MAX PLANCK INSTITUTE FOR HUMAN COGNITIVE AND BRAIN SCIENCES LEIPZIG

Michael A. Skeide: Syntax and Semantics Networks in the Developing Brain. Leipzig: Max Planck Institute for Human Cognitive and Brain Sciences, 2012 (MPI Series in Human Cognitive and Brain Sciences; 143)

# Syntax and semantics networks in the developing brain

Impressum

Max Planck Institute for Human Cognitive and Brain Sciences, 2012



Druck: Sächsisches Druck- und Verlagshaus Direct World, Dresden
Titelbild: Clara Sophia Skeide, 2012

ISBN 978-3-941504-27-1

# Syntax and semantics networks in the developing brain

Von der Fakultät für Biowissenschaften, Pharmazie und Psychologie

der Universität Leipzig

genehmigte

D I S S E R T A T I O N

zur Erlangung des akademischen Grades

doctor rerum naturalium

Dr. rer. nat.

vorgelegt

von Michael Artur Skeide, M.A.

geboren am 7. Juni 1984 in Wernigerode

Dekanin: Prof. Dr. Andrea A. Robitzki

Gutachter: Prof. Dr. Dr. h.c. Angela D. Friederici

Prof. Dr. Axel Mecklinger

Tag der Verteidigung: 1. November 2012

## Acknowledgements

How lucky the author of the present thesis is having Prof. Dr. Dr. h.c. Angela D. Friederici as a supervisor, mentor, inspirator, critic, motivator and furtherer at such a crucial point of his scientific development. Furthermore, the author is grateful that Prof. Dr. Axel Mecklinger showed great interest for his work right from the start and immediately agreed to review his thesis. Prof. Dr. Sharlene Newman dedicated valuable time of her sabbatical to be a member of his examination committee. Dr. Jens Brauer convinced the author that it is possible to make kids having fun with a 3 Tesla MR scanner. Prof. Dr. Christian Fiebach helped him with the first attempts to walk on the field of Neuroscience back in the Heidelberg University days.

The author had great fellow researchers and PhD students at the Neuropsychology department: Lars Meyer showing him that it is advantageous to use matlab for handling complex data, Anja Hubert who knows a lot about how children acquire a language, Sarah Gierhan giving him examples how to use SPM8 in an elegant way, Riccardo Cafiero showing him how to see through the architecture of the MPI's DWI processing pipelines and just all of them, finally the whole world-class institute.

Anke Kummer, Simone Wipper and Mandy Jochemko are the unsung heroes of long and laborious scanning days. Katja Kirsche and Antje Viehweger do great winning participants. Thanks go to the graphics department for designing and equipping, the IT department for debugging and supporting as well as the receptionists for welcoming so many romping kids.

The author is indebted to his loved and esteemed ones who all perfectly know that he is referring to them right now. He dedicates this work to Artur Hermann Skeide.

Book cover artist: Clara Sophia Skeide.

# Contents

# 1. GENERAL INTRODUCTION

Language is one of the most crucial younger evolutionary achievements of the homo sapiens sapiens (Darwin, 1871). Recently, however, remarkable cognitive capacities such as complex auditory and visual pattern learning have also been discovered in non-human primates (Fitch and Hauser, 2004; Grainger et al., 2012) and even in birds (Gentner et al., 2006; Abe and Watanabe, 2011). These sophisticated skills in animals were interpreted by some authors as the precursor of the ability to learn genuine linguistic representations. Nevertheless, in order to produce and comprehend language, it is essential to be able to discriminate, combine and integrate a very complex set of linguistic elements, including phonological, graphematic, morphological, syntactic, semantic, prosodic and pragmatic entities. This faculty is a uniquely human trait.

Syntax and semantics, the two linguistic domains which are in the focus of this thesis, are two core higher-order language functions. Mastering syntactic rules, which determine how small linguistic units are combined to form complex phrase structures, is crucial for understanding a language. In order to interpret the meaning of a sentence, however, a speaker must also be proficient in accessing lexical-semantic information to allow the build-up of semantic relations between words in a sentence and, moreover, to map this lexical-semantic information onto world knowledge. Thus, it is the interplay of syntax and semantics that guarantees language production and comprehension.

The processing of language based on auditory and visual and, if necessary, tactile sensory organs is regulated by an organ which has reached ultimate complexity in the course of the phylogeny of the homo sapiens sapiens – the brain. The neuroanatomical and neurophysiological foundations of language have been scientifically illuminated since about 150 years. Pierre Paul Broca, a

French physician, was the first to anatomically localize the ability to produce language. Based on his autopsy findings that patients suffering from production aphasia had specific nerve tissue lesions, he provided evidence that language functions are located in the left frontal cortex of the brain (Broca, 1863). Slightly later, Carl Wernicke, a German physician, discovered that not all language deficits had their origin in lesions in the cortical area Broca had described before. Rather, he found that damage to the posterior portion of the left superior temporal gyrus is associated with what he called a sensory aphasia, i.e. difficulties in language comprehension. Another important progress Wernicke made, was that he did not only take into account the language selectivity of frontal and temporal cortical areas but rather pointed out that also the connections between these areas are crucial for both producing and comprehending language. Accordingly, he speculated that damage to fronto-temporal association systems would lead to a third type of aphasia which he called conduction aphasia (Wernicke, 1874).

Although the notion of language-selective cortical areas and long-distance language networks was already established in the 19th century (Broca 1863; Wernicke, 1874; Lichtheim 1885), it was not possible to directly assess this notion empirically until the 1990s when magnetic resonance imaging of human tissue was developed (Kwong et al., 1992). This groundbreaking technology together with the already established electroencephalography as well as magnetoencephalography made it possible to investigate the brain basis of language non-invasively and in vivo. Accordingly, our understanding of the neural underpinnings of syntactic and semantic processing has dramatically increased since that time even though the topic is still controversially discussed. Most of what we know about the relationship of syntax, semantics and the brain stems from neuroimaging and event-related potentials studies with adults. However, so far, we do not know much about how these language functions

develop according to the maturation of the brain. Therefore, the magnetic resonance imaging research presented in this thesis has been conducted to shed light on syntax and semantics networks in the developing brain.

In chapter 2, I will give an overview of the current state of research in both the adult and the language acquisition literature reporting influential models as well as important studies. Chapter 3 comprises a description of the experimental methods used covering both the acquisition and statistical analysis of the behavioral as well as the neuroimaging data. In the first part of chapter 4, I will report an event-related functional magnetic resonance imaging (fMRI) study showing how cortical activation patterns for syntactic and semantic processes change as the brain matures. In the second part of chapter 4, I will introduce a diffusion tensor imaging (DTI) study in which we demonstrate how white matter fiber tracts contribute to the propagation of syntactic and semantic information between syntax- and semantics-selective fronto-temporal cortical regions. Chapter 5 contains a summary of our findings and how they expand our knowledge about the brain basis of language development.

# 2. DATA, MODELS AND RESEARCH PERSPECTIVES

In chapter 2, I will outline Friederici's adult model of the structural and functional neural network underlying the processing of syntactic and semantic information in sentence comprehension (Friederici, 2011). This model also serves as a reference frame for the interpretation of the few data available on how language comprehension works in the child brain.

## 2.1. The brain basis of syntactic and semantic processing in adults

Friederici highlights both the spatial extension of the language network and the temporal dynamics of language processing. A scheme of the temporal dynamics of language processing can be seen in **Figure 2.1**. The spatial extension of the language network in the brain is shown in **Figure 2.2**. Note that Friederici argues for a strong left-lateralization of both syntax and – to a lesser extent – semantics.

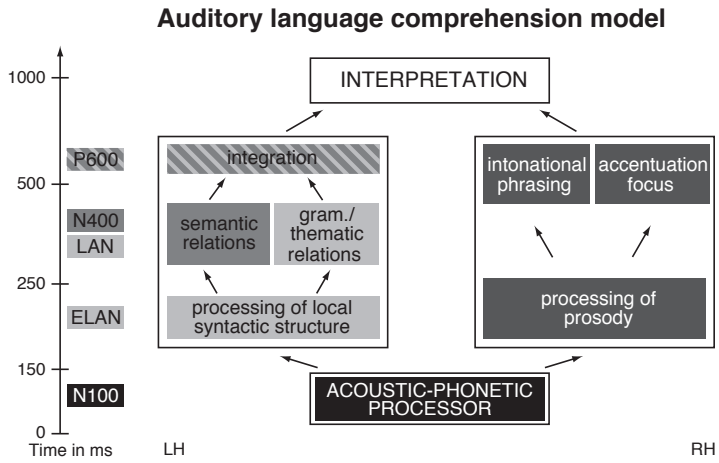


**Figure 2.1.** The time course of several linguistic subprocesses within auditory language comprehension. (Figure adapted from Friederici, 2011.)

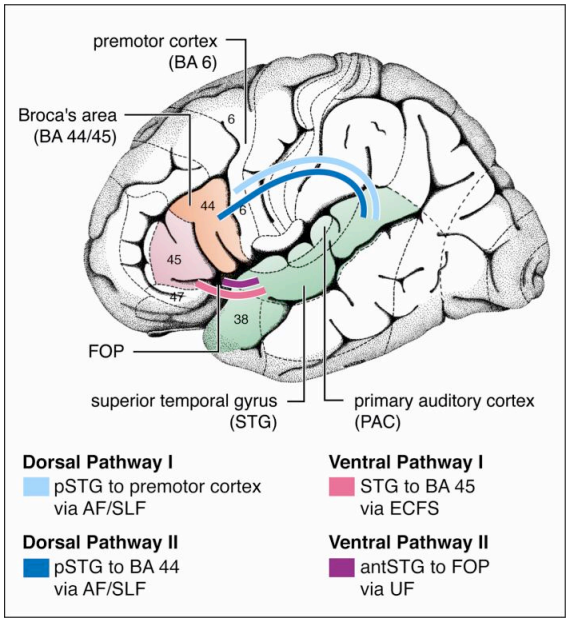


**Figure 2.2.** Fronto-temporal language regions (Broca's area, premotor cortex, frontal operculum (FOP), superior temporal gyrus) and the course of their connecting white matter fiber pathways (arcuate fasciculus (AF), superior longitudinal fasciculus (SLF), extreme capsule fiber system (ECFS), uncinate fasciculus (UF)). (Figure adapted from Friederici, 2011.)

In the first instance, Friederici's model of brain-based language processing takes into account acoustic and phonological analyses going on within 100ms after auditory stimulation by a spoken sentence (Näätänen et al., 1997; Obleser et al., 2006). Both the primary auditory cortex (PAC) and the planum temporale (PT) are involved in these processes (Rauschecker and Scott, 2009; Scott and Johnsrude, 2003). According to Friederici, the information about the acoustic and phonological features of the input sentence is then transmitted to the anterior portion of the left superior temporal gyrus (aSTG) and sulcus (aSTS) as well as the frontal operculum (FOP), on the one hand, and to the posterior portion of the superior temporal gyrus (pSTG) and sulcus (pSTS), on the other hand. The fronto-temporal connection between the aSTG/STS and

the FOP is established by a ventral white matter fiber tract covering the uncinate fasciculus (UF) (Friederici et al., 2006). In Friederici's model, both the aSTG/aSTS and the FOP support early syntactic processes of limited complexity like the initial detection of phrase structures occurring between 120 and 200ms (Knösche et al., 1999; Friederici et al., 2000; Friederici and Weissenborn, 2007; Dikker et al., 2009). More complex syntactic processing, including the identification of hierarchical structures within a sentence, takes place later at around 300 to 500ms in the already mentioned pSTG/STS (Cooke et al., 2002; Vandenberghe et al., 2002; Humphries et al., 2005; Bornkessel and Schlesewsky, 2006; Kinno et al., 2008; Friederici et al., 2009; Snijders et al., 2009; Santi and Grodzinsky, 2010; Newman et al., 2010). However, this is not achieved by the pSTG/STS alone but, as Friederici argues, critically involves the pars opercularis of the inferior frontal gyrus (IFGoper) in Broca's area (Friederici et al., 2006; Makuuchi et al., 2009; Newman et al., 2010; Wilson et al., 2010). Accordingly, information about complex syntax is propagated through a dorsal pathway connecting both regions via the superior longitudinal fasciculus (SLF) and the arcuate fasciculus (AF) (Wilson et al., 2011). Although the semantic network also covers the pSTG (Friederici et al., 2003; Obleser and Kotz 2010), like the syntax network, as well as the pMTG and although semantic processing takes place in a parallel time window (Li et al., 2006), it rather depends on a ventral fiber tract through the extreme capsule fiber system (ECFS) transmitting semantic information to the pars triangularis of the inferior frontal gyrus (IFGtri) and the pars orbitalis of the inferior frontal gyrus (IFGorb), as Friederici points out (Friederici, 2002). Finally, in order to enable a successful interpretation of a sentence, both syntactic as well as semantic information has to be integrated then in the pSTG/STS (Friederici et al., 2009; Grodzinsky and Friederici, 2006). Prosodic information is processed in right-hemispheric brain regions connected via the the posterior corpus callosum both during initial phrase structure building (Eckstein and

Friederici, 2006; Sammler et al., 2010) and more complex syntactic processes occurring later (Steinhauer et al., 1999; Friederici et al., 2007; Bogels et al., 2010). Note, that Friederici also proposes a second dorsal stream via the SLF/AF which she considers responsible for mapping auditory patterns onto motor plans during articulation processes (Hickok and Poeppel, 2007; Rilling et al., 2008; Saur et al., 2008).

In contrary to predecessing dual stream models (Hickok and Poeppel, 2007), Friederici's 4-pathway-model gives a more comprehensive account of how language processing works as a complex interplay between all of its linguistic subcomponents and the underlying structural and functional neural network. Furthermore, it is currently put on a more solid data footing than so-called unification models assuming that representations from all linguistic domains are unified in the left IFG while the dorsolateral prefrontal cortex is responsible for language-related attentional control processes and the temporal cortex supports storage and retrieval of linguistic information (Hagoort, 2005).

### 2.2. The brain basis of syntactic and semantic processing in children

Up to this day, there is no model available describing the development of structural and functional neural networks underlying language acquisition. In contrary to the relatively rich adult literature, the child literature on the neural underpinnings of language processing is scarce. Accordingly, I will provide an overview of the currently available data, rather than discussing a coherent model.

Most of what we know about how linguistic information is processed in the maturing brain, comes from event-related potentials (ERP) studies on infants and toddlers (Friederici, 2005; Kuhl, 2010). On the basis of these data, a relatively clear picture of the timing of various linguistic processes has emerged although the discussions continue (see **Figure 2.3.**).

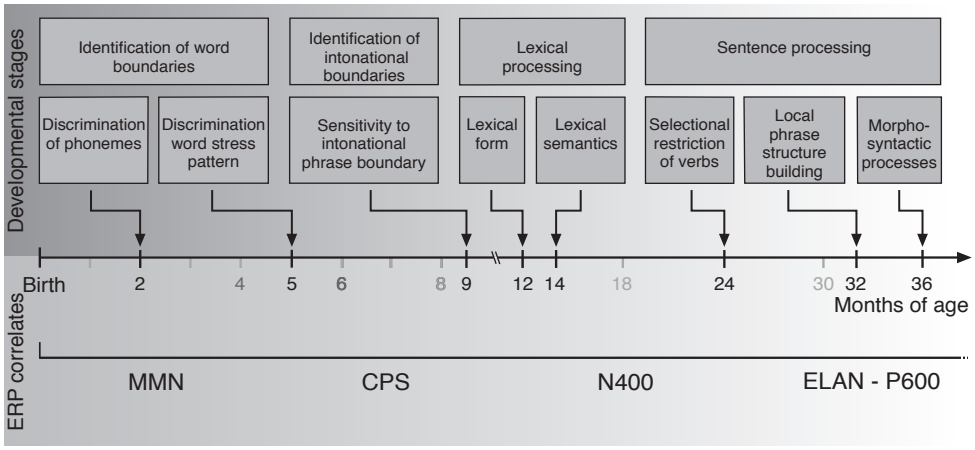


**Figure 2.3.** ERP correlates of phonological, semantic and syntactic processing indicating developmental trajectories of auditory language comprehension in infants and toddlers. (Figure adapted from Friederici, 2005.)

It has been demonstrated that 2-months-old infants already show electrophysiological responses, i.e. the mismatch negativity (MMN), to distinct phonemes (Friedrich et al., 2004) and also to distinct stress patterns at 5 months of age (Weber et al., 2004). Infants use this knowledge to identify word boundaries. Towards the end of the first year of life, the infant's brain starts to become sensitive to certain parameters of the intonational phrase boundary (Männel and Friederici, 2009; Männel and Friederici, 2011), reflected in so-called closure positive shift (CPS) effects in adults (Steinhauer et al., 1999). Word-level lexical-semantic processes are detectable as ERP responses, namely a frontally distributed negativity occurring at roughly 400ms (N400), from around 12 to 14 months on (Friedrich and Friederici, 2005) whereas their sentence-level counterparts do not arise before around 30 months of age (Silva Pereyra et al., 2005). At the end of the third year of life it is also possible to identify the electrophysiological underpinnings of syntactic processing. First local phrase structure building processes occuring at 32 months of age are reflected in the so-called early left anterior negativity (ELAN) (Oberecker et al., 2005). A sensitivi-

ty for decoding morphosyntactic information seems to be measurable only from 36 months of age on in terms of a left anterior negativity (LAN) and a centro-parietally distributed positivity occurring at roughly 600ms (P600) (Schipke et al., 2011). Note that all theses components have higher latencies in children as opposed to adults. Given that all major electrophysiological components which can be detected in adults, are already established in 3-year-old children, ERP studies suggest that language-developmental processing differences between adults and children are quantitative, rather than qualitative in nature (Friederici, 2005).

The view that the structural and functional organization of language relevant perisylvian neural networks in children was similar to their adult counterparts found support in the first functional magnetic resonance imaging (fMRI) and diffusion tensor imaging (DTI) studies on speech processing in infants (Dehaene-Lambertz et al., 2006). However, this view was challenged by the results reported in the first fMRI study investigating the neural basis of syntax and semantics in kindergarten children of 5 to 6 years of age in which the authors describe broader and less specific activation patterns in children compared to adults (Brauer and Friederici, 2007). Recently, also functional and structural connectivity data from a combined fMRI-DTI experiment on 2 days old infants suggested qualitative differences (Perani et al., 2011). In contrast to adults, the newborns demonstrated pronounced interhemispheric but immature intrahemispheric connectivities. Furthermore, it has been demonstrated that these disparities regarding interhemispheric fronto-temporal connections are still present in 7-year-old children (Brauer et al., 2011). While adults rely more on the dorsal SLF/AF, children seem to recruit both the dorsal SLF/AF and the ventral ECFS for processing linguistic representations. Taken together, the current picture of the developmental trajectories related to the localization of language functions in children is not as clear as the current picture of their age-

dependent timing. It is a major goal of the work presented in this thesis, to contribute to the clarification of this picture. So far, a fronto-temporal network involving the STG, MTG and IFG (Moore-Parks et al., 2010; Nunez et al., 2011) as well as dorsal and ventral fiber tracts has been described as playing a role for language processing in the developing brain. Children differ from adults in that they recruit a broader and less left-lateralized network (Vannest et al., 2009). Additionally, infants show stronger interhemispheric but weaker intrahemispheric connectivities than adults. An adult-like maturation of interhemispheric white matter fiber tracts connecting inferior frontal with mid and superior temporal areas is not even reached at 7 years of age.

### 2.3. Research questions and hypotheses

In the present thesis, we investigate how the behavioral, brain functional and brain structural underpinnings characterizing syntactic and semantic processing in auditory language comprehension change during language development and brain maturation from 3 years of age to adulthood. In order to shed light on this topic, we apply a multimodal approach combining the analysis of response accuracy and reaction time data with fMRI-based hemodynamic cortical activity measures on the whole-brain level as well as in regions of interest (ROIs) and also with probabilistic DTI measures defining the course and the constitution of relevant white matter fiber tracts.

There are 3 general research questions we would like to answer in this thesis:

1. How do children at distinct stages of their language development, i.e. children of 3 to 4 years of age, 6 to 7 years of age and 9 to 10 years of age differ from adults with respect to the hemodynamic activation patterns underlying the neural processing of syntactic and semantic information?

2.1. At the behavioral level, a tight interdependence of syntactic and semantic processes in children has been known for a long time (Friederici, 1983). Is this tight interdependence reflected at the functional neural level?

2.2. Is there also evidence for different behavioral processing strategies between the age groups?

3.1. Which functional and structural changes occur in the course of brain maturation within white matter fiber pathways connecting fronto-temporal areas which support the processing of syntax and semantics?

3.2. What are the precise functional roles of the identified tracts? Do they contribute to the propagation of syntactic, semantic or both types of information?
On the basis of the current literature we formulate the following hypotheses:

1. The younger the children are, the more the brain activation patterns for syntactic and semantic processing overlap and the less segregated they are compared to adults (Brauer and Friederici, 2007; Nunez et al., 2011).

2.1. The tight interdependence of syntactic and semantic processes in young children might be reflected in a syntax x semantic interaction effect in the fronto-temporal cortex. This effect should, however, disappear in older children and adults.

2.2. The younger the children are, the more they should rely on semantic information in order to achieve a successful interpretation of a sentence. In contrast, adults are expected to focus more on syntactic cues.
3.1. In adults, we assume to isolate a highly developed dorsal fiber pathway playing a role for the processing of syntax (Wilson et al., 2011) and a ventral pathway playing a role for the processing of semantics (Friederici, 2011). We hypothesize, that this clear division is less pronounced in the maturing brain.

3.2. Although the functional roles of these tracts might be different at earlier developmental stages, we expect to corroborate associations between syntax and a dorsal pathway and semantics and a ventral pathway, respectively.

# 3. GENERAL METHODS

The following chapter includes a theoretical overview of the experimental methods employed in the investigations described in the subsequent chapter. Emphasis rests on the complete introduction of all relevant experimental parameters. At first, I will give a general outline of behavioral and brain measurements followed by an introduction to the principles of nuclear magnetic resonance (NMR) from a classical physics perspective. On this basis, I will explain how NMR is applied to the experimental techniques of functional magnetic resonance imaging (fMRI) and diffusion-weighted imaging (DWI). Chapter 3 closes with general remarks on the statistical methods used to analyze the behavioral, functional and anatomical data presented in chapter 4.

## 3.1. Data acquisition

### 3.1.1. Behavioral measurements

Some psycholinguistic paradigms for behavioral measurements can be combined and synchronized with functional imaging measurements. This approach allows to draw direct conclusions about interrelations between behavioral data and functional brain data. The best-validated and most frequently described tasks in the language-related developmental neuroscience literature are decision, selection and judgment tasks. These task types have been applied to a wide range of linguistic domains including phonology (Wilke and Schmithorst, 2006), the lexicon and semantics (Gaillard et al., 2007; Moore-Parks et al., 2010; Nunez et al., 2011; Newman, 2012), syntax (Brauer and Friederici, 2007) and texts (Wilke et al., 2005).

Following the well-documented positive experience with selection tasks in preschool children, an age-appropriate picture selection task was designed in order to assess the interplay of syntactic complexity and semantic plausibility information during auditory language comprehension. It will be described in more detail in chapters 4.1.1. and 4.1.2. of this thesis. Picture selection tasks have a long tradition in psycholinguistics (McDaniel et al., 1996). However, given that space and time are limited in the MR scanner we pretested the stimulus material following 2 general considerations. First, it had to be technically possible to perform the task inside the MR tube while participants are not allowed to move more than around 3mm. By the way, this requirement made the act-out paradigm, for example, which has been frequently used by developmental psycholinguists especially to test young children (Correa, 1995), incompatible with an fMRI investigation. The same holds true for overt language production tasks including repetition tasks which can induce strong facial muscle movements. Second, the task should not exceed an overall duration of 15 minutes, which has turned out to be the upper limit for kindergarten children. Additionally, in order to increase the probability that the participating children execute the whole experiment from start to finish, we had to make sure that the task is age-appropriate with regard to its difficulty and its desirability. Accordingly, the task was designed as playful and interactive as possible to keep the children motivated.

### 3.1.2. Neuroimaging measurements

Several experimental designs are available to address a wide range of specific research questions in fMRI (**Figure 3.1.**). A good choice is very important because the more appropriate the selection of an experimental design is, the more precise the data acquisition and later data evaluation are.

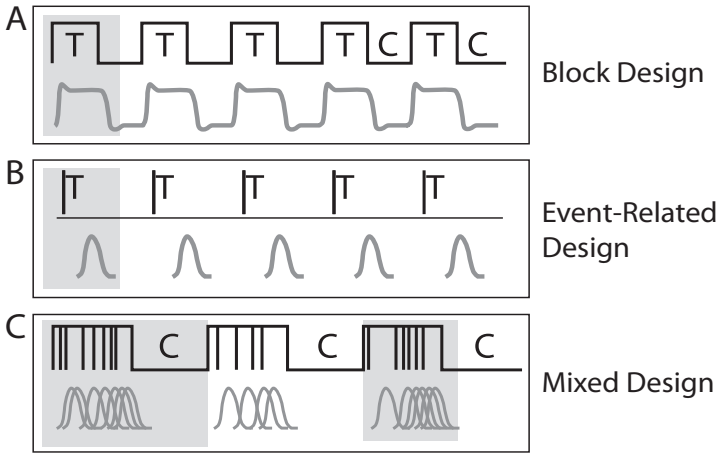


**Figure 3.1.** The three main design types used in fMRI. In a block design (**A**), stimuli of one condition are presented directly after another while in an event-related design (**B**), stimuli of different conditions are presented in a randomized series of individual trials. Both stimulus delivery designs can also be combined into a mixed design (**C**). (Figure adapted from Amaro and Barker, 2006.)

Depending on a certain research question and a certain stimulus material, a so-called block design can be very suitable (Amaro and Barker, 2006). In such a design, a series of multiple stimulus events of only one distinct experimental condition is presented in a coherent time window of mostly about 10 to 60 seconds. After this period, the next time block is started and stimuli belonging to a different experimental condition are presented. Unfortunately, many types of stimuli, especially in language experiments, cannot be presented on the basis of such a rigid architecture. However, the advantage of this traditional design which was the only design used in the first early 1990s fMRI experiments is its good statistical power in detecting hemodynamic effects (Friston et al., 1999). On the other hand, it is not very powerful when applied to estimate the time course of brain activations.

A so-called event-related experimental design (Josephs et al., 1997; Friston et al., 1998) served as a framework of the fMRI study that I introduce in section 4.1. When this design is applied, stimulus events of distinct experimental conditions are presented each in individual trials. This allows to deliver stimuli fully (pseudo-)randomized and jittered (Rosen et al., 1998). Event-related designs are younger than block designs because it took some years of methodical refinement to produce the proof that even very short hemodynamic activity changes leading to transient blood-oxygen-level-dependent (BOLD) signal increases result in measurable effects suitable for successful statistical evaluation (Buckner et al., 1998). But although event-related designs permit to detect hemodynamic activation differences they are nevertheless still not as powerful as block designs regarding their sensitivity. However, a big advantage of event-related designs is their broad applicability to a much wider range of research questions. Furthermore, they lead to much higher temporal resolution of the hemodynamic response signal than block-designs do (Buxton et al., 2004).

Some studies also employ a mixed design in which some of the experimental factors are delivered in blocks and some as (pseudo-)randomized events within blocks (Donaldson et al., 2001). In principal, this hybrid method allows to disentangle both transient as well as sustained activation because good time course estimation and good activation detection can be combined. In practice, however, only very few research questions fit to this approach.

MR scanning of healthy young adults has become a routine investigation in neuroscience. Prior to the measurements, participants undergo safety instructions and give informed consent to take part in a study. Additionally, it is checked whether there are any contraindications making it necessary to withhold MR scanning, e.g. ferro-magnetic objects in the body which are suscepti-

ble to electro-magnetic fields. Depending on the purpose of a certain study, participants might have to fulfill further criteria in order to be suitable for an experiment. Most linguistic experiments, for example, require right-handedness to increase the likelihood of left-lateralization of language functions. Adult participants can remain up to 2 hours in a MR scanner without moving excessively, meaning that a large amount of high quality data can be acquired in a short time. Very few participants have to stop the scans because of being claustrophobic.

It is more difficult to acquire MR data of children. First of all, it is less efficient because many more children than adults interrupt scanning, stop scanning or do not even enter the scanner. Accordingly, drop-out rates are much higher in children compared to adults and they increase exponentially the younger the children are.

**Figure 3.2.** The mock scanner at the Max Planck Institute for Human Cognitive and Brain Sciences. Children go through a training session in which the real MR environment can be simulated playfully in order to familiarize them with the experimental procedures.

Based on our data and the literature (Byars et al., 2002; O'Shaughnessy et al., 2008), we estimate that drop-out rates are around 50% in 3- to 4-year-old children, up to 25% in 6- to 7-year-old children and up to 10% in 9- to 10-year-old children, if they are unprepared for scanning. In order to reduce drop-out rates, children are trained in a mock scanner prior to the actual measurement (**Figure 3.2.**).

The rationale behind a mock-up session is, first, to assess whether a child would make a suitable participant based on its current emotional, cognitive and motivational development and, second, to familiarize the child with an MR environment, the measurement procedures and the tasks it has to solve. In practice, it is important to help the participants not to be afraid of the scanner but rather to have fun with the experiment. Therefore, the experimenter has to set up the training as a game, especially in younger children. Sometimes it is necessary to include the parents as well. Additionally, young participants have to train lying still in the scanner and, most importantly, not to move their heads. This can be achieved by giving them encouraging feedback on-line during a mock-up session. Motion sensors stopping the presentation of a video, for example, in case of head movement have also proven useful. All in all, it is crucial to simulate the actual measurement session as precise as possible so that the children do not get distracted or scared in the real MR environment. Although mock-up sessions are time consuming, they significantly reduce drop out rates to about less than 40 % in 3- to 4-year old children and less than 10% in 6- to 7-year-old children while 9- to 10-year-old children, like adults, show no noteworthy drop out anymore. An optimal result with respect to data quantity as well as data quality is achieved in a child-friendly, low-noise scanner with a wide tube. Further remarks on the MR measurements we took from the 3 child samples can be found in chapter 4.1.2.

## 3.2. Nuclear magnetic resonance imaging

### *Nuclear magnetic resonance*

Nuclear Magnetic Resonance (NMR) is a phenomenon demonstrated independently in 1946 by the research groups of Felix Bloch (Bloch et al., 1946) and Edward Purcell (Purcell et al., 1946). It occurs when the nuclei of certain atoms are immersed in an external static magnetic field $B_0$ and exposed to a second oscillating magnetic field $B_1$. If an atomic nucleus experiences nuclear magnetic resonance, depends on whether it possesses an intrinsic angular momentum, i.e. a nuclear spin. It is a fundamental characteristic property of elementary particles. Hydrogen ($^1$H) nuclei of water molecules for example – the principal component of the brain and the whole body – are composed of single protons that do have a spin.

As spinning protons of hydrogen nuclei behave like moving electrical charges they possess a magnetic dipole moment quantifying the force a nucleus can exert on electric currents but also the torque any magnetic field will exert on it. This phenomenon bases on the fact that hydrogen protons have two distinct energy states ($N_E$) determined by the equation $N_E = 2S(^1H) + 1$ where S is the spin quantum number and $S(^1H) = 1/2$. The effect is that a hydrogen proton spins along axes of opposite directions. One spin axis points north, i.e. parallel to $B_0$ and the other spin axis points south, i.e. anti-parallel to $B_0$. Now the reason why hydrogen nuclei possess a magnetic dipole moment and hence induce an electromagnetic field is that they have an odd number of protons. If there were an even number of protons in the nuclei, every proton would be paired, i.e. for every parallel spinning proton there would be an antiparallel spinning proton. The result would be that the two electromagnetic fields of these paired protons would cancel each other out. Nuclei with an odd number

of protons, however, always contain an unpaired proton inducing an electromagnetic field (Hashemi et al., 2010).

As the static magnetic field $B_0$, the $^1H$ nucleus is exposed to, exerts a torque on its electromagnetically charged protons, the $^1H$ nucleus would tend to align with $B_0$. However, as described above the $^1H$ nucleus also has an intrinsic angular momentum, a nuclear spin, so that it instead initially keeps spinning at a certain angle around the $B_0$ field axis (**Figure 3.3.**). This so-called precession movement proceeds at a certain frequency which is directly proportional to the strength of $B_0$ and the constant ratio of the magnetic dipole moment to its angular momentum, called the gyromagnetic ratio γ of the proton. Thus, the precession frequency $\omega_0$ – often called Larmor frequency – of a nucleus can be described by the equation $\omega_0 = \gamma B_0$. In a 3 Tesla scanner, as used for the experiments described in chapter 4, $\omega_0$ of $^1H$ = 42.576 MHz/T * 3T = 127.728 MHz (Hashemi et al., 2010).

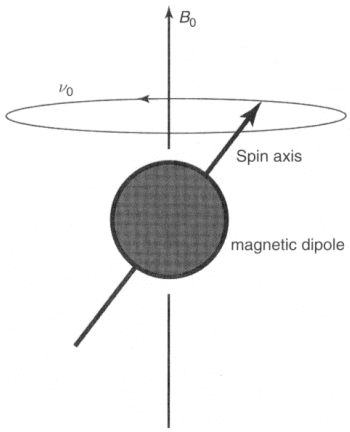


**Figure 3.3.** Precession – a core principle of Nuclear Magnetic Resonance. Although the static magnetic field $B_0$ exerts a torque on the hydrogen nucleus, it does not immediately align with it but keeps spinning for a while, i.e. precessing at a frequency $\nu_0$, at an angle around it because the nucleus forms a magnetic dipole with an angular momentum. (Figure adapted from Buxton, 2009.)

NMR bases on applying electromagnetic field gradient pulses of a certain radiofrequency introducing a linear magnetic field inhomogeneity to create a second weak magnetic field $B_1$ as mentioned above. Inducing a dynamic $B_1$ ($B_{xy}$) transversal to $B_0$ ($B_z$) results in a so-called excitation of the spinning $^1H$ nuclei. Therefore, the frequency of $B_1$ must equal the Larmor frequency $\omega_0$ of the precessing nuclei (**Figure 3.4.**).

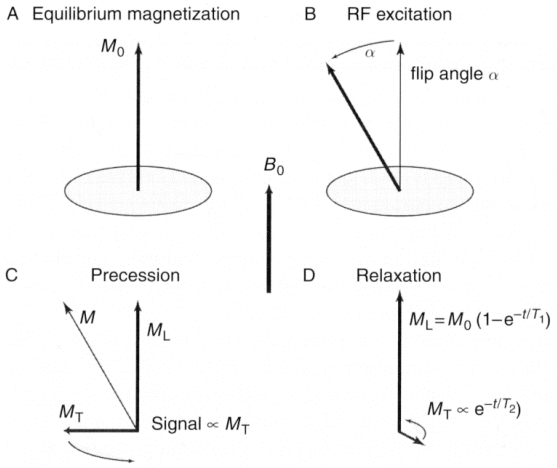


**Figure 3.4.** The 4 main phases of Nuclear Magnetic Resonance. Initially, a nucleus is aligned with the static magnetic field $B_0$ (**A**). When a radiofrequency (RF) pulse is introduced, the nucleus tips over at a certain angle α (**B**) and precesses (**C**). When the RF pulse is deactivated, the nucleus realigns to $B_0$, i.e. it relaxates (**D**) generating an NMR signal. (Figure adapted from Buxton, 2009.)

During excitation a nucleus takes up electromagnetic energy while absorbing the $B_1$ radiation. As a consequence, the direction of the nucleus' spinning axis gets alternated from the z plane towards the xy plane. If the flip angle is limited to 90°, as it is the case in the fMRI study to be presented in chapter 4, the hydrogen nuclei are at their highest energy state during maximal transversal alignment against $B_0$. After a certain time $B_1$ is turned off so that the proton's spinning axis gradually reorients towards the longitudinal $B_z$ direction. During

this reorientation process which is called longitudinal relaxation the nucleus releases photons carrying the energy it has absorbed before as radio frequency radiation during transversal excitation. Relaxation continues until the nucleus reaches maximal longitudinal alignment with $B_0$ when it is at its lowest energy state again. This process of going back to the lowest energy state, i.e. the equilibrium state, is often called saturation recovery. Saturation refers to the energy uptake during excitation (Hashemi et al., 2010).

Hydrogen protons emitting energy during relaxation create a transient NMR signal which can be measured as currents induced in a nearby detection coil. This fast decaying signal is called Free Induction Decay (FID). It can be recorded and visualized by assigning color values to signal strength values. As every tissue probe is characterized by a heterogeneous hydrogen proton density, it generates a distinct FID signal strength and hence also a distinct color value which is mostly a grey value contrast (Levitt, 2008).

***Magnetic resonance imaging***

As already mentioned, the NMR signal contrast depends on the proton density in a given tissue probe. In the human body there is a relatively high hydrogen proton density because of the abundance of water molecules in most of the tissues. Brain tissue for example contains approximately 71% of water in white matter, 84% of water in grey matter and even 97% of water in cerebrospinal fluid (CSF) (Buxton, 2009).

Proton density, however, is not the only factor influencing the NMR signal contrast. It also depends on the time it takes a spinning proton to realign towards the z-axis during longitudinal relaxation and to recover to the state of magnetic equilibrium. This time is generally called T1, but also longitudinal relaxation

time, thermal relaxation time or spin-lattice relaxation time (**Figure 3.5.**). The latter term refers to the time it takes a spinning proton to release the energy obtained during excitation back to the surrounding lattice of macromolecules in the course of its saturation recovery. T1 is a time constant depending on the tissue of interest and the strength of $B_0$. In a 3 Tesla scanner – as used for the investigations to be presented in this thesis – it is approximately 832ms for white matter, 1331ms for grey matter and 2300ms for CSF (Wansapura et al., 1999). It is important to note that T1 is the time it takes a spinning proton to only partially align with the z-axis and to recover to the state of magnetic equilibrium. Optimal alignment and full recovery takes 3 to 5 times longer than T1 (Hashemi et al., 2010).

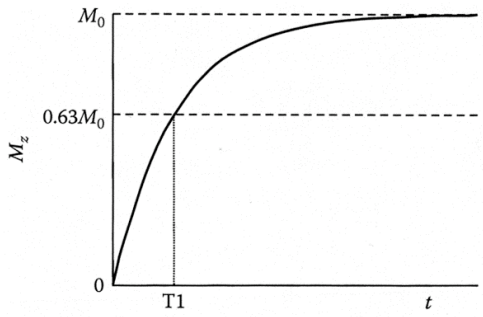


**Figure 3.5.** The time constant T1 denotes the time it takes a spin to start releasing energy and hence induce an NMR signal during longitudinal relaxation. (Figure adapted from Berry and Bulpitt, 2009.)

The second time constant affecting the NMR signal contrast is called T2. It denotes the time it takes protons for transverse relaxation along the xy direction so that T2 is often called the transverse relaxation time (**Figure 3.6.**). T2 relaxation is the irreversible process by which a proton's net magnetization ($M_0$) value decreases exponentially to about 37% of its initial value in the xy plane during longitudinal relaxation. It measures the rate of the signal's intrinsic de-

cay after an excitatory radiofrequency pulse is delivered. The basis of this effect is that shortly before deactivating the radiofrequency pulse, every single proton precesses at the same frequency $\omega_0$. Furthermore, each proton's precessional cycle phase is synchronized. These two properties allow the proton to absorb the energy released by another nearby excited proton. According to this process, T2 relaxation is also called spin-spin relaxation. However, this energy transfer is transient as $\omega_0$ starts fluctuating due to molecular vibrations or rotations leading to a gradual loss of phase coherence and hence causing signal decay. The T2 signal decay is much shorter than the T1 signal decay. It is about 80ms in white matter, about 110ms in grey matter and about 1800ms for CSF at 3 Tesla (Buxton, 2009).

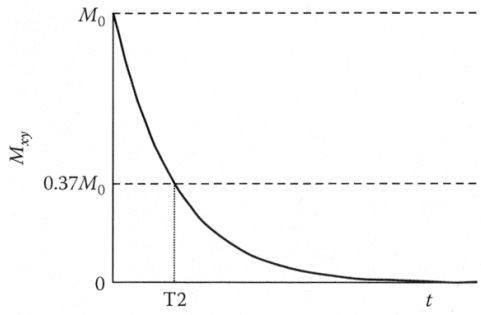


**Figure 3.6.** The time constant T2 denotes the time it takes a spin to start releasing energy and hence induce an NMR signal during transverse relaxation. (Figure adapted from Berry and Bulpitt, 2009.)

In addition to dephasing processes caused by molecular vibrations or rotations as described above, there is another dephasing process caused by constant main field inhomogeneities, gradient field inhomogeneities or sample-induced inhomogeneities. The effect of this phase coherence loss is that the T2 signal decay is slightly accelerated. Such a spin-spin relaxation speeded up by additionally occuring dephasing is called T2* relaxation (**Figure 3.7.**). T2* is slightly

shorter than T2 (Hashemi et al., 2010). Measurement sequences determined by T1, T2 and T2* relaxation times are called T1-, T2- or T2*-weighted imaging sequences.

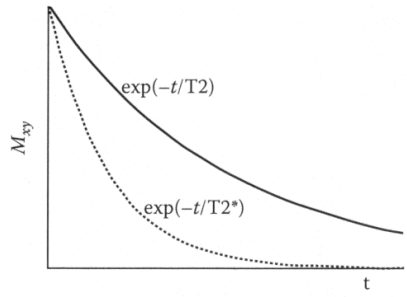


**Figure 3.7.** T2* relaxation occurs faster than T2 relaxation because of stronger dephasing caused by additional field inhomogeneities. (Figure adapted from Berry and Bulpitt, 2009.)

A very important imaging parameter decisively influencing the T1 signal contrast is the so-called repetition time (TR). To clarify what the TR is, it has to be pointed out that the magnetic field induced in a sample, e.g. the brain, is virtually determined as a cuboid divided into several slices of a certain thickness which are again divided into cuboids of a certain size called voxels (volume pixels). During acquisition of an MR image, slices are excited one after another in an ascending, descending or interleaved order. This so-called slice selection requires multiple recordings of each slice in order to generate an MR image. Exactly the time between two excitations of one and the same slice in a certain probe is the TR. Its influence on T1 bases on the fact that the longer the TR is, the more time the spinning protons have for saturation recovery and longitudinal magnetization, which in turn enables them to absorb more energy and to emit a stronger signal. Hence, a long TR, i.e. less T1 weighting, gives all of the three main brain tissues sufficient time to relaxate so that white matter, grey matter and CSF emit a comparably strong signal. A short TR on the other hand,

i.e. T1 weighting, only allows quickly relaxating tissue like white matter to generate a strong signal while CSF, for example, which has a much longer T1, is only very slightly relaxated and therefore emits only a weak signal (Brown and Semelka, 2010).

The echo time (TE) also called time to echo or echo delay time is a further substantial imaging parameter. It has a fundamental impact on the T2 signal contrast. TE is defined as the time span between the application of the 90° RF excitation pulse and the signal detection after transversal realignment. This temporal delay during data collection is necessary as gradient field inhomogeneities occur causing the protons to spin out of phase, as already described above. Measurement cannot take place until the time point is achieved when the spins are in phase again. When a short TE is chosen, measures are taken at an early stage of relaxation and hence T2 weighting is low. Hardly any contrasts would appear between white matter, grey matter and CSF. A long TE, i.e. strong T2 weighting, however, increases signal intensities. Tissue with a relatively long T2, like CSF, would induce a strong signal when a long TE is chosen as opposed to grey matter and white matter who have a short T2 (Buxton, 2009).

So far, proton density and relaxation time constants have been described as the two main factors contributing to the intensity of the MR signal. The next step is to explain how spatial information is obtained from this signal and how this information is used to compute a three-dimensional image.

In order to localize signal sources in a slice, a technique called slice selection is applied (**Figure 3.8.**). Slice selection requires inducing distinct magnetic field strengths within the entire set of slices in a probe. Once a slice differs to all other slices with regard to its field strength, it also possesses a different Larmor frequency. Hence, when a gradient pulse of a certain radiofrequency is

applied, only the slice carrying the corresponding Larmor frequency gets excitated. This method is technically implemented by using a so- called gradient coil creating a linear increase or decrease of a magnetic field in the z-direction. As soon as all z-directed signal values within a slice are fully measured, they can be decomposed into a 2D image matrix, the k-space or Fourier space, in which every voxel is represented by a pixel (picture element) of a specific grey value. However, to complete this matrix it is necessary to identify signals also along the x- and y-axis which is called spatial encoding (Buxton, 2009).

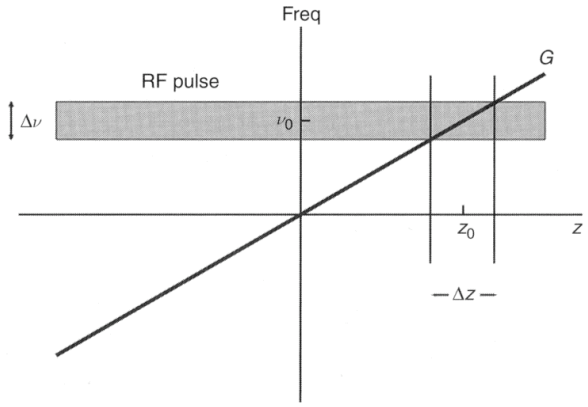


**Figure 3.8.** Slice selection. Gradient coils induce additional magnetic fields of individual strengths in each slice so that only slices matching the Larmor frequency of the applied radiofrequency pulse get excitated. (Figure adapted from Buxton, 2009.)

Spatial encoding comprises two operations which are frequency coding and phase coding (**Figure 3.9.**). Frequency coding is again achieved by applying a magnetic field gradient along the x-axis. The result is that a distinct set of voxels represented by a pixel column of the later k-space 2D image matrix differs in frequency from all of the other columns. Now the relative amplitude of every voxel set's frequency corresponding to a certain pixel column can be calculated (Stehling et al., 1991). The spectrum of spin frequencies to be captured is determined by an MR imaging parameter called acquisition bandwidth. Its extent defines the thickness of the slices under investigation (Brown and Semelka, 2010).

In order to define the entire k-space frequency spectrum, frequency values of each pixel set which is arranged row wise in the 2D image matrix must also be calculated. This second step comprises phase coding. Therefore, a so-called phase coding gradient is applied transiently in y-direction immediately after excitation. The effect is that spins located in a range where the magnetic field is stronger, precess faster than more distant spins who are exposed to a weaker magnetic field. This so-called phase shifting allows to identify phase-separated spins along the y-axis of a probe (Hashemi et al., 2010).

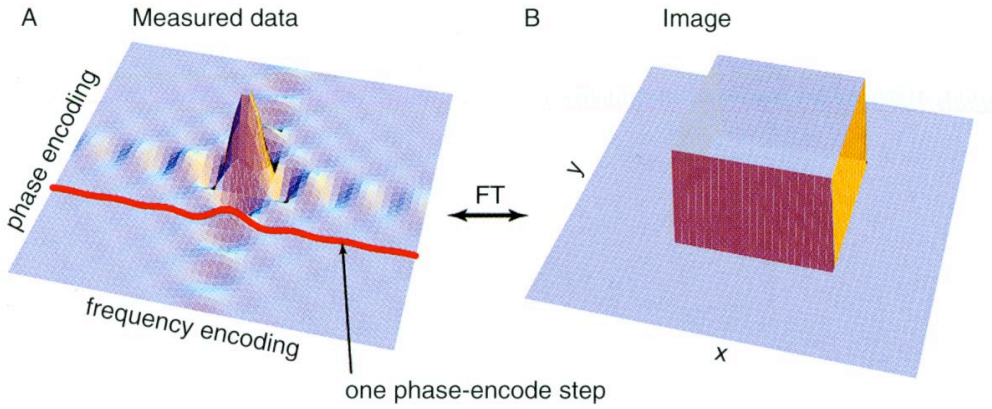


**Figure 3.9.** Spatial encoding and Fourier transform. An image matrix containing a spectrum of spin frequencies and spin phases is decomposed into real space constituent frequencies applying a Fourier transform (FT) and finally converted into a 3D image. (Figure adapted from Buxton, 2009.)

In order to compute a 3D image out of the now defined image matrix, a so-called Fourier transform is applied (**Figure 3.9.**). This mathematical operation allows to decompose signals, i.e. time functions, into a series of constituent frequencies in real space and therefore is the foundation of MR image reconstruction. The size of an actual image section is configured by another important MR imaging parameter called field of view (FOV) (Hashemi et al., 2010).

After the discovery of NMR by Bloch and Purcell, it was mainly developed further for chemical and physical molecular analysis. In 1971, however, a breakthrough towards the applicability of NMR for imaging living tissue was achieved, when Raymond Damadian could demonstrate differences in relaxation times between healthy and tumor tissue (Damadian, 1971). Magnetic resonance imaging in the true sense was first shown on small water-filled test tube samples by Paul Lauterbur in 1973 (Lauterbur, 1973). Later that same year, Peter Mansfield succeeded in performing magnetic resonance imaging in solids (Mansfield and Grannell, 1973). Another milestone in developing the technique was set in 1975 when Richard Ernst introduced phase and frequency encoding and applied Fourier transform for image reconstruction (Kumar et al., 1975). In 1977, Peter Mansfield developed the so-called echo-planar imaging (EPI) method which decisively accelerated image acquisition. It enabled Mansfield to acquire a complete image slice from one excitation in a fraction of a second (Mansfield, 1977).

### *Functional magnetic resonance imaging*

It took another 15 years until initially Kenneth Kwong (Kwong et al., 1992) and then after him also Peter Bandettini (Bandettini et al., 1992) and Seiji Ogawa (Ogawa et al., 1992) published the first human functional images created using the BOLD effect. 2 years before that, in 1990, Ogawa (Ogawa et al., 1990) had already demonstrated that brain microvasculature in cats interacts with T2* signal intensity. Keith Thulborn and co-workers paved the way for these findings in the early 1980s showing that hemoglobin carries distinct MRI signals as a function of its oxygenation state (Thulborn et al., 1982).

However, the relationship between local neural activity and subsequent changes in cerebral blood flow, i.e. neurovascular coupling, has been at least roughly known since the late 19th century (Roy and Sherrington, 1890; James, 1890). Crucial for Ogawa's and Kwong's breakthrough was Linus Pauling's discovery that oxy- and deoxyhemoglobin differ in magnetic susceptibility (Pauling and Coryell, 1936). Based on this finding, it could be assumed that oxygen concentration changes in a brain area have an impact on the MR signal. Another important milestone was reached in the early 1940s when Kety & Schmidt were the first to confirm that cerebral blood flow is regulated by the brain itself. They observed that when oxygen consumption increases, neurons emit biochemical signals causing surrounding blood vessels to dilate (Kety and Schmidt, 1945; Kety and Schmidt, 1948).

The BOLD contrast is the key effect utilized for functional MRI of cerebral neural activity. It foots on the assumption that activated brain tissue shows an increased cerebral metabolic rate (CMRO2) as well as an increased regional cerebral blood flow (rCBF) and local cerebral blood volume (lCBV) in its surrounding cerebrovascular bed (Logothetis et al., 2001; Arthurs and Boniface, 2002) (**Figure 3.10.**). As a consequence, activated brain tissue undergoes an increased delivery of oxygenated hemoglobin as opposed to less-activated brain tissue thereby changing its magnetic susceptibility, i.e. its degree of magnetization in response to the external magnetic fields. Hemoglobin molecules in red blood cells (erythrocytes) are iron-ions-containing ($Fe^{2+}$) metalloproteins binding up to 4 oxygen ($O_2$) molecules from the pulmonary alveoli to release it into the nerve cells and to collect carbon dioxide ($CO_2$) resulting from converting biochemical energy from nutrients into adenosine triphosphate (ATP) in the course of a complex redox reaction. The more oxygen molecules are bound in hemoglobin, the stronger they shield the ferromagnetic properties of the iron ions making oxygenated hemoglobin diamagnetic, i.e. practically

non-magnetic. The opposite effect occurs in deoxygenated hemoglobin which makes it paramagnetic, i.e. magnetic. Now given that paramagnetic deoxygenated hemoglobin induces a local magnetic field gradient, i.e. magnetic field inhomogeneities, around blood vessels and given that its concentration drops in activated brain tissue, the strength of this gradient decreases. As a consequence, the spinning protons in each excited slice dephase more slowly and hence the T2*-weighted imaging signal intensity increases. This effect is most pronounced in the venous capillaries, venules, and surrounding brain parenchyma. Recently, also glucose, ATP and aerobic glycolysis have been found to contribute to the actual MR signal (Raichle and Mintun, 2006) whereas changes in lCBV per se do not.

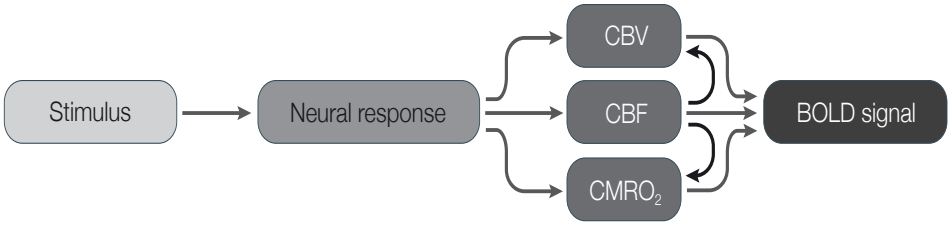


**Figure 3.10.** The three constitutive components of the BOLD signal. Neural activity influences cerebral blood volume (CBV), cerebral blood flow (CBF) and cerebral blood oxygen consumption ($CMRO_2$) in surrounding blood vessels and finally causes an increased delivery of diamagnetic oxygenated hemoglobin. (Figure adapted from D'Esposito et al., 2003.)

The temporal dynamics of the BOLD effect are characterized by the so-called hemodynamic response function (HRF) (**Figure 3.11.**). Initially, the MR signal goes below baseline very shortly immediately after stimulus onset because the cerebrovascular response to activity in a neuronal population is delayed by a couple of seconds. After this so-called "initial dip", typically around 1-3 seconds after stimulus onset, the signal begins to rise (Malonek and Grinvald, 1996). During this "overshoot" phase it reaches its peak normally after 4-6 seconds in adults and usually about 2 seconds later in children depending on the region of

interest (Brauer et al., 2008). If the stimulation continues, the BOLD signal remains at a local overshoot plateau slightly below peak. As soon as the stimulation stops, the signal decreases and finally falls below baseline again. This signal suppression after stimulation is called the "post-stimulus undershoot" (Bandettini et al., 1997).

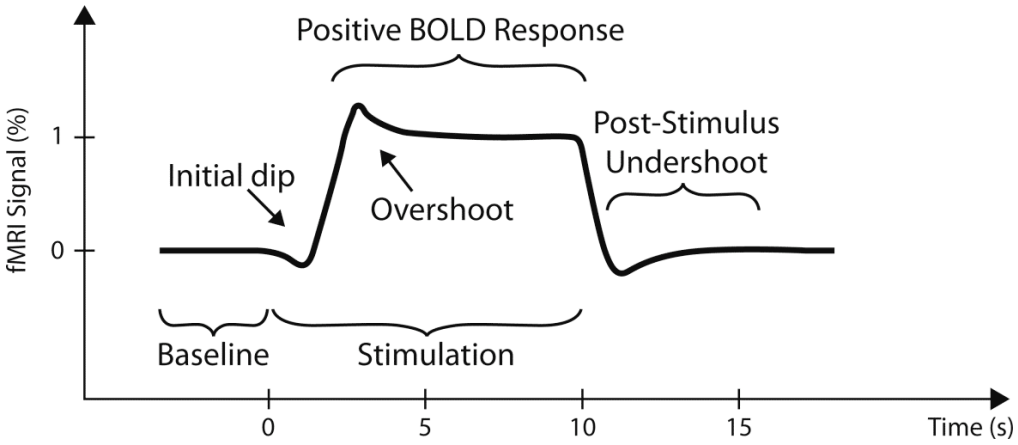


**Figure 3.11.** The hemodynamic response function. After stimulus onset, the fMRI signal shortly falls slightly below baseline, then overshoots and keeps at a plateau level. As soon as the stimulation stops, the signal transiently drops below baseline and then realigns to it.

At first sight, the BOLD response seems to be linear (D'Esposito et al., 2003). However, several non-linear characteristics were discovered in the course of fMRI research. One of the most important observations was that rCBF and lCBV transients underlie different temporal dynamics. Accordingly, several models were proposed in order to take this problem into account.

The oxygen limitation model (Buxton and Frank, 1997) is based on the central assumptions that increased rCBF is coupled to increased capillary blood velocity and not to the more extensive recruitment of capillaries, i.e. higher lCBV, and that all of the oxygen leaving the brain capillaries is completely metabo-

lized by the surrounding brain tissue. The main observation supporting these assumptions was that increased rCBF shortens capillary transit time and hence that less oxygen can be extracted by the bordering brain tissue. Now given that the oxygen delivery rate is defined by the product of rCBF and oxygen extraction fraction, rCBF has to increase much more than the actual oxygen metabolic rate in order to ensure higher delivery of oxygen to the brain.
In order to provide a more comprehensive account of the interrelations between rCBF, lCBV, CMRO2 and the BOLD response, Buxton and colleagues also established the so-called balloon model (Buxton et al., 1998). In this model, the cerebral blood vessels are modeled as a balloon with a blood inflow rate $F_{in}$ and a blood outflow rate $F_{out}$. While during resting state it is assumed that $F_{in} = F_{out}$, the balloon inflates when $F_{in} > F_{out}$ and deflates when $F_{in} < F_{out}$. An inflow rate $F_{in}(t)$ forms the driving function of the system and the outflow rate is a function of the balloon's volume $F_{out}$ (v). Whenever the balloon expands its internal pressure rises and hence the outflow rate increases (Buxton, 2009).

***Diffusion-weighted imaging***

When obtaining spatial information from the MR signal as described above, one assumes that all hydrogen protons remain at a constant location within a probe. In practice, however, spins constantly move. Accordingly, in order not to violate the stationarity hypothesis, a motion correction technique, which will be explained the section 'motion correction', has to be applied to the MR data before analyzing them. Nevertheless, residual motion remains and limits the spatial resolution of MR imaging to around 10µm.

Brownian motion – one of the main intrinsic factors for the constant movement of hydrogen protons – is the source for another import MR imaging technique: diffusion-weighted imaging (DWI). Note that Brownian motion refers to the very

general property of thermally driven, theoretically random mobility of particles. In the case of the brain it is mainly water diffusing based on a diffusion constant D (Stejskal and Tanner, 1965) driven by body heat. Here, motion of water molecules is not absolutely random and equal in all directions (isotropic) but constrained by tissue properties and hence to a certain degree directed (anisotropic). The most important neuroanatomical structure showing a characteristic anisotropic water diffusion is the white matter of the brain as it is shows pronounced alignment. Accordingly, DWI has proven to be especially useful for imaging the macroanatomy of white matter fiber tracts. It gives a better representation of in vivo white matter anatomy than other MR imaging contrasts and also provides a clear progress compared to conventional histological studies on the postmortem brain. The first application of DWI to the human brain was reported in 1986 by Le Bihan and colleagues (Le Bihan et al., 1986).

DWI is based on the same principles as MRI in general. The special feature of DWI is that intra-voxel incoherent motion is used to create the actual image contrasts. Therefore the gradient field is applied in the direction of a predetermined diffusion axis of interest. Now the spins that move along this axis change their precession frequency and hence the rephasing pulse is no longer equivalent to the original phasing pulse. Accordingly, spins showing large diffusion and thus strong dephasing induce a weak signal whereas areas which show less extensive diffusion and are thus less dephased induce a stronger signal (**Figure 3.12.**). The strength of the actual contrast depends on the apparent diffusion coefficient (ADC) of the tissue on the one hand, and on the strength, the duration and the TR of the gradient field on the other hand (Mori, 2007).

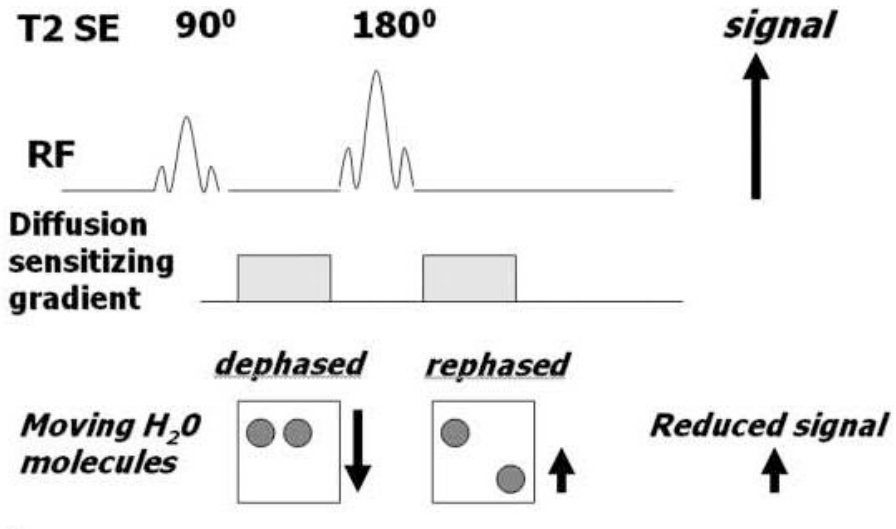


**Figure 3.12.** The basics of diffusion-weighted imaging. Prior to the radiofrequency (RF) pulse, a dephasing gradient field, i.e. a diffusion-sensitizing gradient, is applied to the water molecules causing phase shifts. As water molecules move through nerve fibers, the refocusing pulse applied subsequently to the RF pulse induces a second gradient field, which does not completely rephase them with the first gradient field. Accordingly, the more dephased the water molecules are, the more they reduce the strength of the MR signal. (Figure adapted from Qayyum, 2009.)

### *Diffusion tensor imaging*

DWI is limited to isotropic diffusion because diffusion can only be measured along the axis of the applied gradient. In order to capture also anisotropic diffusion in other directions, Basser and co-workers (Basser et al., 1994a; Basser et al., 1994b) modeled molecular movement on the basis of a so-called tensor, i.e. a symmetric matrix comprising at least 3 eigenvectors with 3 eigenvalues. Accordingly, the technique was called diffusion tensor imaging (DTI). In DTI, a diffusion tensor, quantifying direction and distance of the molecular motion in three spatial dimensions, is calculated for each voxel. The longest eigenvector within the diffusion tensor codes the direction of the strongest diffusion where-

as the shortest eigenvector within the diffusion tensor codes the direction of the weakest diffusion. Accordingly, diffusion tensors in more isotropic media are spherical whereas diffusion tensors in more isotropic media like white matter rather have an ellipsoid shape as motion perpendicular to the fiber directions is limited by tissue barriers like myelin. All directionality and distance values are converted into scalar indices ranging from 0 (isotropy) to 1 (anisotropy). These so-called fractional anisotropy values finally reveal a ratio between anisotropic and isotropic diffusion tensor components (Moritani et al., 2009).

## 3.3. Data analysis

### 3.3.1. Behavioral data statistics

Behavioral measurements were taken only in the functional imaging study to be presented in chapter 4.1., in which both the child participants as well as the adult control participants had to perform a picture selection task. Response correctness as well as reaction times were recorded based on response button presses to measure the participants' performance. Response correctness was evaluated including only trials in which a response was given. Trials in which a participant missed to give a response were not considered because it was not possible to clearly determine what the actual source of theses misses was. Reaction time was taken in milliseconds and averaged to get the mean reaction time. Only correct reaction times were analyzed. Basic descriptive measures (means, standard deviation, standard error) were calculated in order to obtain a first overview of differences in performance within the samples.

Before any inferential statistics were used, we checked whether the data fulfilled the conditions for the application parametric tests. As this was the case, repeated-measures analyses of variance (ANOVA) were calculated for statisti-

cal evaluation of the results. Bonferroni correction was applied whenever it was necessary. For post-hoc analyses, we also used two-sided paired t-tests and a Fisher's exact test. How all these statistical approaches were concretely applied to the behavioral data, is explained in detail in the chapters 4.1.2. and 4.1.3.

### 3.3.2. Functional magnetic resonance imaging data statistics

#### *Raw data preprocessing*

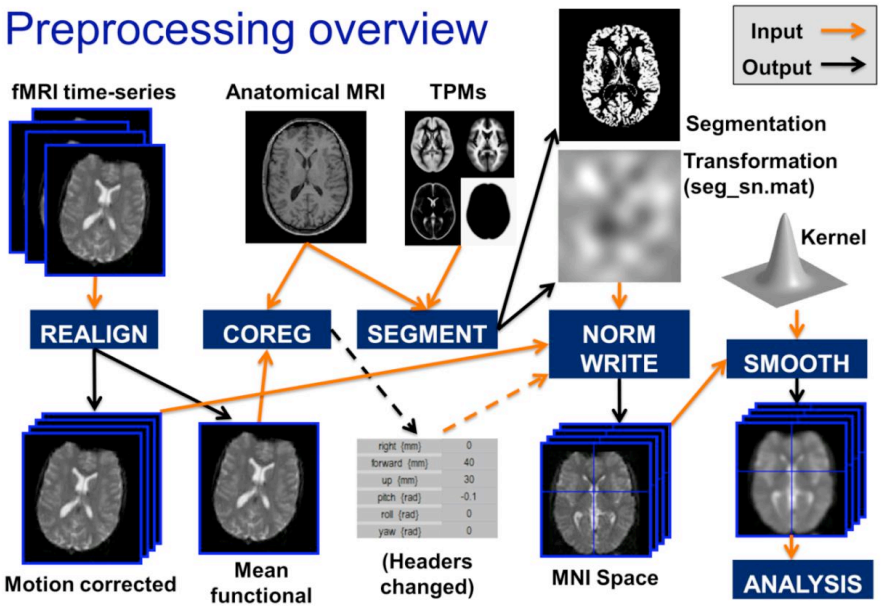


**Figure 3.13.** Preprocessing of fMRI data. The raw functional images undergo motion correction (including realignment to their original position), coregistration with the corresponding high-resolution anatomical images, slice timing correction (not shown in the picture), normalization on a standard brain template (comprising the segmentation and transformation of distinct types of tissue) and spatial smoothing with a Gaussian kernel as well as temporal smoothing (not shown in the picture). All preprocessing steps are explained in the main text. (Figure adapted from http://www.fil.ion.ucl.ac.uk/spm/course/slides12-zurich/.)

To maximize the validity of statistical analyses applied to raw data sets acquired in the MR scanner, these data sets undergo a series of preprocessing procedures before being statistically assessed. The preprocessing steps explained in the following sections are motion correction, slice timing correction, registration, normalization and smoothing (**Figure 3.13.**). These procedures are introduced in detail because they crucially influence the later data analysis.

***Motion correction***

When statistically analyzing MR data, one assumes that each volumetric picture element (voxel) of brain tissue acquired in the course of the imaging procedure remains exactly at a certain fixed position constantly over the whole acquisition period (Brown and Semelka, 2010). Human participants, however, are no perfectly static probes. Sources of the participant's head movements are generally involuntary muscle contractions occurring for example during breathing (Paling and Brookeman, 1986), pulsation (Weisskoff et al., 1993) and fasciculation but also voluntary muscle contractions due to certain events (Birn et al., 1998; Birn et al., 1999) or – what it is not the case in present study – task demands. Whenever head movement occurs, each voxel's time series is derived from more than one coordinate in the brain so that the static probe premise is violated and data are confounded or at least less sensitive (Yetkin et al., 1996). Especially in young child populations excessive head movement occurs much more frequently than in adult populations. Data quality can be severely reduced sometimes to the point of complete data loss. Furthermore, as head movement causes signal changes in a voxel, it can happen that this signal change cannot be differentiated from task driven brain signal changes anymore if both are correlated with each other (Hajnal et al., 1994; Thacker et al., 1999).

Motion prevention is an important factor for ensuring good data quality. Motion prevention firstly comprises constraining the test participant's head and ensuring the person's comfort while lying on the table. Secondly, the participant should be instructed to remain as still as possible during the whole experiment, not to talk, not to adjust head and to swallow as rarely as possible. Thirdly, head motion can be prevented by designing an experiment in that way that the scanning length can be maximally reduced. Fourthly, a training session in a mock scanner can help participants getting used to hold the head still in the MR scanner.

As motion prevention of course cannot completely exclude motion and as hence the data acquired may contain motion-related artifacts, post-hoc motion correction is needed in order to correct for misalignment of MRI data. Therefore, every single image acquired undergoes realignment to be transferred into a coherent geometric space. Realignment involves two stages: registration and transformation. Registration comprises an estimation of 6 motion parameters describing the rigid body transformation between each image and a reference image. The 6 motion parameters consist of 3 translational and 3 rotational vectors in which translation is defined as motion along the x-,y- and z-coordinate axes and rotation as pitch about the x-axis, roll about the y-axis and yaw about the z-axis. Once the whole series of images is registered, each image can be transformed, i.e. it can be resampled according to the transformation parameters determined during its registration so that it exactly matches the reference image's grid of voxels. In the study to be presented in section 4.1., a B-Spline Interpolation algorithm was used to achieve that (Friston et al., 1994).

Still after realignment movement occurs between and within slice acquisition. Furthermore, interpolation can create artifacts due to resampling. Also non-linear distortions and even complete drop-out appear from time to time due to

inhomogeneity of the magnetic field caused by tissue composition differences across the brain. The effect is that image distortions vary with movement. That means that the rigid body transformation assumption made in conjunction with realignment is not strictly followed anymore. To correct for that, images have to undergo unwarping which is a post-hoc method to estimate these changes in distortion. Unwarping helps to reduce the amount of variance in the data that can be accounted for by effects of movement (Andersson et al., 2001).

### *Slice timing correction*

An image of the whole brain is not acquired as once, but slice-by-slice. For example, in the experiment to be discussed in chapter 4.1. slices were collected in an interleaved fashion. That means slices 1, 3, 5 ... 25 were collected first and after that slices 2, 4, 6 ... 26. Moreover, during MR scanning brain volumes are not acquired simultaneously, but serially. Every single voxel of a slice within a volume is collected with a certain temporal delay throughout a specified TR. When evaluating BOLD signals statistically, however, one implies that these signals originate from one and the same point in time in all collected volumes. To achieve this coherent temporal representation of functional signals, each voxel activation value must be virtually returned to a fixed reference time. Exactly this is how slice timing correction works. A voxel's time course is examined, then phase shifted via Fourier transformation and finally a cubic-spline-interpolation algorithm is applied to get back the time course as it would have turned out to be if every voxel would have been sampled at the very same time (Dale and Buckner, 1997).

### *Functional-structural coregistration*

Functional images acquired during MR scanning are of low resolution and of little anatomical contrast. As there is a special interest in a precise neuroanatomical localization of brain activations it is necessary to map functional images onto structural images of high-resolution and high-contrast. Exactly this is achieved by applying a coregistration algorithm linking functional T2* EPI 2D images to T1 MP-RAGE 3D images for each participant. This algorithm bases on the same principles as realignment during slice-timing correction described in section 3.3.2.1.1. above. 6 motion parameters are estimated to compute a transformation matrix that can be applied to the functional T2* EPI 2D images as well as to the T1 MP-RAGE 3D images.

### *Spatial normalization*

As each human brain is individual, there are remarkable differences regarding weight, volume and morphology such as shape and organization of gyri and sulci. In order to compute powerful 2nd level group statistics across all participants, however, all individual datasets must be converged into a common anatomical reference space. This is again achieved by employing a transformation matrix to virtually compensate volume and morphology differences between the functional data set of each participant and a standard brain image template. For the purposes of the investigations to be discussed in the present work, the Montreal Neurological Institute space (MNI space) has been used as a probabilistic reference space. Its coordinates are derived from an average of more than one hundred individual structural MR images (Fonov et al., 2011). The 2nd very common and traditional reference space for normalization found in the neuroscience literature is the Talairach space. Although still widely in use,

it is questioned how representative it can be for a whole population as it foots on measurements from just one dissected post-mortem brain.

***Temporal smoothing***

Three types of temporal filters are used to obtain temporally smoothed MR data. These are high-pass filters, low-pass filters and band-pass filters. Voxel time series of fMRI data often show low-frequency drifts. These drifts may be caused by physiological noise such as respiration but also by physical, i.e. scanner-induced system noise such as inhomogeneities of the static field due to imperfect shimming or instabilities in the gradient fields. If not taken into account, low-frequency drifts severely reduce the power of statistical data analysis. They also invalidate event-related averaging, which assumes stationary time courses, i.e. time courses with a constant signal level. Since the signal drifts are slowly rising and falling, they are removed by using a high-pass filter of a certain cut-off frequency. This filter lets high frequencies representing stimulus-related activity pass, but removes low frequencies, i.e. the signal drifts. However, low-pass filtering may bring along the risk of removing task-related signal of interest variation. This may happen if the filter is not properly adjusted to the maximum of every stimulus condition's frequency. By the way, this frequency is sampled at twice the rate of any stimulation according to the Nyquist frequency limitation implying that the maximum frequency that can be identified equals one half of the actual sampling rate (Friston et al., 2000).

A low-pass filter leaves low frequencies intact while attenuating high frequency noise. It has not been applied in the study that is reported in chapter 4.1., as this study bases on an event-related experimental design. In these designs stimulus presentation and respiration can occur at similar frequencies which would substantially complicate filtering.

Of course, low-pass and high-pass filters can also be combined. This is called band-pass-filtering, if low- as well as high frequencies are filtered out as soon as they reach two predefined cut-off frequency values. The other possibility is to attenuate only a specified range of frequencies lying within an interval limited by a lower and an upper cut-off frequency value. This is called band-stop-filtering.

***Spatial smoothing***

Spatial smoothing means applying a low-pass filter to the acquired images in order to remove high frequencies of the signal from the data while enhancing low frequencies. This works that way that voxel values are averaged with surrounding voxel values. The size of the voxel clusters to be smoothed depends on the size of the used kernel. As standard practice in neuroscience, a Gaussian kernel is applied. That means that the fMRI signal is convolved with a Gaussian function (Friston et al., 1994). The width of the Gaussian "bell curve", specified by its full width at half maximum (FWHM), determines how many voxels are smoothed. This procedure improves the signal-to-noise ratio (SNR) and better pronounces spatial correlation within the data, but also reduces image resolution and may introduce false-positive or false-negative activations, so that a balance must be found. A FWHM of 4mm has proven most appropriate for the fMRI experiment described in chapter 4.1.

***1st and 2nd level statistical analysis***

After preprocessing the functional images, they were statistically assessed on the first-level using the Statistical Parametric Mapping (SPM) (Friston, 2007) approach implemented in the SPM8 software. Within this univariate framework, all single voxel time series are passed to a general linear model (GLM), con-

cretely a regression model of the form y = xβ+ε where *y* is the voxel's hemodynamic (BOLD) response function (i.e. the response variable), *x* is a regressor (in our case a certain stimulus condition) represented as a column vector in a design matrix, *β* is the beta value (parameter) quantifying the contribution of the stimulus condition *x* to the explanation of *y* and *ε* is the error term accounting for noise fluctuations. When all parameters are estimated, the data are decomposed into the actual BOLD effects and errors for each voxel. As a next step, the parameter estimates can be passed to *t* tests in order to create condition-wise *t* maps and *z* maps, respectively. However, as the GLM is applied to a large number of voxels (mostly more than 100 000), the data have to be thresholded in order to correct for multiple comparisons. SPM8 includes cluster-level thresholding based on the Gaussian Random Field Theory identifying both improbably high and improbably broad activation peaks. Finally, the corrected *t* maps are subtracted from each other in order to directly compare experimental conditions.

At the second level, inferences about parameter estimates and accordingly about the impact of certain regressors can be made employing statistical models which best fit the specific experimental design and the samples under investigation. The actual 2nd level models applied in our fMRI experiment are explained in chapter 4.1.2.

SPM8 has become the standard for the analysis of fMRI data. However, there are several other general linear model based software packages (Cox, 1996; Lohmann et al., 2001; Smith et al., 2004). Furthermore, there are also model-free approaches (Rombouts et al., 2009).

### 3.3.3. Diffusion tensor imaging data statistics

The preprocessing of Diffusion MRI raw data comprises motion correction and registration procedures I do not explain in detail because they follow similar principles like the corresponding fMRI preprocessing procedures described in chapter 3.3.2. In the next crucial step, a diffusion tensor model has to be fitted on the motion corrected and registered diffusion images before fractional anisotropy maps can be created for each participant. I have already introduced these concepts in chapter 3.2. 'Diffusion Tensor Imaging'. For group-level statistics, the single-subject fractional anisotropy maps have to be normalized (see 3.3.2.). For this purpose, we derived template maps from each of our 4 samples separately in order to identify the most representative one within each group. This was done by registering all FA maps onto each other in order to detect the map which required minimal warping for registering the remaining images on it. Alternatively, this can also be done by using a standard brain template. As a result of warping all FA maps onto the most typical FA map, we obtained deformation fields which we then applied to the single-subject FA maps. The resulting normalized single-subject FA maps were finally averaged and thresholded in order to create group-mean FA maps. Based on these group-mean FA maps, we used specific fMRI activation clusters as starting points for probabilistic tracking in order to isolate fiber tracts relevant for syntax and semantics. Additionally, we extracted FA values corresponding to the identified group tracts from single-subject FA maps. These analyses are explained in more detail in chapter 4.2.2. of this thesis.

# 4. INVESTIGATIONS

Two contiguous studies, which have been in the main focus of the dissertation work, are reported in the present chapter. In section 4.1., I describe an event-related fMRI experiment, in which we investigated the development of cortical areas supporting syntactic and semantic processing in auditory sentence comprehension. In the subsequent section 4.2., I report a DTI experiment, in which we examine how the functional organization of white matter fiber tract connections between the previously identified frontal and temporal language regions changes in the maturing brain.

## 4.1. Functional neural segregation of syntactic and semantic processing from 3 years of age to young adulthood

### 4.1.1. Introduction

Although there is a tight functional interrelation between syntax and semantics, both language functions are represented in clearly segregated neural networks in the adult brain (Bookheimer, 2002; Newman et al., 2010; Friederici, 2011), with the pars opercularis of the left inferior frontal gyrus (left IFGoper) supporting complex syntactic processes and the pars triangularis of the left inferior frontal gyrus (left IFGtri), as well as the pars orbitalis of the left inferior frontal gyrus (left IFGorb), subserving higher-level semantic processes.

There is, however, indirect evidence that these underlying neural networks are not fully specialized in children. Rather, the few studies available report overlapping activation for processing syntactic and semantic information, even in late primary school age children (Brauer and Friederici, 2007; Nunez et al.,

2011). When tested behaviorally on-line, children up to the age of 11 years old show an interaction of syntactic and semantic processes, whereas adults demonstrate a clear independence of these two processing components (Friederici, 1983). With respect to the underlying brain structures, it has been found that the leftward asymmetry of the IFGoper and the IFGtri observed in adults only develops later in childhood, with the asymmetry of the IFGtri emerging around the age of 5 years, and that of the IFGoper emerging around the age of 11 years (Amunts et al., 2003). These neuroanatomical data suggest a late specialization of the cortex supporting syntactic processes. The developmental trajectories of the functional neuroanatomy of syntax and semantics in the course of language acquisition, however, are poorly studied and far from being understood.

In the present event-related fMRI study, we used a cross-sectional design to investigate whether children of 3 to 4 years of age, 6 to 7 years of age and 9 to 10 years of age do, or do not, already show an adult-like segregation of activation patterns for syntactic and semantic processes, or whether the behaviorally observed interdependence of syntactic and semantic information is reflected at the neural level.

One major experimental challenge was the requirement for an extremely flexible paradigm, applicable to samples of very heterogeneous cognitive maturity. Numerous test versions of the behavioral experiment had to be piloted, especially in the youngest age range, until we achieved an optimal operationalization.

We selected relative clauses to provide the basis for analyzing syntactic complexity across the target age range, for two principal reasons. Firstly, based on the literature (Kidd et al., 2007) and on our own pilot studies on 3- to 4-year-old children, we reasoned that even our youngest participants should be able to

master at least a simple canonical version of these syntactic structures. Secondly, it is feasible to control relative clauses for all of the possible confounding variables (see 4.1.2.). Here, we profited from the fact that both the acquisition of relative clauses and their processing in adults are well-studied within psycholinguistic frameworks (Kidd, 2011; Fedorenko et al., 2012). In order to achieve different levels of syntactic complexity, we contrasted canonical subject relative clauses (SR: "Where is the [subject], who [verb] the [object]?") with more difficult non-canonical object relative clauses (OR: "Where is the [object], who the [subject] [verb]?"). Using interrogative sentences in a picture selection task, enabled us to increase the interactivity of the experimental setting, and hence the motivational attractiveness of the stimulus material for young participants.

The starting point of our considerations in operationalizing semantic processing was that 3- to 4-year-old children are familiar with natural sizes of animals, which are among the first things they develop a prototype-semantic concept of (Rosch, 1975). Crucially, our pilot studies showed that children of this age are, furthermore, able to derive plausibility constraints for certain simple actions ("carry", "catch", "chase", "pull", "push", "throw") dependent on world knowledge about the natural sizes of the animals involved. Accordingly, it seemed plausible to the children that a tall animal could act out these actions on a small animal. So, we used 6 "tall" animals ("bear", "dog", "fox", "lion", "tiger", "wolf") prototypically taller than 6 "small" animals ("monkey", "beetle", "bird", "frog", "hedgehog", "rabbit") for our stimulus material. A semantically plausible proposition was established if one of the 6 tall animals ("the big A") was the agent performing one of the 6 possible actions on one of the 6 small animals ("the small B"), which was the patient undergoing this action. An inversion of this argument structure resulted in a semantically implausible proposi-

tion. See 4.1.2. for a comprehensive report on participants, stimulus material and experimental procedure.

| **Semantic Plausibility** (high → low) | **Example sentences** | **Syntactic Complexity** (low → high) |
|---|---|---|
| Plausible Proposition | Wo ist **der große** Fuchs, **der den kleinen** Käfer trägt?<br>Where is **the big** fox, [**who**]$_{NOM}$ [**the**]$_{ACC}$ **small** beetle carries?<br>Where is the big fox, who carries the small beetle? | Subject Relative Clauses |
| Implausible Proposition | Wo ist **der kleine** Käfer, **der den großen** Fuchs trägt?<br>Where is **the small** beetle, [**who**]$_{NOM}$ [**the**]$_{ACC}$ **big** fox carries?<br>Where is the small beetle, who carries the big fox? | Subject Relative Clauses |
| Plausible Proposition | Wo ist **der kleine** Käfer, **den der große** Fuchs trägt?<br>Where is **the small** beetle, [**who**]$_{ACC}$ [**the**]$_{NOM}$ **big** fox carries?<br>Where is the small beetle, who the big fox carries? | Object Relative Clauses |
| Implausible Proposition | Wo ist **der große** Fuchs, **den der kleine** Käfer trägt?<br>Where is the **big fox,** [**who**]$_{ACC}$ [**the**]$_{NOM}$ **small** beetle carries?<br>Where is the big fox, who the small beetle carries? | Object Relative Clauses |

**Table 4.1.** The 2x2 factorial design. Illustrated are example sentences the participants listened to while a corresponding picture set (**Figure 4.1.**) was presented simultaneously during the sentence-picture matching task.

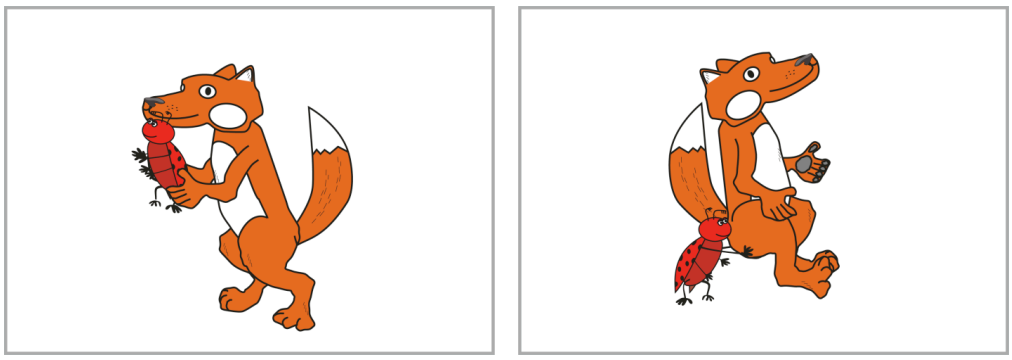

**Figure 4.1.** Example picture set used in the picture selection task. Participants had to select one out of two pictures showing the agent-patient-scheme (who does what to whom) matching the argument structure of the corresponding sentence.

This pioneering paradigm (**Table 4.1.**, **Figure 4.1.**) has allowed us to shed first light on the effects of semantic plausibility during language development. To the best of our knowledge, there is no other language acquisition literature available at present, which addresses this topic. Our work provides first insights on how brain-functional language development progresses after infancy (Sakai, 2005; Dehaene-Lambertz et al., 2006; Kuhl, 2010).

For adults, we expected that fMRI activation for syntactic and semantic processes would occur in segregated brain regions, with the factor syntactic complexity, in particular, being located in the left IFGoper, and the posterior portion of the left superior temporal gyrus (left pSTG) and sulcus (left pSTS) (Newman et al., 2010; Friederici, 2011). Accordingly, we hypothesized that semantic implausibility would lead to increased activation in the left IFGtri and the left IFGorb. Moreover, we hypothesized that, for children, the brain activation patterns for syntactic and semantic features would be less segregated.

### 4.1.2. Methods

#### *Participants*

89 children (age 3y 9m to 4y11m, *n*=40; age 6y 7m to 7y 11m, *n*=20; age 9y 7m to 10y 11m, *n*=29) were recruited on a voluntary basis from kindergartens and primary schools in Leipzig. During an informative briefing about the study, parents gave written informed consent and children gave verbal assent to participate in the study. All experimental procedures were approved by the University of Leipzig Ethical Review Board.

All children underwent a training session in a mock scanner to familiarize them with the experimental procedure. Thereby, they practiced the task with stimuli similar to but not identical to those used for the actual fMRI experiment. In order to reduce head motion, children were equipped with a motion sensor fixed to their forehead in the training session, and the presentation stopped every time too much movement occurred. To further reinforce this feedback, motivating verbal advice to lie still was also given. If a child fulfilled the motivational and cognitive preconditions to take part in the fMRI study, handedness (Edinburgh Handedness Inventory) (Oldfield, 1971), intelligence (Kaufman ABC Sequential Processing Scale) (Melchers and Preuss, 2009) and language comprehension skills (German version of the Test for Reception of Grammar TROG-D) (Fox, 2011) were assessed. Additionally, parents completed a questionnaire to ensure their children had neither a history of neurological or neurologically relevant diseases, nor psychiatric disorders. 83 children (age 3y 9m to 4y11m, *n*=35; 6y 7m to 7y 11m, *n*=20; age 9y 7m to 10y 11m, *n*=28) received a positive evaluation (handedness laterality quotient ≥+60, KABC and TROG-D test results within normal range as well as no history of relevant diseases) and were invited for fMRI scanning.

20 participants had to be excluded from data analysis because fMRI data could not be collected or could not be analyzed because of too much movement during scanning. 3 more datasets were discarded because spikes occurred on several images. Datasets from a total of 60 children (age 3y 9m to 4y11m, *n*=20, 12 female, mean age 4y 4m; age 6y 7m to 7y 11m, *n*=20, 11 female, mean age 7y 5m; and age 9y 7m to 10y 11m, *n*=20, 8 female, mean age 10y 3m) were considered for the final fMRI analysis.

Furthermore, 26 adult participants were recruited from the University of Leipzig community, who were all right-handed, had normal intelligence and language skills and no history of relevant diseases. All gave written informed consent to participate on a voluntary basis. 2 datasets which revealed movement artifacts and 2 further datasets containing spikes had to be excluded. 2 more datasets were not included in the actual analysis because the participants showed outlying behavioral data. A total of 20 adult datasets (7 female, age 21y 8m to 33y 6m, mean age 26y 5m) were analyzed.

***Behavioral data acquisition***

While lying in the scanner, participants listened to interrogative sentences (duration range: 3.571 s to 3.999 s, mean duration: 3.81 s ) via MR compatible headphones (VisuaStim XGA, Resonance Technology Inc.) and watched 2 parallel pictures of equal size through an MR compatible eyeglass display (VisuaStim XGA, Resonance Technology Inc.). When auditory stimulation was over, but the visual stimulus was still present, they performed a picture selection task in which they were given a maximum response time of 2.5 s to decide, via button press, which picture showed the correct agent-patient (who does what to whom) scheme. Button presses were recorded with Presentation (http://www.neurobs.com). Sentences were spoken by a professional female

native speaker in a unisonous and moderately child-directed prosody, and recorded at a sampling rate of 44,100 Hz (Stereo). For the purpose of the experimental presentation, the recordings were downsampled to 22,050 Hz (Mono), their intensities were normalized, and fade-ins as well as fade-outs of 50 ms (silence) were added to them using Praat (http://www.fon.hum.uva.nl/praat/). Pictures were designed with Adobe Illustrator (Adobe Systems Inc.). Participants were instructed to attentively watch the pictures, to attentively listen to the sentences and to respond as fast as possible, as soon as auditory stimulation was over.

After finishing the experiment, participants were asked if any problems occurred with respect to the stimulation. During this post-hoc interview, participants were also surveyed in order to evaluate if they applied a certain strategy to solve the task ("How did you find out which was the correct picture?"). If participants only reported that they focused on features of the visual scenarios ("I was looking at the animals." or "I was looking at what the animals did." etc.) without referring to linguistic features of the sentences, they were assigned a semantic strategy. If, on the other hand, they reported that they paid attention to certain nouns, verbs and relative pronouns or to case marking and sentence structure, they were assigned a syntactic strategy. Participants describing both aspects were assigned a hybrid strategy.

The whole experiment comprised of 96 target trials (24 trials per condition) and 12 null event trials, with a duration of approximately 8 seconds. Before the onset of the first target trial, a child-friendly oral introduction, together with a picture of a girl, was presented for about 32 s followed by a pause of approximately 2 s (blank screen). After the last trial run, the picture of the girl appeared again and the end of the experiment was announced for around 2 s. Each target trial started with a jitter (blank screen) of variable length (0 s, 0.5 s,

1 s or 1.5 s). Then the picture appeared and with a delay of 0.5 s the sound stimulus was presented. Pictures disappeared as soon as a response button was pressed. The total experiment time was about 15 min.

The trial order was pseudo-randomized for each participant, using a MATLAB (The MathWorks Inc.) script, so that identical factor levels did not occur in more than 4 succeeding trials. Maximum succession of identical conditions was limited to 2 trials. These restrictions were set in order to avoid priming of factor levels and conditions, respectively. Furthermore, randomization was constrained in that a gap of at least 1 trial was established before identical verbs and identical nouns could appear again. This was intended to avoid lexical-semantic priming. Each of the 12 nouns occurred 8 times and each of the 6 verbs 16 times within the whole experiment. Each noun-verb-noun combination appeared exactly 4 times (once per condition) and was not presented elsewhere.

Biases related to any unwanted systematic arrangement of the pictures and their contents were prevented by counterbalancing the position of the correct picture and the position of agent and patient within the picture so that each correct picture was on the left side of the display and each agent was on the left side within a picture in 50% of all trials. Succession of identical between-pictures positions and identical within-pictures positions, respectively, was limited to 4 trials. Jitter durations were pseudo-randomized so that jitters of the same length did not occur in more than 3 successive trials, in order to be able to exclude a timing bias.

Because only the nouns and verbs were the varying elements within the stimulus material, their frequency had to be controlled in order to exclude this as a confounding variable. Nouns had a Mannheim spoken corpora (http://celex.mpi.nl/) frequency ranging from 1 to 45 matches and verbs had a

Mannheim spoken corpora frequency ranging from 5 to 109 matches. To ensure there were no outliers in the material, each noun and each verb was checked for possible frequency effects. This item analysis did not reveal any correlations. None of the items had a systematic influence, either on response accuracy, or on reaction time. Considering the adult psycholinguistic literature cited above, it is unlikely that frequency differences between subject and object relatives in general could have confounded the experiment. From case and corpus studies reported in the psycholinguistic literature on language acquisition it is known that frequency differences between both sentence types are not even present (Brandt et al., 2008). Another variable controlled within a separate item analysis was age of acquisition of nouns and verbs. Parents had to assign a value from 1 (very early acquisition age) to 7 (very late acquisition age) for each lemma used. The results revealed a narrow range from 2.21 to 2.94. Again, no correlation between this variable and the behavioral data was detected. Animacy was controlled by including only animate arguments in each sentence (Bornkessel-Schlesewsky, 2006). Working memory confounds caused by effects of item length were excluded because only very limited differences in numbers of phonemes (range 3-5) and syllables (range 1-2) were allowed for the nouns and verbs, while the rest of the stimulus elements were of constant length. Because no optional syntactic elements (adjunctions) occurred between the arguments and the verb of any sentence, it is very unlikely that the syntactic complexity manipulation implemented by short-distance movement of the object noun phrase, inherent in the object relative clause, introduced a working memory confound.

### *Behavioral data analysis*

Responses, as well as reaction times, were recorded to measure performance of the participants. As a first approach to the data, simple descriptive statistical measures (means, standard deviation, standard error) were computed in order to identify outlying subsamples. Next, in order to ensure applicability of parametric tests, datasets were tested for approximate normality by applying the Kolmogorov-Smirnov test. No significant differences from normal distribution were found in any of the 4 samples.

A 4 (group) x 2 (syntactic complexity) x 2 (semantic implausibility) repeated measures analysis of variance (ANOVA) was then computed in order to draw conclusions from mean accuracy rates and mean reaction times of the samples, on the level of between-group inferential statistics. For post-hoc assessment of within-group effects, this procedure was applied again to each of the 4 samples separately by running isolated 2 (syntactic complexity) x 2 (semantic implausibility) ANOVAs. Results were Bonferroni-corrected at $P < 0.05$ for the 4 comparisons, so that only $P$ values smaller than 0.0125 (0.05 divided by 4) were considered to indicate significant effects. Additionally, in order to explore post-hoc whether there were any further selective response accuracy or reaction time differences between groups, with respect to syntactic complexity and semantic implausibility, we computed two-sided paired *t*-tests on all sample combinations.

Only trials in which a response (correct or incorrect) was given were included into the comparison of response accuracy means. For the assessment of reaction times, only correct answers were modeled. $P$ values are reported exactly to the fourth decimal place and reported as $P < 0.0001$ whenever $P$ exceeded

this cutoff. All statistical analyses reported so far were calculated using IBM SPSS 19 (IBM Corp.).

Processing strategies across age groups were assessed by running a Fisher's exact test on the 4 (group) x 3 (processing strategy) contingency tables which examined the significance of the association between both variables. These computations were carried out with MATLAB (The MathWorks Inc.).

### *fMRI data acquisition*

The experiment was carried out at the Max Planck Institute for Human Cognitive and Brain Sciences in Leipzig on a 3.0-Tesla Siemens TIM Trio (Siemens AG) whole-body magnetic resonance scanner using a 12-radiofrequency-channel head coil. With the goal of investigating brain functional activity on the basis of a scanning protocol sensitive to BOLD contrasts, a T2*-weighted gradient-echo echo-planar imaging (EPI) sequence was applied to 26 slices with TR = 2 s, TE = 30 ms, FOV = 192mm, matrix size = 64 x 64 voxels and voxel size 3 x 3 x 3 mm. In order to correct for geometric distortions in EPI caused by magnetic field inhomogeneity, a field map was obtained for each dataset. For anatomical localization, T1-weighted three-dimensional magnetization-prepared rapid-acquisition gradient echo (MPRAGE) pulse sequences with TR = 1.480 ms, TE = 3.46 ms, TI = 740 ms, FOV = 256 mm, matrix size = 256 x 240 x 192 and voxel size = 1 x 1 x 1.5 mm were acquired.

### *fMRI data analysis*

Functional images were preprocessed using SPM8 (http://www.fil.ion.ucl.ac.uk/spm/software/spm8/). Firstly, a cubic spline interpolation algorithm was applied to the time series of individual slices, to correct for time differences between

slices recorded within the same scan, and to resample them afterwards (slice time correction). Secondly, images were realigned (i.e., spatially registered and transformed) to the first acquired image to correct for movement between scans, and then unwarped to correct for distortions caused by magnetic field inhomogeneities and interpolation artifacts (motion correction). Thirdly, low-resolution functional images of each participant were mapped (i.e., coregistered) onto the corresponding high-resolution T1-weighted structural images and subsequently normalized to age-appropriate Montreal Neurological Institute (MNI) templates (Fonov et al., 2011) (spatial normalization). Finally, data were spatially low-pass filtered using a 4 mm full width half-maximum (FWHM) Gaussian kernel, which proved to be the best tradeoff between a good signal-to-noise ratio and a good resolution. A temporal high-pass filter with a cut-off frequency of 1/120 Hz was applied in order to remove low-frequency drifts within voxel time series (spatial and temporal smoothing). After preprocessing, the data were checked for the impact of residual head motion. 13 datasets corrupted by outlying movement exceeding 3 mm (> 1 voxel width) were discarded as outliers.

For statistical analysis, functional whole-brain data were passed to a general linear model to run a least-squares parameter estimation (regression analysis), as implemented in SPM8. Design matrices were created on the basis of a hemodynamic response function and its derivatives. First-level contrast images were computed for all 4 conditions against the baseline (null events). Only correct trials were modeled in all samples. Realignment parameters were included as regressors into the model. As a second-level approach, a 4 (groups) x 2 (syntactic complexity) x 2 (semantic implausibility) full factorial ANOVA was run on the first-level contrasts, using age and gender as covariates, to detect between group effects. Hereby, activation clusters for the 3 interaction effects, as detected in the between-group analysis, served as masks. Only within-group

main effects for syntactic complexity, located within the group x syntactic complexity interaction mask; within-group main effects for semantic implausibility, located within the group x semantic implausibility interaction mask; and within-group main effects for syntactic complexity x semantic implausibility interaction, located within the group x syntactic complexity x semantic implausibility interaction mask, were considered to be valid effects.

It was necessary to use a single template in order to provide a common space for group comparison. However, the risk of creating artifacts by applying spatial transformations which were too large had to be minimized (Muzik et al., 2000). Normalizing all 4 groups on the MNI 4.5-18.5 atlas proved to be the best solution to this problem. A 4 (group) x 6 (mean values of 3 translational and 3 rotational parameters obtained by spatially normalizing anatomical T1 images of all participants to the MNI 4.5-18.5 template) repeated-measures ANOVA on the spatial transformation data of each participant did not reveal a significant main effect of group ($F_{3,76}$ = 2.07, $P$ = 0.1045).

First-level contrasts, compared to baseline, were then entered into a post-hoc second-level random effects model, based on flexible factorial 2 (syntactic complexity) x 2 (semantic implausibility) ANOVAs, in order to investigate within-group effects of the factors. Effects of interest were syntactic complexity (contrasting the 2 conditions in which object relative clauses occur against those 2 conditions in which subject relative clauses occur), semantic implausibility (contrasting the 2 conditions in which implausible semantic information was provided against those 2 conditions in which plausible semantic information was provided), and the interaction of both factors (contrasting the simple-syntax-plausible-semantics condition and the simple-syntax-plausible-semantics condition with the two remaining conditions). Effects of no interest (i.e., syntactic simplicity and semantic plausibility) were also analyzed, but did

not reveal any significant or informative results. Condition-wise activation differences between groups were explored computing several post-hoc two-tailed paired samples *t*-tests.

In the post-hoc 2 x 2 ANOVA performed on the adult datasets, only effects surviving a conservative family-wise error correction at an alpha level of 0.01 were considered significant. Given that the effects were very robust and broadly distributed across the left IFG, cluster-level thresholding would have made it impossible to disentangle the precise location of the activation peak. However, a more liberal correction for multiple comparisons had to be applied for the post-hoc ANOVAs within the child groups. Possibly due to worse signal-to-noise-ratios, induced by stronger residual movement in child datasets – a repeated-measures ANOVA on the root mean square values of the realignment parameter time series for all groups revealed a significant main effect of group ($F_{3,76}$ = 6.17, $P$ = 0.0065) – restrictive voxel-by-voxel thresholding, like in adult datasets, was inappropriate. Instead, the probability of a false detection was determined by dual thresholding of both type I error and cluster size, running 10 000 iterations of a Monte Carlo Simulation using AFNI AlphaSim (http://afni.nimh.nih.gov/afni). Only clusters extending over more than 11 voxels were considered significant, minimizing the probability of false detection to max. 0.0440 for uncorrected alpha rates of 0.005 given that voxels were smoothed with a 4 mm FWHM kernel. This thresholding procedure was also used for the results of the between-groups 4 x 2 x 2 ANOVA.

Functional regions of interest (ROIs) were investigated using the MarsBaR toolbox (http://marsbar.sourceforge.net/). As both effects of interest were implemented in a 2 x 2 factorial design, liberal sub-threshold effects for the 2 x 3 corresponding orthogonal contrasts qualified as intrinsic functional localizers (Friston et al., 2006). However, the lower limit for sub-threshold activation was

set to $P < 0.1$ (uncorrected for multiple comparisons). Only clusters that showed activations equal to or stronger than this sub-threshold limit were considered in the analysis. Furthermore, only clusters located within one of the 5 brain regions, in which significant whole-brain effects had previously been observed in one of the samples, were assessed. However, this procedure, did not apply to cases where a significant whole-brain level activation cluster was already present in one of these regions. If this was the case, the corresponding whole-brain level activation cluster was used as an exploratory ROI. After having defined and created all relevant ROIs, beta-weights and time courses were extracted from these clusters to compute mean percent signal changes for all conditions in each group. The resulting values for the syntactic complexity and the semantic implausibility contrast were then compared using two-sided paired *t*-tests. Significance values were Bonferroni-corrected, i.e., divided by the number of regions (5) assessed.

### 4.1.3. Results

#### 4.1.3.1. Effects of syntactic complexity on mean response accuracy rates

In order to get a first overview of the behavioral performance across the whole age range, we calculated mean response accuracy rates for all groups and all conditions from the responses given during fMRI scanning (**Figure 4.2.A**). In the adult group, we observed a ceiling effect covering all syntactic complexity levels (99.46% accuracy in SR, 99.17% accuracy in OR). Remarkably, children as young as 3 to 4 years old performed above chance both in the 2 SR conditions (72.08% correct responses) and in the 2 OR conditions (59.33% correct responses). This performance is better than the results reported in the psycholinguistic literature, but in line with the findings of our pilot studies. We assume that our semantic plausibility manipulations acted as world knowledge cues,

easing comprehension and hence increasing overall performance. The 6- to 7-year-old children demonstrated a performance of 92.30% correct responses in trials containing SR and 78.78% correct responses in trials containing OR. In syntactically simple SR conditions the 9- to 10-year-old children gave a correct response in 94.83% of all trials. For the syntactically more complex OR conditions they achieved a response accuracy of 94.54%.

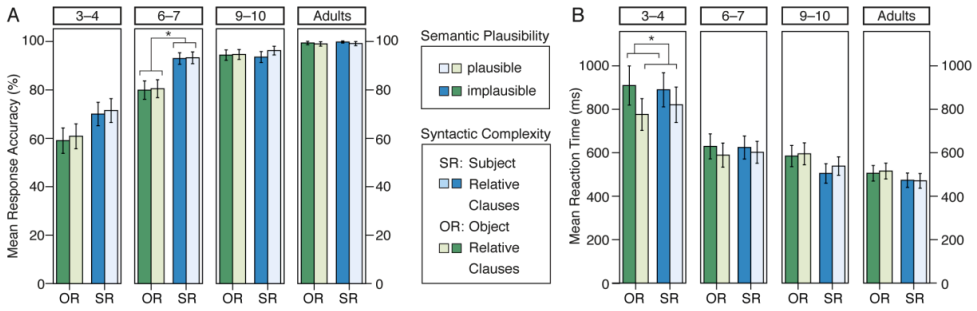


**Figure 4.2.** Behavioral results. (**A**) Mean response correctness (%) for the adult group and the child groups. (**B**) Mean reaction time (ms) for the adult group and the child groups. Asterisks indicate significant main effects. Error bars indicate s.e.m.

As a next step, we explored whether the differences in processing syntactic complexity, as reflected in the reported mean response correctness values, revealed any effects between groups. Therefore, we computed a 4 (group - GROUP) x 2 (syntactic complexity - SYN) x 2 (semantic implausibility - SEM) repeated measures ANOVA on the mean response correctness data. This revealed a significant main effect of GROUP ($F_{3,76}$ = 66.34, $P$ < 0.0001) and of SYN ($F_{3,76}$ = 19.40, $P$ < 0.0001) as well as a GROUP x SYN interaction ($F_{3,76}$ = 4.26, $P$ = 0.0078). We observed neither a significant main effect of SEM ($F_{3,76}$ = 0.63, $P$ = 0.4266), nor a significant GROUP x SEM interaction ($F_{3,76}$ = 0.40, $P$ = 0.7527). Furthermore, there was no significant SYN x SEM interaction ($F_{3,76}$

= 0.98, $P$ = 0.3255) and also no GROUP x SYN x SEM interaction ($F_{3,76}$ = 0.16, $P$ = 0.9209).

Finally, we ran 4 separate 2 (SYN) x 2 (SEM) repeated measures ANOVAs within each group to disentangle post-hoc the extent to which the mean accuracy results of each sample contributed to the GROUP x SYN interaction reported above. We found a significant main effect of SYN after Bonferroni correction for the 4 comparisons (see 4.1.2.) in the 6- to 7-year-old children ($F_{1, 76}$ = 12.76, $P$ = 0.0018) but in neither the 3- to 4-year-old children ($F_{1,76}$ = 4.69, $P$ = 0.0433) nor in the 9- to 10-year-old children ($F_{1,76}$ = 0.03, $P$ = 0.8682) nor in adults ($F_{1,76}$ = 0.46, $P$ = 0.5074). Hence, we reasoned that the GROUP x SYN interaction was mainly driven by the performance of the two youngest child groups, especially the 6- to 7-year-old children.

In order to explore post-hoc whether there were any further selective response accuracy differences between groups with respect to syntactic complexity, we additionally computed two-sided paired *t*-tests, combining all samples with each other. Given that the reported ANOVAs revealed significant results only for syntactic complexity, we did not consider it informative to look into semantic implausibility differences.

The performance of the adults was significantly better compared to all 3 of the child groups, both with respect to simple subject relative clauses (SR; $t_{19}$ = 6.77, $P$ < 0.0001 vs. the 3- to 4-year-old children; $t_{19}$ = 4.13, $P$ = 0.0013 vs. the 6- to 7-year-old children; $t_{19}$ = 2.38, $P$ = 0.0284 vs. the 9- to 10-year-old children) and more complex object relative clauses (OR; $t_{19}$ = 7.83, $P$ < 0.0001 vs. the 3- to 4-year-old children; $t_{19}$ = 4.43, $P$ < 0.0001 vs. the 6- to 7-year-old children; $t_{19}$ = 2.50, $P$ = 0.0224 vs. the 9- to 10-year-old children).
Mean accuracy rates in the 9- to 10-year-old children were significantly better than in both of the two younger child groups when looking at OR ($t_{19}$ = 6.80, $P$

< 0.0001 vs. the 3- to 4-year-old children; $t_{19}$ = 3.50, $P$ = 0.0019 vs. the 6- to 7-year-old children). When looking at SR, however, the accuracy of the 9- to 10-year-old children was better compared to the 3- to 4-year-old children ($t_{19}$ = 4.81, $P$ < 0.0001) but not compared to the 6- to 7-year-old children ($t_{19}$ = 1.08, $P$ = 0.2944). Compared to the 3- to 4-year-old children, the 6- to 7-year-old children demonstrated a significantly better performance both in trials containing SR ($t_{19}$ = 4.73, $P$ < 0.0001) and in trials containing OR ($t_{19}$ = 3.64, $P$ = 0.0021).

In the last stage of our post-hoc analyses we assessed within-group differences of syntactic complexity separately for each sample. In the adults no significant within-group differences occurred between SR and OR ($t_{19}$ = 0.68, $P$ = 0.5071). However, we detected a significant accuracy rate difference between SR and OR in the 3- to 4-year-old children ($t_{19}$ = 2.17, $P$ = 0.0434) and also in the 6- to 7-year-old children ($t_{19}$ = 3.57, $P$ = 0.0022). The 9- to 10-year-old children performed equally high regardless of the syntactic complexity ($t_{19}$ = 0.17, $P$ = 0.8675) within the sentences.

#### 4.1.3.2. Effects of semantic implausibility on mean reaction times

Reaction times provided another measure for the behavioral performance of all 4 age groups. Mean reaction times (**Figure 4.2.B**) in the adults were 494 ms in sentences containing semantically plausible information, and 490 ms in sentences containing semantically implausible information. The 3- to 4-year-old children needed on average 811 ms to give a response when the semantic scenario was plausible and an average of 935 ms when it was implausible. Mean reaction time for plausible semantics was 613 ms, and 641 ms for implausible semantics, in the 6- to 7-year-old children. The 9- to 10-year-old chil-

dren responded after 574 ms on average to semantically plausible sentences and after 558 ms on average to semantically implausible sentences.

We used testing procedures that were analogous to those applied to the mean response correctness data, to investigate if mean reaction time differences for semantic implausibility would also reveal between-group effects. We found a significant main effect of GROUP ($F_{3,76}$ = 12.61, $P$ < 0.0001) and of SEM ($F_{3,76}$ = 5.64, $P$ = 0.02), as well as a significant GROUP x SEM interaction ($F_{3,76}$ = 5.22, $P$ = 0.0023). We could detect neither a significant main effect of SYN ($F_{3,76}$ = 2.36, $P$ = 0.1287), nor a significant GROUP x SYN interaction ($F_{3,76}$ = 0.50, $P$ = 0.6863). Additionally, we did not observe a significant SYN x SEM interaction ($F_{3,76}$ = 0.56, $P$ = 0.4577), or a significant GROUP x SYN x SEM interaction ($F_{3,76}$ = 0.5002, $P$ = 0.6844).

An isolated main effect of SEM occurred exclusively in the 3- to 4-year-old children ($F_{1,76}$ = 8.29, $P$ = 0.0103) but not in the adults ($F_{1,76}$ = 0.73, $P$ = 0.4032), the 6- to 7-year-old ($F_{1,76}$ = 0.98, $P$ = 0.3333) or in the 9- to 10-year-old children ($F_{1,76}$ = 0.63, $P$ = 0.4374), when we calculated 4 separate 2 (SYN) x 2 (SEM) repeated measures ANOVAs. On the basis of the result of this post-hoc test, we reasoned that the 3- to 4-year-old children's reaction time differences in response to semantically plausible and semantically implausible sentences had the main impact on the interaction.

We applied the post-hoc testing procedure described in the last section on the response accuracy data to the mean reaction time data as well, focusing on semantic implausibility differences, given that this was the only factor we found a significant main effect for. When comparing conditions in which sentences were semantically plausible, the adults responded significantly faster than the 3- to 4-year-old children ($t_{19}$ = 3.42, $P$ = 0.0031) but not significantly faster than the 6- to 7-year-old children ($t_{19}$ = 1.99, $P$ = 0.0635) or the 9- to 10-year-old

children ($t_{19}$ = 0.62, $P$ = 0.5454). For semantically implausible sentences, reaction times of the adults were significantly shorter than both the 3- to 4-year-old children ($t_{19}$ = 4.98, $P$ < 0.0001) and the 6- to 7-year-old children ($t_{19}$ = 2.19, $P$ = 0.0422), but not the 9- to 10-year-old children ($t_{19}$ = 1.21, $P$ = 0.2432).
The 3- to 4-year-old children responded significantly slower than the 6- to 7-year-old and the 9- to 10-year-old children when looking at both plausible semantics ($t_{19}$ = 3.78, $P$ = 0.0011 vs. the 6- to 7-year-old children; $t_{19}$ = 3.30, $P$ = 0.0043 vs. the 9- to 10-year-old children), as well as implausible semantics ($t_{19}$ = 5.40, $P$ < 0.0001 vs. the 6- to 7-year-old children; $t_{19}$ = 4.21, $P$ < 0.0001 vs. the 9- to 10-year-old children).

The 6- to 7-year-old and 9- to 10-year-old children differed from each other with respect to neither semantic plausibility ($t_{19}$ = 1.03, $P$ = 0.3141) nor semantic implausibility ($t_{19}$ = 0.89, $P$ = 0.3844). From a within-group perspective, only the 3- to 4-year-old children showed significantly longer reaction times for processing semantically implausible versus semantically plausible sentences ($t_{19}$ = 2.88, $P$ = 0.0102). However, we could not detect any significant differences in the adults ($t_{19}$ = 0.33, $P$ = 0.7454), the 9- to 10-year-old children ($t_{19}$ = 0.79, $P$ = 0.4373) or the 6- to 7-year-old children ($t_{19}$ = 0.99, $P$ = 0.3333).

#### 4.1.3.3. Syntactic and semantic processing strategies

In order to gain more information about the possible processing strategies applied by the different age groups, we asked all participants post-scanning, if they followed a certain strategy for solving the sentence-picture matching task. The design of this survey is summarized in section 4.1.2. The background of this additional assessment is that each of the trials could be solved by relying more on either syntactic or semantic features of the stimuli: Applying a formal syntactic strategy, focusing on the initial noun phrase preceding the actual

relative clause and on the case-marked relative pronoun that follows, could substantially ease performance and would be expected to minimize semantic processing load. On the other hand, a semantic strategy would be based more on the propositional schemes (agents and actions) of the visual scenario.
17 out of the 20 (85%) participants in the 3- to 4-year-old age group made a statement. They all reported that they focused on the animals and the actions they performed. We took this as evidence that they followed a semantic strategy. A slightly different picture emerged in the 6- to 7-year-old children. While 11 of them (55%) still reported the circumscribed semantic strategy, 9 of them (45%) reported that they looked out for both the semantic scenario and the arrangement of the relevant linguistic constructions. A similar hybrid processing strategy was described by only 1 of the 9- to 10-year-old children (5%). For the representative majority of this group (19 out of 20 children; 95%), we documented that they just relied on the syntactic cues they detected. All 20 adult participants consistently reported a formal syntactic strategy. We confirmed these systematic associations between age and chosen sentence processing strategies by running a Fisher's exact test on the 4 (group) x 3 (processing strategy) contingency tables, which was significant ($P < 0.0001$).

#### 4.1.3.4. Whole-brain fMRI

As a first analytical step to explore whole-brain blood-oxygen-level-dependent (BOLD) effects between groups, we submitted first level contrast images to a 4 (GROUP) x 2 (SYN) x 2 (SEM) full factorial ANOVA. We discovered main effects of GROUP ($P < 0.001$), of SYN ($P < 0.001$) and of SEM ($P < 0.001$) as well as a GROUP x SYN interaction ($P < 0.005$), a GROUP x SEM interaction ($P < 0.005$), and a SYN x SEM interaction ($P < 0.005$). Additionally, we found a GROUP x SYN x SEM interaction ($P < 0.005$). All *P*-values were corrected on the cluster-size level (see 4.1.2.).

Post-hoc, we tried to isolate the within-group effects driving the 3 interactions with the factor GROUP. In order to achieve this, we ran flexible factorial 2 (SYN) x 2 (SEM) ANOVAs on the first level contrast images, separately for each of the 4 samples (**Figure 4.3.**). Further remarks on additional work steps preceding this analysis can be found in section 4.1.2.

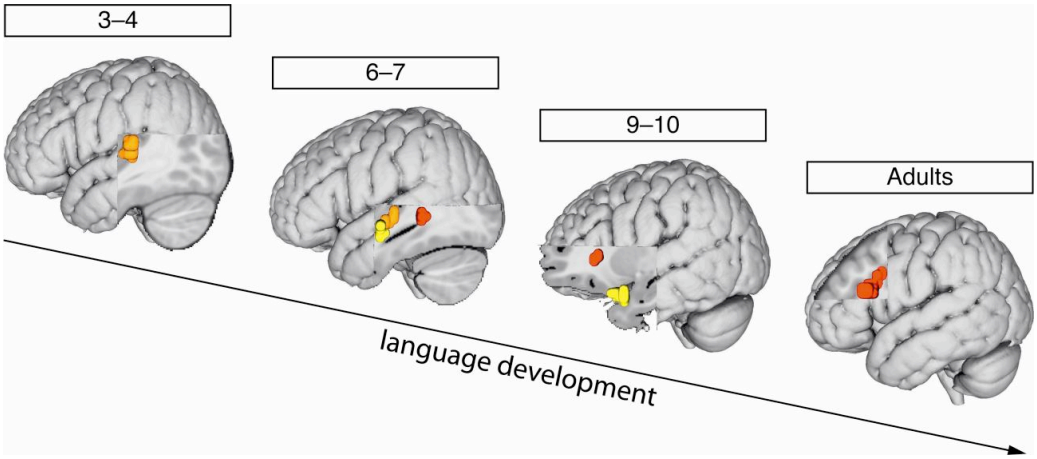


**Figure 4.3.** Whole-brain level fMRI results. Activation clusters indicate significant blood-oxygen-level-dependent (BOLD) main effects of syntactic complexity (red) and semantic plausibility (yellow), as well as the interaction of both factors (orange) thresholded at $P < 0.01$ (family-wise error corrected) in adults, and at $P < 0.005$ (cluster size corrected) in the 3 child groups. See **Table 4.2.** for cluster sizes, MNI coordinates and $T_{Max}$ scores of all activated regions.

In the adults, the only observable BOLD contrast was a significant main effect for SYN in the left IFGoper ($P < 0.01$, family-wise error corrected). In the 3- to 4-year-old children we did not observe significant main effects of either SYN or SEM, but we did find an interaction between both factors in the left temporal cortex, extending from the mid to the posterior portion of the left superior temporal gyrus (left mSTG/pSTG; $P < 0.005$). In contrast to the procedure applied for the adult group, this, and all further *P*-values reported in this section were

corrected on the cluster-size level. (See 4.1.2. for a discussion of this issue.) In the 6- to 7-year-old children, we also found an interaction of SYN and SEM ($P < 0.005$), which was located in the mid portion of the left superior temporal gyrus and sulcus (left mSTG/STS). Furthermore, we detected a main effect for SYN ($P < 0.005$) in the posterior portion of the left superior temporal gyrus and sulcus (left pSTG/STS). Additionally, we observed a SEM main effect ($P < 0.005$), covering the left mSTG/STS. The 9- to 10-year-old children demonstrated a significant main effect of SYN in the left IFGtri ($P < 0.005$) and also a main effect for SEM in the left anterior superior temporal gyrus and sulcus (left aSTG/STS; $P < 0.005$). However, unlike in the 3- to 4-year-old and 6- to 7-year-old children, an interaction effect was not present in the 9- to 10-year-old children. In accordance with the literature, an adult-like left-lateralization characteristic for auditory language comprehension was clearly established in all groups, even the youngest. A complete list of all activations comprising cluster sizes, MNI coordinates and $T_{Max}$ scores including two right-hemispheric clusters can be found in **Table 4.2**.

**A**

| **Macroanatomical region** | **Cluster size** | **MNI coordinates** | | | **$T_{Max}$** |
|---|---|---|---|---|---|
| | | **x** | **y** | **z** | |
| *Interaction Syntactic Complexity & Semantic Implausibility* | | | | | |
| Left anterior cingulate cortex | 19 | -15 | 17 | 34 | 5.05 |
| Left posterior superior temporal gyrus<br>Left middle superior temporal gyrus | 74 | -54 | -25 | 7 | 4.41 |
| Left anterior cingulate cortex | 17 | -30 | -1 | 40 | 4.20 |
| Left occipital cortex | 27 | -15 | -79 | 13 | 4.00 |
| Right anterior cingulate cortex | 10 | 30 | -1 | 49 | 3.53 |

**B**

| Macroanatomical region | Cluster size | MNI coordinates x | y | z | $T_{Max}$ |
|---|---|---|---|---|---|
| *Main Effect Syntactic Complexity* | | | | | |
| Left posterior superior temporal sulcus<br>Left posterior superior temporal gyrus | 12 | -48 | -37 | 1 | 3.38 |
| *Main Effect Semantic Implausibility* | | | | | |
| Left middle superior temporal sulcus<br>Left middle superior temporal gyrus | 14 | -45 | -10 | -11 | 3.28 |
| *Interaction Syntactic Complexity & Semantic Implausibility* | | | | | |
| Left middle superior temporal gyrus<br>Left middle superior temporal sulcus | 24 | -42 | -19 | -2 | 3.65 |

**C**

| Macroanatomical region | Cluster size | MNI coordinates x | y | z | $T_{Max}$ |
|---|---|---|---|---|---|
| *Main Effect Syntactic Complexity* | | | | | |
| Left inferior frontal gyrus, pars triangularis | 28 | -30 | 29 | 1 | 4.25 |
| *Main Effect Semantic Implausibility* | | | | | |
| Right occipital cortex | 84 | 24 | -73 | -5 | 4.13 |
| Left anterior superior temporal sulcus<br>Left anterior superior temporal gyrus | 14 | -39 | 11 | -20 | 4.12 |

**D**

| Macroanatomical region | Cluster size | MNI coordinates x | Y | z | $T_{Max}$ |
|---|---|---|---|---|---|
| *Main Effect Syntactic Complexity* | | | | | |
| Left inferior frontal gyrus, pars opercularis | 37 | -45 | 23 | 16 | 6.78 |

**Table 4.2.** Activation clusters for all whole-brain fMRI effects of interest. Displayed are cluster sizes, MNI coordinates and $T_{Max}$ scores for (**A**) 3- to 4-year-old children, (**B**) 6- to 7-year-old children, (**C**) 9- to 10-year-old children (all thresholded at $P < 0.005$ and corrected on the cluster size level) and (**D**) adults thresholded at $P < 0.01$ (FWE).

In order to investigate activation differences for syntactic complexity, semantic implausibility as well as the syntax semantics interaction effects between groups we computed several post-hoc two-tailed paired samples *t*-tests (**Figure 4.4.**).

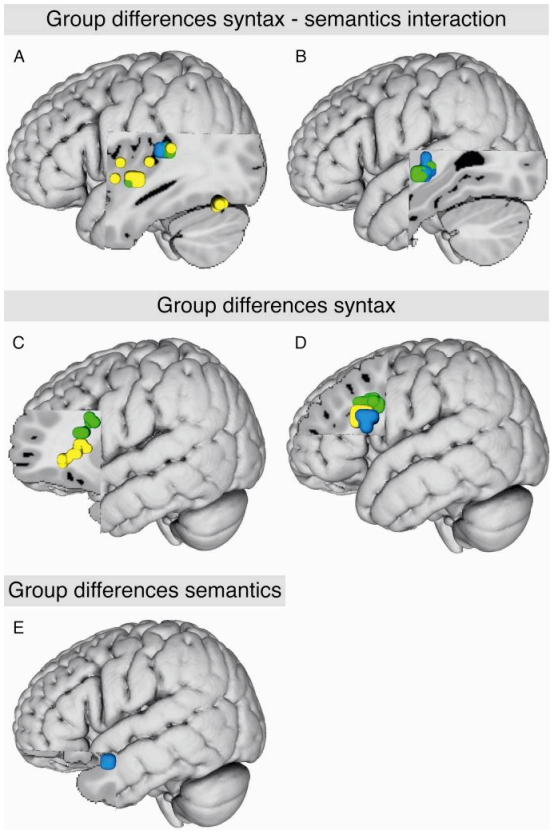


**Figure 4.4.** (**A**) Whole-brain level group activation differences of the syntactic complexity & semantic implausibility interaction between the 3- to 4-year-old children and the 6- to 7-year-old children (yellow, $P < 0.01$), the 9- to 10-year-old children (green, $P < 0.01$), and the adults (blue, $P < 0.001$). (**B**) Activation differences of the syntactic complexity & semantic implausibility interaction between the 6- to 7-year-old children and the 9- to 10-year-old children (green, $P < 0.005$), and the adults (blue, $P < 0.001$). (**C**) Whole-brain level group activation differences of syntactic complexity between the 9- to 10-year-old children and the 3- to 4-year-old children (yellow, $P < 0.005$), as well as between the 9- to 10-year-old children and

the 6- to 7-year-old children (green, $P < 0.005$). (**D**) Activation differences of syntactic complexity between the adults and all 3 child groups, i.e., the 3- to 4-year-old children (yellow, $P < 0.0001$), the 6- to 7-year-old children (green, $P < 0.001$), and the 9- to 10-year-old children (blue, $P < 0.0001$).
(**E**) Whole-brain level group activation difference of semantic implausibility between the 9- to 10-year-old children and the adults ($P < 0.05$).

A group comparison of syntactic complexity between the adults and each of the three child groups consistently revealed a significant difference in the dorsal part of the pars opercularis of the left inferior frontal gyrus ($P < 0.0001$ vs. the 3- to 4-year-old children, $P < 0.001$ vs. the 6- to 7-year-old children and $P < 0.0001$ vs. the 9- to 10-year-old children). The interaction effect in the 3- to 4-year-old children was significantly different compared to all three older age groups. It was most pronounced when testing against the adults ($P < 0.001$, left pSTG) and became gradually weaker when testing against the 9- to 10-year-old children ($P < 0.01$, left mSTG and left pSTG) as well as the 6- to 7-year-old children ($P < 0.01$, left mSTG and left pSTG). It also turned out that the interaction observed in the 6- to 7-year-old children revealed a significant group effect when compared to the 9- to 10-year-old children ($P < 0.005$, left mSTG) as well as the adults ($P < 0.001$, left mSTG) in this area. Syntax activation in the left lFGtri, as detected in the 9- to 10-year-old children, proved to be significantly different from both the 3- to 4-year-old children ($P < 0.005$) and the 6- to 7-year-old children ($P < 0.005$). Furthermore, a group comparison of semantic implausibility between the 9- to 10-year-old children and the adults revealed a significant difference in the left aSTG/STS ($P < 0.05$).

### 4.1.3.5. Region-of-interest selectivity to syntax and semantics

In order to analyze more closely the activation clusters which are potentially relevant for processing syntactic complexity and semantic implausibility information, we investigated BOLD signal changes in 5 functionally defined ROIs located within one of the 5 brain regions in which significant whole-brain-level effects were detected. These are the left IFGoper and the left IFGtri, as well as the anterior, middle and posterior portions of the left STG/STS (**Figure 4.5.**).

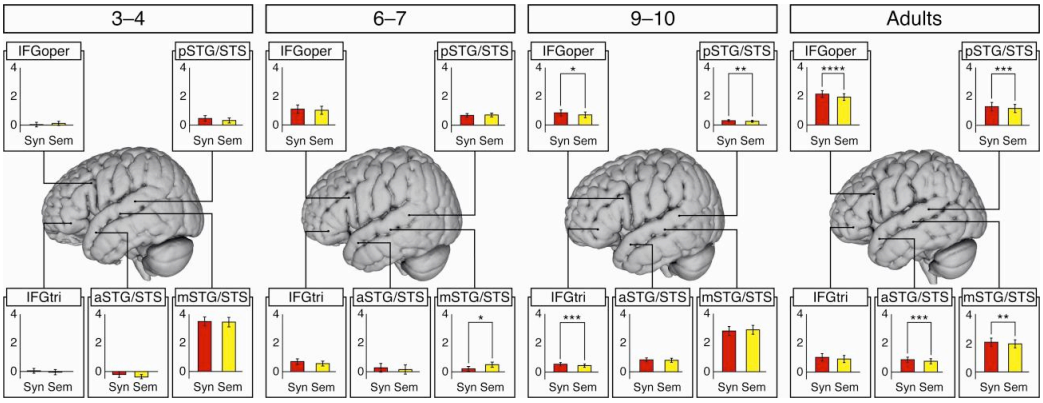


**Figure 4.5.** Region-of-interest fMRI results. Bar charts indicate BOLD signal changes in 5 functional regions of interest (ROIs) relevant for processing syntactic complexity (Syn) and semantic implausibility (Sem) within a sentence: the pars opercularis of the left inferior frontal gyrus (left IFGoper), the pars triangularis of the left inferior frontal gyrus (left IFGtri), the anterior portion of the left superior temporal gyrus and sulcus (left aSTG/STS), the middle portion of the left superior temporal gyrus and sulcus (left mSTG/STS) and the posterior portion of the left superior temporal gyrus and sulcus (left pSTG/STS). Asterisks indicate Bonferroni corrected significance levels (**** = $P < 0.001$, *** = $P < 0.005$, ** = $P < 0.01$, * = $P < 0.05$) for differences between both factors. Error bars indicate s.e.m. See 4.1.2. for an explanation of the applied cluster size correction method, as well as a description of how the ROI analysis was performed.

In the adults, we consistently observed that percent signal change values were higher for syntactic complexity than for semantic implausibility in 4 of the 5 ROIs covering language-relevant perisylvian regions, with the exception of the left IFGtri. However, we found no significant differences between syntax and semantics in the 3- to 4-year-old children. In the 6- to 7-year-old children, only a slightly different picture emerged, with the left mSTG/STS demonstrating a significantly higher BOLD percent signal change for semantic implausibility in contrast to syntactic complexity. Finally, the 9- to 10-year-old children showed significantly stronger signal changes when syntactically more complex sentences had to be processed both in the left IFGoper and in the left IFGtri, as well as in the left pSTG.

### 4.1.4. Discussion

A principle finding of this study is that the neural basis of language development is characterized by an increasing segregation of syntax- and semantic-related brain systems. In the youngest age groups, including 3- to 4-year-old children, these two aspects of language comprehension interacted in one single brain region, i.e. the mid-to-posterior left superior temporal cortex. Even at 7 years of age, syntactic complexity and semantic implausibility were not yet independent at the neural level. Both types of linguistic information still revealed significant interactions in the left mSTS, mSTG, pSTS and the pSTG, that is in brain structures crucially involved in processing features from both language domains (Grodzinsky and Friederici, 2006; Humphries et al., 2007). It was only by the age of 9 to 10 years that syntactic complexity was processed in the left IFGtri independent from semantic implausibility which recruited the left aSTG/STS.

Thus, both syntax and semantics processes are not yet independent in young kindergarten children of 3 to 4 years of age. Rather, it appears that syntactic complexity and semantic implausibility interact in the mid and posterior temporal cortex during language comprehension at this age. However, in the 6- to 7-year-old children a selectivity for semantic versus syntactic processes in the left mSTG/STS was observed, although in addition to an interaction effect. Our behavioral data indicate that this first step in the neural segregation of syntax and semantics in the left temporal cortex goes along with more generally efficient language comprehension performance, as the 6- to 7-year-old children responded more accurately and faster than the 3- to 4-year-old children.

A second major step of developmental change can be observed around the age of 9 to 10 years. At this age children demonstrated adult-like dissociable brain activations for the processing of syntactic complexity and semantic implausibility. We revealed the left IFGtri to be critically responsible for processing syntactic complexity at 9 and 10 years of age. The syntax-selectivity of this region has already been reported in the adult literature (Musso et al., 2003; Santi and Grodzinsky, 2007; Caplan et al., 2008; Kinno et al., 2008; Pallier et al., 2011). A developmental shift from the recruitment of the left mSTS, mSTG, pSTS and the pSTG to the recruitment of the left IFGtri may causally relate to the better performance for object relative clauses compared to the two younger age groups. The left IFGtri seems to provide a highly efficient system for processing complex syntax at a late primary school age. Further support for this conclusion comes from the results of our ROI analysis. Full selectivity to syntactic complexity features in relative clauses within the left IFG did not arise until the end of the 10th year of life. Note, however, that the 9- to 10-year-old children still differed slightly from the adults in that the latter show no semantic plausibility effect at all and primarily recruit the left IFGoper for complex syntax, whereas the former show a significant effect for semantic implausibility in the left aSTG/STS (Vandenberghe et al., 2002; Reilly and Peelle, 2008; Rogalsky

and Hickok, 2009). These age differences were also clearly reflected in the ROI analyses of the left IFG. While the the 9- to 10-year olds showed the strongest selectivity in the left IFGtri, the adults demonstrated a syntax-specific selectivity in the left IFGoper. Although both the adults and the 9- to 10-year old children reported that they applied a purely syntactic strategy during the comprehension task, they do this on a different neural basis. While adults are able to filter out irrelevant semantic information by employing their highly specialized system for syntax in the left IFGoper, 9- to 10-year-old children rather recruit the left IFGtri which is less selective for syntax.

In line with earlier studies, the adults showed a significantly increased activation for complex syntax in the left IFGoper (Friederici et al., 2006; Makuuchi et al., 2009; Newman et al., 2010; Wilson et al., 2010). This area, especially, was proven to become more fine-tuned towards syntactic complexity as the brain matures. We interpret this functional specification in the context of anatomical findings showing that the leftward asymmetry of the IFGoper develops late and is only present at the age of 11 years, whereas a left IFGtri asymmetry is present much earlier (Amunts et al., 2003). The left IFGoper may only be able to serve as an efficient syntax processor once it is fully matured neuroanatomically. Clearly, the observed age difference of the involvement of the left pars opercularis activation in the adults and the pars triangularis activation in the primary school children for syntactic complexity in German language demonstrated here, must await replication in neurotypologically different languages, since in word-order fixed languages, such as English, syntactic complexity effects in adults are often reported for both the pars opercularis and the pars triangularis (Grodzinsky, 2000; Cooke et al., 2002; Ben-Shachar et al., 2003; Ben-Shachar et al., 2004; Constable et al., 2004; Fiebach et al., 2005; Santi and Grodzinsky, 2010; Pallier et al., 2011; Tyler et al., 2011). However, the present data indicate that a developmental shift towards a primary involvement

of the pars opercularis holds true for a morphosyntactically rich free-word-order language such as German.

In summary, our results indicate that 3- to 4-year-old children process syntax and semantics in strongly overlapping and interacting left-lateralized superior temporal brain regions. As sentence comprehension becomes faster and less bound to the primacy of semantics at 6 to 7 years of age, the selectivity for syntactic and semantic information in the superior temporal cortex increases. A fronto-temporal neural segregation of the two functions is accomplished only by the age of 9 to 10 years. This important language-developmental change towards a highly-efficient comprehension system goes along with an increased syntax selectivity in Broca's area. The present results demonstrate that language development is characterized by the neural segregation of the syntactic and semantic processing systems. Neural segregation may serve as a general principle underlying the increasing efficiency of performance during cognitive development.

## 4.2. The development of white matter fiber pathways supporting the processing of syntax and semantics

### 4.2.1. Introduction

Recent studies described several dorsal and ventral white matter fiber tracts and ascribed different functional roles for language processing to them. By now, there is strong evidence that both a dorsal pathway, namely the superior longitudinal fasciculus (SLF) and the arcuate fasciculus (AF) as well as a ventral pathway comprising the extreme capsule fiber system (ECFS) are generally involved in syntactic processing (Friederici, 2011; Papoutsi et al., 2011; Rolheiser et al., 2011; Griffiths et al., 2012). Complex syntactic information, in particular, is propagated via the dorsal fiber tract (SLF/AF) (Friederici, 2011; Wilson et al., 2011). Both the dorsal tract covering the SLF/AF and the ventral tract covering the ECFS have also been discussed as playing a decisive functional role for processing semantics. On the one hand, it has been argued that semantic information is propagated via the AF and that the specific termination of the AF in the left temporal cortex determines this functional involvement. The sub-portion of the AF terminating in the MTG was interpreted to selectively support the transmission of semantic information (Glasser and Rilling, 2008). On the other hand, there is stronger evidence that it is rather a ventral tract via the ECFS which is mainly involved in the propagation of semantic information (Catani et al., 2005; Friederici, 2011; Rolheiser et al., 2011).

In the last years, progress has been made in exploring how cortical connectivity between perisylvian language areas changes in the course of development (Friederici, 2012). However, the current literature focuses either on young infants (Dehaene-Lambertz et al., 2006; Dubois et al., 2009; Perani et al., 2011) or on primary school children (Lebel and Beaulieu, 2009; Brauer et al., 2011).

How language-related structural maturation progresses after infancy and before school entry, however, has not been investigated yet. Accordingly, we intended to shed first light on this developmental stage of the language network.

The specific goal of our cross-sectional fMRI-DTI study of 3- to 4-year-old and 9- to 10-year-old children as well as adults was to identify developmental changes in neural fiber pathways connecting functional areas which support the processing of complex syntax and semantics in sentence comprehension. We used blood-oxygen-level-dependent (BOLD) activation peaks of syntactic and semantic processing from the fMRI experiment reported in the previous chapter 4.1. of this thesis as starting points for probabilistic fiber tracking. We assumed that the tracts derived from the resulting fractional anisotropy (FA) maps are functionally involved in transmitting information from a cortical area which was modulated by syntactic information to another syntax-sensitive cortical area and analogical from a cortical area which was modulated by semantic information to another cortical area showing selectivity for semantics. Furthermore, in order to corroborate these findings, we tested whether we could detect any correlations between behavioral measures of performance in comprehending either syntactically complex or semantically implausible sentences and FA values in the corresponding fiber tracts we identified.

In view of the adult group, we hypothesized to isolate a dorsal fiber tract connecting the left IFGoper, which is involved in processing complex syntax, with the left pSTG. Given that we did not find a main effect for semantic implausibility in the adults because we chose a very simple experimental manipulation suitable for preschool children, we could not derive a seed specifically representing semantics and hence did not have any hypothesis for this language function.

For 9- to 10-year-old children, we assumed a dorsal pathway connecting the left IFGtri and the left pSTG to be responsible for the propagation of syntactic complexity information. Additionally, we expected a ventral pathway in this age group, playing a supportive role for syntax, to connect the left IFGtri via the left frontal operculum with the left pSTG. Based on our fMRI results revealing a main effect for semantic implausibility in the left aSTG/STS, we expected to be able to isolate a second ventral tract playing a role for transmitting information about the semantic plausibility of a sentence.

In 3- to 4-year-old children, we hypothesized that all dorsal and ventral tracks running through the left MTG/STG, we would observe, would be less differentiated than in adults and in 9- to 10-year-old children. Additionally, we expected that the corresponding FA values would be lower at 3 and 4 years of age compared to adults and to 9- to 10-year-old children.

### 4.2.2. Methods

#### *Participants*

29 children and 19 adults from 3 of the 4 age groups who took part in the previously reported fMRI study, participated in this DWI study. Note, that we did not include 6- to 7-year-old children because DWI data of 7-year-old children were already collected in a previous study in our laboratory (Brauer et al., 2011). We acquired 12 datasets of 3- to 4-year-old children (8 female, mean age 4y 7m), 17 datasets of 9- to 10-year-old children (7 female, mean age 10y 3m) and 19 datasets of adult participants (7 female, mean age 26y 4m). The selection process as well as exclusion criteria are reported in detail in section 4.1.2. Adult participants as well parents, who all have given written informed consent before the fMRI study, were asked whether they wanted to participate

in a second follow-up experiment. Children gave explicit verbal assent to take part in the second session. All experimental procedures were approved by the University of Leipzig Ethical Review Board.

### *Procedure*

The experimental procedures for the fMRI study have been described in chapter 4.1.2. In the DWI study, participants were only instructed to lie as still as possible in the scanner. During the overall experiment time of approximately 20 minutes, participants watched a video via the MR compatible VisuaStim system (VisuaStim XGA, Resonance Technology Inc.).

### *DWI Data Acquisition*

The experiment was carried out at the Max Planck Institute for Human Cognitive and Brain Sciences in Leipzig on a 3.0-Tesla Siemens TIM Trio® whole-body magnetic resonance scanner using a 12-radiofrequency-channel head coil.

In a first scanning session we collected functional and structural data. All aspects of both the acquisition and the analysis of these data are comprehensively described in 4.1.2.

In a second scanning session we collected diffusion-weighted data using a twice-refocused spin EPI sequence (Reese et al., 2003) with echo time = 100 ms, repetition time = 9300 ms, matrix size = 128 x 128, voxel size = 1.7 x 1.7 x 1.7 mm, 65 axial slices providing 60 isotropically distributed diffusion-encoding gradient directions with $b_0$ = 1000 s/mm$^2$. 7 anatomical reference images without diffusion weighting were acquired once at the beginning of the sequence

and after each block of 10 diffusion-weighted images for off-line motion correction. Fat saturation was applied together with 6/8 partial Fourier imaging and generalized auto-calibrating partially parallel acquisitions (GRAPPA) with acceleration factor = 2 (Griswold et al., 2002).

### *DWI Data Analysis*

T1-weighted structural images as well as diffusion-weighted images were skull-stripped using the FSL Brain Extraction Tool (Smith, 2002) and afterwards coregistered into Talairach space (Talairach and Tournoux, 1988). We used the images without diffusion-weighting for estimating motion correction parameters applying a rigid-body transformation algorithm (Jenkinson et al., 2002) implemented in FSL. Motion correction for diffusion-weighted images was combined with a global registration to the T1-weighted structural images. Therefore, the gradient direction for each volume was corrected with the rotation parameters. After registration, images were interpolated to the new reference frame with an isotropic voxel resolution of 1 mm and then a voxel-wise diffusion tensor was fitted to the datasets.

Probabilistic fiber tracking was performed taking seeds from the fMRI analysis reported in chapter 4.1. Therefore, we extracted global as well as local peak activation coordinates from fMRI within-group effects and used FSL to project them onto the individual T1-weighted structural images applying the coefficients obtained by inverse linear and nonlinear registration of the individual anatomical images to age-appropriate MNI templates (Fonov et al., 2011). Individual fractional anisotropy maps thresholded at 0.25 were then created to generate a white matter skeleton for each participant running tract-based spatial statistics (TBSS) as implemented in FSL (Smith et al., 2006). These white matter skeletons enabled us to control if the extracted fMRI activation coordinates were effectively located in the white matter. Individual white matter

voxels closest to the group activation coordinates served as seed points for the actual fiber tracking.

Probabilistic fiber tracking was performed computing a series of random walks (number of repetitions fixed by Monte Carlo Simulations) starting from a seed point and running through surrounding voxels in order to obtain a probabilistic map based on this trajectory. Random walks are constrained by the orientation of the diffusion tensor in the seed voxel and the surrounding voxels. The number of times the random walk terminates in a specific voxel determines how the degree of connectivity strength between voxels is calculated. All these analytical steps were performed using the vdconnect algorithm implemented in LIPSIA (Lohmann et al., 2001; Anwander et al., 2007). The resulting single-subject connectivity maps were then normalized onto the most typical participant's map for each group. Therefore, a deformation field was applied to the single-subject maps. Target subjects maps were identified by aligning each probability map to every other one in order to compute for which map spatial transformation to all remaining maps within the group was minimal. The connectivity values correspond to the number of tracks per voxel and range between zero and 100.000. To reduce the dynamic range, a logarithmic transformation was applied to these values followed by a scaling between zero and one. Group connectivity maps were finally averaged and thresholded at 0.25.

FA values within the obtained tracts were extracted applying the vistat function implemented in LIPSIA. Prior to this, we created inclusion masks for all regions of interest based on the literature on the anatomy of the relevant tracts in adults (Mori et al., 2005; Galantucci et al., 2011) and children (Lebel and Beaulieu, 2009; Brauer et al., 2011) using the vledit tool implemented in LIPSIA. In order to limit our analysis to the tracts of interest and to exclude neighboring tracts not sharing any projections with the original tracts we creat-

ed exclusion masks for 9- to 10-year-old children and adults. This was not possible for 3- to 4-year-old children, however, because we could not build on data on the literature and did not have strong a priori hypotheses.

Functional associations between DTI (FA) measures and behavioral measures (mean response accuracy percentages) modeled as linear dependencies between both factors were computed with IBM SPSS 19 (IBM Corp.). We reported Pearson correlations. Correlations including reaction times were not mentioned because we did not detect any significant results based on this measure.

### 4.2.3. Results

#### 4.2.3.1. fMRI results revisited

The whole-brain fMRI results have already been reported in section 4.1.3.4. of the present thesis. In brief, in adults, we observed a significant main effect for complex syntax (SYN) in the left IFGoper ($P < 0.01$, family-wise error corrected, MNI coordinates: -45, 23, 16). Further local activation peaks could be detected in the immediate vicinity of this global cluster ($P < 0.005$, MNI coordinates: -42, 17, 25 and -54, 26, 16). In the 3- to 4-year-old children, we detected neither a significant main effect of SYN nor of SEM but a SYN x SEM interaction extending from the mid to the posterior portion of the left superior temporal gyrus (left mSTG/pSTG) ($P < 0.005$, MNI coordinates: -54, -25, 7). The 9- to 10-year-old children demonstrated a significant main effect of SYN in the left ventral IFGtri ($P < 0.005$, MNI coordinates: -30, 29, 1). Additional local peak activity was found in the left ventral IFGoper ($P < 0.005$, MNI coordinates: -57, 19, 17). Furthermore, we discovered a main effect of semantic implausibility in the left aSTG/STS ($P < 0.005$, MNI coordinates: -39, 11, -20). All *P*-values of the child samples were corrected on the cluster-size level.

Assessing regions of interest (ROIs) in adults, we consistently observed that percent signal change values were higher for syntactic complexity than for semantic implausibility in 4 of 5 left-hemispheric language ROIs (IFGtri, aSTG/STS, mSTG/pSTG, pSTG/pSTS but not IFGoper). The 9- to 10-year-old children showed significantly stronger signal changes when syntactically more complex sentences had to be processed both in the left IFGoper and the left IFGtri as well as in the left pSTG. No significant differences between syntax and semantics could be observed in any of the 5 ROIs in the 3- to 4-year-old children.

#### 4.2.3.2. Probabilistic fiber tractography of syntactic complexity

We used the syntax-related fMRI effects to derive group-specific functional seeds which we took for probabilistic fiber tracking (**Figure 4.6.**).

Seeding in the syntax-relevant BOLD activation peak within the left IFGoper in adults, we obtained a dorsal long-distance fiber tract running to the posterior part of the left STG and the left MTG (left pSTG/MTG) via the left SLF and the left AF. Dense short-distance connections to the remaining left IFGoper and to dorsal portions of the left IFGtri could be observed as well (**Figure 4.6.A**).

In the 9-to 10-year-old children, long-distance fibers passing through the ventral portion of the left IFG tri, i.e. the corresponding area for complex syntax defined by maximum BOLD activity, connect it with the posterior portion of the left superior and middle temporal cortex and finally the occipital cortex following the left inferior fronto-occipital fasciculus (IFOF) via the extreme and external capsule. When seeding in the ventral portion of the left IFGoper, which was also found to be involved in syntactic processing on the basis of a local BOLD

activation peak, we obtained a connectivity map linking this area to the superior temporal cortex following the left SLF and the left AF (**Figure 4.6.B**).

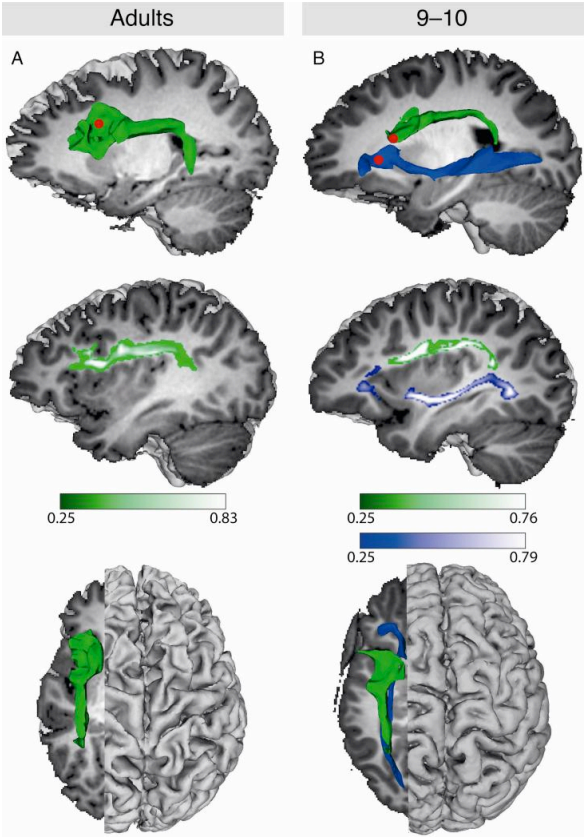


**Figure 4.6.** White matter fiber tracts supporting the transmission of syntactic complexity information. (**A**) In the adults, we placed a functional seed in the left IFGoper where we observed the maximum BOLD activation for syntax and isolated a dorsal pathway terminating in the left posterior STG/MTG (green). (**B**) In the 9- to 10-year-old children, we obtained a ventral pathway extending into the posterior temporal and the occipital cortex when seeding in the activation peak located in the ventral part of the left IFGtri (blue). A seed placed in a ventral portion of the left IFGoper, where a local activation peak was detected, revealed a dorsal pathway terminating in the left posterior STG/MTG (green).

Post-hoc, we used the MNI coordinates of a local activation maximum for syntactic complexity (MNI coordinates: -51, 26, 7), which we found in adults when choosing a more liberal threshold of $P < 0.005$ (cluster size corrected) at the whole-brain level, as seed coordinates for probabilistic fiber tracking in order to examine the connectivity of the left IFGtri. Following this procedure, we identified a ventral pathway covering the left IFOF and extending into the left posterior MTG/STG (**Figure 4.7.**).

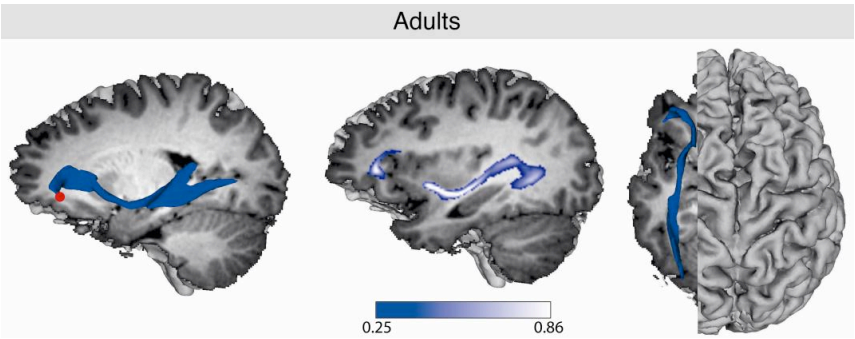


**Figure 4.7.** The ventral white matter pathway in adults connecting the left IFGtri with the left posterior MTG/STG. This connectivity map was found in a post-hoc analysis using a syntax-related local peak activation cluster in the left IFGtri (MNI coordinates: -51, 26, 7) at a liberal threshold of $P < 0.005$ (cluster size corrected).

### 4.2.3.3. Fractional anisotropy correlates of complex syntax

The response accuracy results obtained from behavioral measures acquired during fMRI scanning have already been described in section 4.1. To summarize, in the adult group, we observed a ceiling effect (99.32% mean response correctness) covering all syntactic complexity levels. Accordingly, the within-group variance was very low (s.e.m. ±0.58%). The 9- to 10-year-old children performed slightly less accurate than adults but also very similar regardless of the syntactic complexity of the sentences (94.69% overall mean response cor-

rectness). Furthermore, the variance within subjects was higher compared to adults (s.e.m. ±1.83%). The 3- to 4-year-old children showed a response accuracy of 59.33% (s.e.m. ±5.54%) for syntactically complex sentences and 72.08% (s.e.m. ±4.15%) for syntactically more simple sentences. We do not recapitulate the reaction time results here, because they did not reveal any significant results in the following analyses.

Looking at linear dependencies between white matter anisotropy and the behavioral measures in the adults, we found that FA values in the left SLF/AF were positively correlated (r = 0.61, *P* = 0.008) with mean response accuracy rates for syntactically complex sentences (**Figure 4.8.A**).

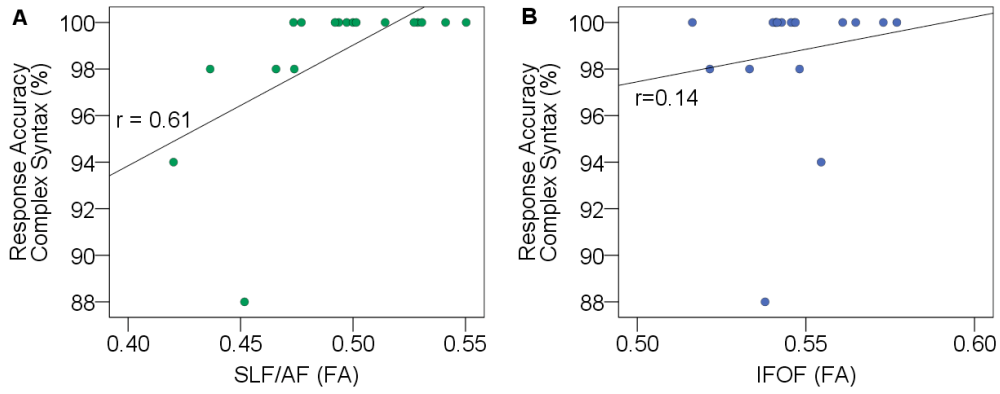


**Figure 4.8.** Functional associations between the processing of complex syntax and FA values in fronto-temporal white matter pathways in adults. Mean response accuracy rates for syntactically complex sentences positively correlated with FA values in a dorsal tract via the left SLF/AF (green) starting in the left IFGoper (**A**). However, this dependency was not present in a ventral tract via the left IFOF which we identified post-hoc seeding in the left IFGtri (blue) (**B**).

In the adults, we did not find any correlations between the mean response accuracy rates for complex syntax and the FA values in the ventral pathway including the left IFOF which we isolated post-hoc seeding in the left IFGtri (**Figure 4.8.B**).

Performing the same analysis with the data of the 9- to 10-year-old children, we observed a positive correlation between mean response accuracy rates for syntactically complex sentences and FA values in the left SLF/AF (r = 0.6, *P* = 0.011) but not in the left IFOF (r = -0.19, *P* = 0.472) (**Figure 4.9.**).

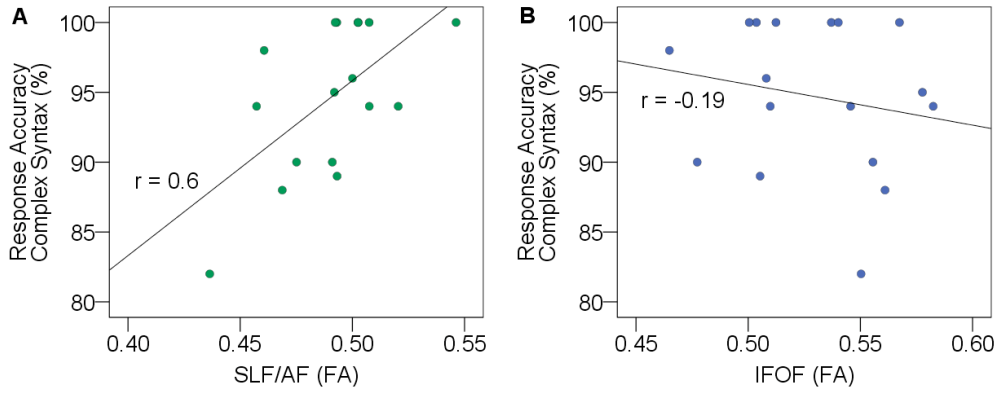


**Figure 4.9.** Functional relationships between syntax measures and FA values in relevant white matter tracts at 9 and 10 years of age. Mean response accuracy rates for syntactically complex sentences positively correlated with FA values in a dorsal tract via the left SLF/AF (green) (**A**) but not in a ventral tract via the left IFOF (blue) (**B**).

### 4.2.3.4. Probabilistic fiber tractography of semantic implausibility

Given that a separable main effect for semantic implausibility was only found in the 9- to 10-year-old children, our investigations concerning the white matter fiber pathways underlying the transmission of semantic information were limited to this age group. On the basis of our whole-brain fMRI results, we placed a seed at the observed activation peak located in the left aSTG/STS. Following

this procedure, we isolated a ventral fiber tract connecting the left aSTG/STS with the left orbitofrontal cortex via the uncinate fasciculus (UF) (**Figure 4.10.**).

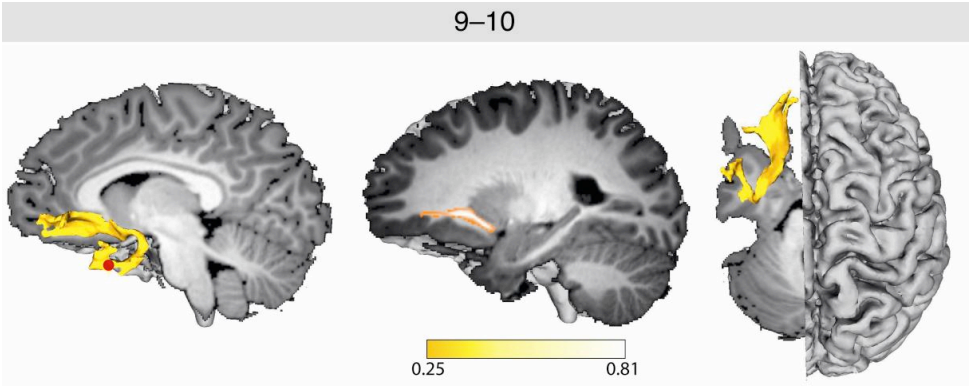


**Figure 4.10.** White matter fiber tracts involved in the propagation of semantic information at 9 and 10 years of age. Seeding in the left aSTG/STS, we detected a ventral pathway comprising the uncinate fasciculus which branches out into the left orbitofrontal cortex.

Given that we did not find any plausibility effects at the behavioral level in the 9- to 10-year-old children, we did not expect any linear dependencies between the fractional anisotropy within the UF and the performance measures related to semantics. Accordingly, there was no correlation between the mean response accuracy rates and the corresponding FA values (r = -0.135, *P* = 0.605).

#### 4.2.3.5. Probabilistic fiber tractography in 3- to 4-year-old children

In order to assess syntax- and semantics-related white matter connectivity also in children of age 3 to 4, we created a seed from the reported SYN x SEM interaction in the left mSTG/pSTG. We could not detect long-distance but only short-distance connections which were largely limited to mid and posterior portions of the left inferior longitudinal fasciculus (ILF) parallel to the left

mSTG/pSTG where they were most dense. One dorsal sub-branch also covered the mid and the posterior part of the left SLF/AF but ended at the precentral gyrus and did not reach the IFG (**Figure 4.11.**).

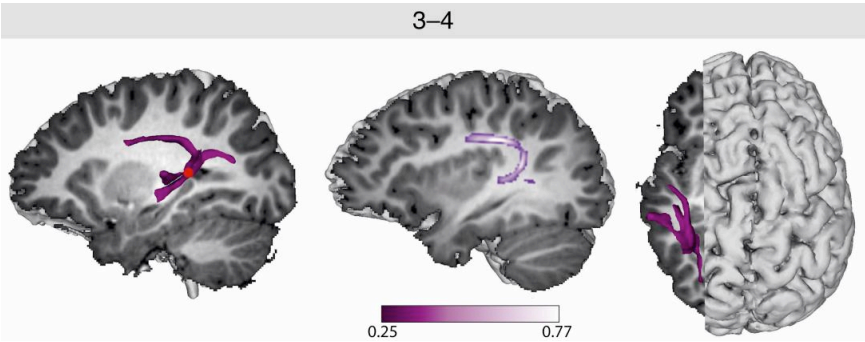


**Figure 4.11.** White matter fiber tracts in the 3- to 4-year-old children. Given that we could not disentangle cortical areas which were selectively involved in either syntactic or semantic processing at this age, we placed a seed in the left mSTG/pSTG where both language functions interacted hemodynamically. The resulting connectivity map comprised a posterior portion of the left SLF/AF as well as mid and posterior branches of the left ILF.

In the 3- to 4-year-old children, we did not detect any correlations between FA values and performance in both syntax and semantics neither in the dorsal tract nor in the ventral tract. The FA values in the posterior sub-branch of the left SLF did not correlate with the mean response accuracy rates for complex syntax (r = 0.201, *P* = 0.531) or implausible semantics (r = 0.039, *P* = 0.904). Analogical, the FA values in the mid and posterior sub-branches of the ILF did not correlate with the mean response accuracy rates for complex syntax (r = 0.075, *P* = 0.816) or implausible semantics (r = 0.064, *P* = 0.844).

We also investigated if there were any associations between the age of the individual participants in each group and the corresponding FA values in language-relevant white matter fiber tracts. There were no such correlations present in the 9- to 10-year-old children or the adults. We did find, however, a

positive correlation between age and FA values in the mid and posterior portion of the left SLF/AF (r = 0.76, *P* = 0.004), but not in the mid and posterior portion of the left ILF (r = 0.47, *P* = 0.123) in the 3- to 4-year-old children (**Figure 4.12.**).

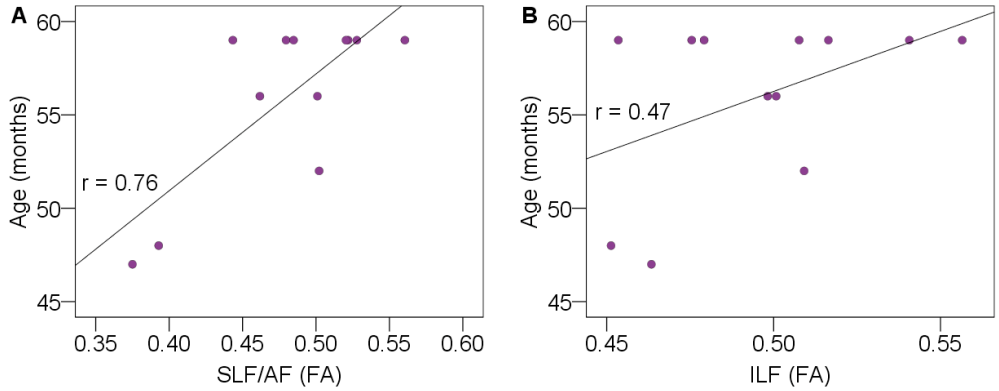


**Figure 4.12.** Maturation processes in white matter fiber pathways at 3 and 4 years of age. While FA values in mid and posterior parts of the SLF/AF still considerably differ as a function of age (**A**), they are already more homogenous in mid and posterior parts of the ILF (**B**).

Post-hoc, we used the peak activation coordinates for syntax and semantics detected in the 9- to 10-year-old children as seed points for probabilistic fiber tracking in the 3- to 4-year-old children starting at the left IFGoper, the left IFGtri and the left aSTG/STS. We roughly replicated the anatomical course of the fiber tracts identified in the 9- to 10-year-old children, but we did not observe any specific involvements of these tracts in processing complex syntax or information about the plausibility of a sentence.

### 4.2.4. Discussion

In the present study, we aimed to investigate developmental changes in neural fiber pathways connecting functional areas which support the processing of complex syntax on the one hand, and the processing of semantic plausibility differences on the other hand. Using probabilistic fiber tracking within the framework of a combined fMRI-DTI approach as well as related behavioral measures, we tried to identify white matter fiber tracts playing a functional role either in transmitting syntactic information between syntax-sensitive cortical areas or in transmitting semantic plausibility information between cortical areas which are sensitive for semantic processes.

In the adults, we obtained a dorsal fiber connection between the left IFGoper and the posterior portion of the left STG and MTG via the SLF/AF. This dorsal connection could also be reproduced when seeding in both of the local fMRI activation peaks. We were only able to isolate a ventral fiber pathway, i.e. large portions of the left IFOF, when placing a seed in a more liberally thresholded local activation cluster of the left IFGtri.

Mean response accuracy rates for syntactically complex sentences positively correlated with FA values in the dorsal fiber pathway. The better the task performance, the higher the corresponding FA values were. Given that the within-group variance was very low and given the limited sample size, this result alone does not allow a strong claim. Nevertheless, our finding that the processing of complex syntax depends on dorsal rather than on ventral fiber tracts is in line with the recent literature on patient studies (Wilson et al., 2011) as well as artificial grammar learning studies (Friederici et al., 2006; Flöel et al., 2009). Additional support comes from our post-hoc findings. We did not find any correlations between the performance in processing syntactically complex

sentences and the FA values in the ventral tract we identified post-hoc. There is evidence that ventral tracts in adults only play a role for syntactic processes occurring on the phrase level but not on the level of complex sentences (Friederici, 2011).

In the 9- to 10-year-old children, we first used the global BOLD activation peak for syntactic complexity, located in the ventral part of the left IFGtri, as a seed for probabilistic tracking. The resulting ventral white matter fiber tract, i.e. the left IFOF, passed through the extreme and external capsule into the temporal cortex and branched out into the occipital cortex. As a second step, we computed a connectivity map seeding in the local activation peak for syntactic complexity located ventrally within the left IFGoper. This time, we identified a dorsal tract, namely the SLF/AF leading into the left pSTG.

Up to this point of our analysis, the data suggested that both a dorsal (SLF/AF) as well as a ventral fiber tract (IFOF) contribute to the propagation of syntactically complex information. A similar finding was already reported for younger, i.e. 7-year-old children (Brauer et al., 2011). However, given that the 9- to 10-year-old children showed very different hemodynamic activation patterns compared to the 6- to 7-year-old children in our fMRI study, we assumed that these differences should also be reflected in the functional involvement of the two fiber tracts. Accordingly, we aimed to disentangle the specific contributions of the dorsal SLF/AF and the ventral IFOF connection, respectively, to the transmission of complex syntactic information. In order to achieve this, we related subject-specific FA values of each of the two tracts with the corresponding mean response correctness rates for the syntactic comprehension task. Crucially, we observed that FA values positively correlated with complex syntax in the dorsal pathway (SLF/AF), but not the ventral pathway (IFOF). These findings provide strong evidence that only the SLF/AF, but not the IFOF, is special-

ized on the propagation of complex syntactic features, such as the identification of hierarchical phrase structures, in children at the age of 9 to 10 years, like in adults. However, similar to 7-year-old children and contrary to adults, the IFOF still seems to play a more pronounced role in syntactic processing, maybe supporting the detection of less complex syntactic features at the local phrase level in 9- to 10-year-old children. Support for this relatively late functional specialization of the dorsal syntax tract comes from a neuroanatomical study showing that the leftward asymmetry of the IFGoper develops late and is only present at the age of 11 years, whereas a left IFGtri asymmetry is present much earlier (Amunts et al., 2003). Furthermore, this finding is in line with the results of our ROI fMRI analysis. While in adults, we observed a clearly segregated syntax selectivity in the left IFGoper but not in the left IFGtri, it is still both regions which showed a syntax selectivity at the age of 9 and 10 years.

On the basis of a main effect of semantic implausibility located in the left aSTG/STS (Vandenberghe et al., 2002; Reilly and Peelle, 2008; Rogalsky and Hickok, 2009) which we detected in the 9- to 10-year-old children, we identified a ventral connection to the left orbitofrontal cortex via the uncinate fasciculus. The specific contributions of this white matter fiber tract to the processing of linguistic information are not well understood yet. A recent study suggested its involvement in semantic processes but pointed out that the functionality of this tract is compensable by the IFOF (Duffau et al., 2009). Future investigations will have to shed more light on the functional role of the uncinate fasciculus.
Given that the fMRI analysis in the 3- to 4-year-old children did not reveal a separable main effect for syntax but only a syntax-semantics-interaction, we placed our seed at the peak of this BOLD activation. The resulting connectivity map comprised a short dorsal pathway, i.e. a mid and posterior sub-portion of the SLF/AF, as well as a short ventral pathway including a mid and posterior sub-portion of the ILF. The FA values we extracted from these sub-portions

were not correlated with the performance in comprehending both syntactically complex and semantically implausible sentences in this age group on the whole. However, we found a significant association between the age of the individual participants in this group and the FA values in the dorsal pathway, i.e. the mid and posterior sub-portion of the SLF/AF, but not the ventral pathway, i.e. the mid and posterior sub-portion of the ILF. These results suggest, that although the SLF/AF undergoes substantial maturational processes between the 4th and the 5th year of life, it does not yet play a functional role in processing complex syntactic features which just start to emerge as representations in the developing brain at this age.

Coming back to the results reported in our fMRI study, all syntactic and semantic processing in 3- to 4-year-old children seems to take place in the temporal cortex. Given that there was no systematic relation between the FA values in the ventral short-distance pathway, which we detected, and the syntactic complexity and semantic implausibility measures we took, it can be assumed that the language-relevant maturational processes within the temporal cortex at this age take place on a more microstructural level.

In conclusion, we report three main findings shedding light on important developmental trajectories regarding the changing functional organization of language-relevant white matter fiber pathways. First, our data support the hypothesis that in adults it is a dorsal tract, linking together the left IFGoper and the left pSTG/pMTG via the SLF/AF, which is primarily involved in the processing of complex syntax rather than both a dorsal and a ventral tract. Second, syntactic processing in 9- to 10-year-old children still depends more on both a dorsal (SLF/AF) and a ventral pathway (IFOF). However, a particular specialization on complex syntax is limited to the dorsal tract and does not include the ventral tract at this age. Third, in 3- to 4-year-old children, all processing of complex syntax and semantics occurs within the left temporal cortex. There-

fore, it does not yet depend on long-distance fiber tracts connecting the temporal cortex with the frontal cortex. The mid and posterior sub-portion of the SLF/AF still undergo intense maturation between the 4th and the 5th year of life. Generally, we present the first study systematically assessing the dynamic interplay between the functional organization of the white matter and syntax and semantics acquisition from 3 years of age into adulthood. The findings we reported, critically advance our understanding of the relationship between brain maturation and language acquisition.

# 5. GENERAL DISCUSSION AND CONCLUSION

In chapter 5.1., I will focus on summarizing the results of the event-related fMRI experiment reported in chapter 4.1. It will be explained, which answers these results provide to the research questions 1., 2.1. and 2.2. presented in chapter 2.3. of this thesis and how they corroborate, substantiate and expand the corresponding hypotheses. In chapter 5.2., I will give a synthesis of the central findings of the probabilistic fiber tracking DTI experiment described in chapter 4.2. I will discuss answers to the research questions 3.1. and 3.2. framed in chapter 2.3., thereby outlining a clear picture on the basis of the given hypotheses. I want to emphasize that both studies support and complement one another.

## 5.1. From the interaction to the segregation to the shift of syntax- and semantics-selective cortical areas

The cross-sectional, event-related fMRI experiment we conducted, shed light on the neurobiological basis underlying the processing of syntactic and semantic information from 3 years of age to young adulthood. We discovered that young children, in contrast to adults, do not process complex syntax and semantics in distinct brain regions. Rather, our results indicated that 3- to 4-year-old children process syntax and semantics in strongly overlapping mid and superior temporal brain regions. A similar finding has already been reported in a study describing baseline contrasts in 5- to 6-year-old children (Brauer and Friederici, 2007). However, using a more sensitive direct contrast of syntax against semantics, we demonstrated how pronounced this non-specificity is in 3- to 4-year-old children. Interestingly, we could not isolate separate main effects of syntax or semantics in this age group although adults generally show

clearly distinguishable activity patterns for both linguistic representations (Newman et al., 2010; Friederici, 2011).

In contrary, in 6- to 7-year-old children, we were able to disentangle syntax and semantics in left temporal regions but without an involvement of left inferior frontal regions (Brauer and Friederici, 2007). These findings match the results reported in the event-related potentials (ERP) literature on the development of syntactic processing. 2-year-old as well as 3- and 4-year-old children do not show the syntax-related ELAN component, which has its sources in the left IFG and in the left aSTG (Friederici et al., 2000), but only a centro-parietal P600 component with sources in the STG (Hahne and Friederici, 1999) when confronted with syntactic violations in a sentence (Silva Pereyra et al., 2005; Oberecker and Friederici, 2006). Moreover, there is ERP evidence that this pattern is still present at 6 years of age for syntactically complex sentences (Hahne et al., 2004).

We provided first evidence that there is a strong functional dependence between syntactic and semantic representations characterized by interaction effects present not only in children aged 3 to 4 years but also still in children aged 6 to 7 years. This observation complements a study demonstrating a behavioral interaction of syntactic and semantic processes which is still present even at the age of 9 and 10 years (Friederici, 1983).

A functional specialization comparable to the mature adult brain is still not established at 7 years of age. The observation that ELAN-like effects seem to arise at 7 years of age (Hahne et al., 2004), could not be corroborated neither by global nor by local BOLD activity in our sample with a mean age of 7 years and 5months. Nevertheless, Hahne et al.'s data and our data of 9- to 10-year-old children converge in the observation that robust hemodynamic activity related to the processing of complex syntactic features in the left IFG going along

with an ELAN seems to establish between the late 8th and the early 10th years of life in normally developing children. Note that this only holds true for complex syntactic processes. As shown in a recent study (Schipke et al., 2011), more simple morphosyntactic processes, like the decoding of case marking information, are detectable as broadly distributed LAN effects present already at the age of 3 years. Future studies will have to uncover the physiological and anatomical underpinnings of this activity.

It is only at the end of the 10th year of life that neural selectivity for complex syntax, similar to that of adults, is established in the left inferior frontal and the left superior temporal cortex. However, qualitative differences between children and adults remain. A highly specialized system for syntax in the left IFGoper seems to enable adults to filter out irrelevant semantic information from the speech input in a very flexible way. Syntax selectivity in the left IFGoper has been frequently demonstrated in the adult literature (Friederici et al., 2006; Makuuchi et al., 2009; Newman et al., 2010; Wilson et al., 2010). 9- to 10-year-old children rather recruit the left IFGtri which has been mentioned in the adult literature as well (Musso et al., 2003; Santi and Grodzinsky, 2007; Caplan et al., 2008; Kinno et al., 2008; Pallier et al., 2011). However, a recent study testing 10- to 15-year-old children, reported syntax-related hemodynamic cortical activation in the left IFGoper (Nunez et al., 2011). These data suggest that an adult-like selectivity for complex syntax in the left IFGoper but not in the left IFGtri seems to establish during early puberty.

In contrast to our findings, a recent fMRI study on semantic processing reported a stronger involvement of the pars opercularis for semantics rather than for syntax (Moore-Parks et al., 2010). The authors interpreted their result as an increase in top-down control mechanisms during language processing. However, our behavioral data suggest no change with respect to task solving strat-

egies between 9- to 10-year-old children and adults. Rather, we suggest that the reported shift within the inferior frontal gyrus goes along with final finetuning for the processing of complex syntactic information increasing the computational efficiency of this cortical area. This view is supported by the fMRI study introduced in the preceeding passage (Nunez et al., 2011) and furthermore by a neuroanatomical study demonstrating that the leftward asymmetry of the IFGoper develops late and is only present at the age of 11 years, whereas a leftward asymmetry of the IFGtri is present much earlier (Amunts et al., 2003).

Even at age 9 and 10, children still seem to be more bound to semantic cues in the speech input than adults are. Children might still automatically co-process semantic features although their syntax system is already highly developed. Future studies will have to concretize this observation. Evidence for the involvement of the anterior portion of the left superior temporal gyrus in semantic processing as seen in 9- to 10-year-old children but not in adults has been previously reported in the adult literature (Vandenberghe et al., 2002; Rogalsky and Hickok, 2009) and was supported by patient data (Reilly and Peelle, 2008).

Taking together our own findings and the data available from the current literature, we propose a schematic overview illustrating how hemodynamic patterns of cortical activation underlying syntactic and semantic processing change from 3 years of age to adulthood (**Figure 5.1.**).

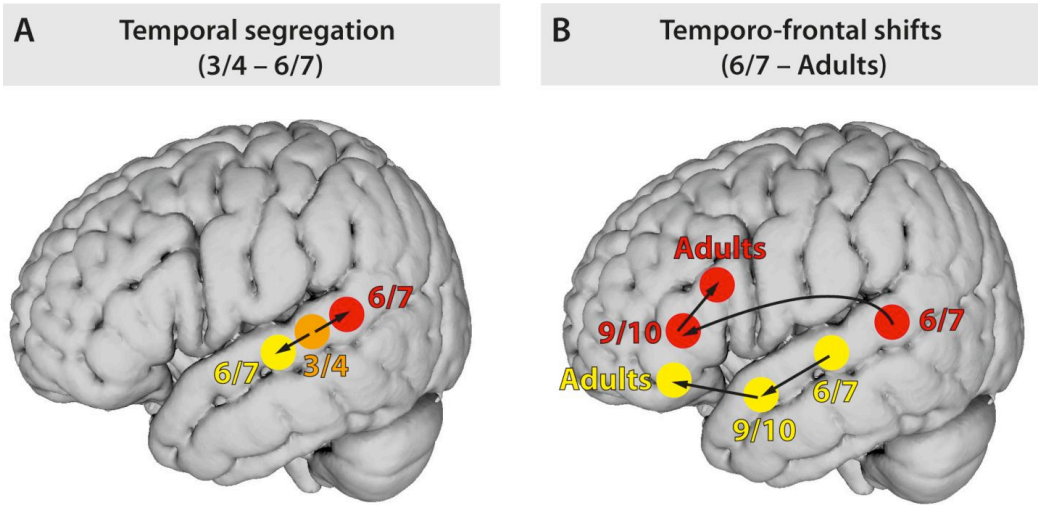


**Figure 5.1.** Developmental dynamics of hemodynamic patterns of cortical activation underlying syntactic and semantic processing. (**A**) While syntax and semantics interact in the mid portion of the left superior temporal cortex (orange) in 3- to 4-year-old children, both language functions are segregated in 6- to 7-year-old children. A mid portion of the left superior temporal cortex shows higher selectivity for processing semantic information (yellow) whereas a posterior portion of the left superior temporal cortex shows higher selectivity for processing syntactic information (red). (**B**) Between the age of 6 to 7 years and the age of 9 to 10 years, the hemodynamic activity underlying syntax shifts into the left inferior frontal gyrus (red). Ongoing maturation towards adulthood is characterized by a dorsal shift within the left inferior frontal gyrus (red). Selectivity for processing semantic information shifts frontally from mid to anterior portions of the left superior temporal cortex between the age of 6 to 7 years and the age 9 to 10 years and finally occurs in the pars orbitalis as well as in the pars triangularis of inferior frontal cortex (yellow).

In our scheme, we distinguish two general developmental stages, the first one occuring between 3 to 4 and 6 to 7 years of age (A) and the second one starting between 6 to 7 and 9 to 10 years and continuing into adulthood (B).

In 3- to 4-year-old children, syntax and semantics are not yet distinguishable but rather interact in mid portions of the left superior temporal cortex. This pat-

tern seems to be associated with the behavioral observation that children at that age rely more on semantic rather than syntactic cues in language comprehension.

The first trajectory is characterized by a segregation of both functions at 6 to 7 years of age. While a selectivity for syntactic information establishes in posterior portions of the left superior temporal cortex, selectivity for semantic information remains in mid portions of the left superior temporal cortex. Note, that this segregation is intralobar, meaning that it is spatially limited to the left temporal cortex and does not extend it. In the course of the described trajectory, children show faster and more accurate language processing and they also seem to be less bound to semantics.

A first interlobar segregation takes place between 6 to 7 and 9 to 10 years of age when syntax selectivity is no longer restricted to the posterior portions of the left superior temporal cortex but also shifts temporo-frontally into the left inferior frontal cortex. Behaviorally, this diversification seems to be the neural basis for the beginning primacy of syntactic cues over semantic cues in 9- to 10-year-old children. The sensitivity for processing semantics shifts in an intralobar fashion from mid to anterior portions of the left superior temporal cortex in the developmental trajectory between both age groups. This shift, however, might be specific to plausibility information and must await further support concerning other semantic aspects.

Our data suggest another intralobar shift within the left inferior frontal gyrus underlying the selectivity for complex syntax. This selectivity seems to migrate from pars triangularis to the pars opercularis in the course of puberty thereby increasing performance efficiency.

It is not our own data but rather several experiments reported in the adult literature (Friederici, 2002; Newman et al., 2010) which suggest another temporo-frontal shift from anterior portions of the left superior temporal cortex to the pars orbitalis and the pars triangularis of the left inferior frontal gyrus. Selectivity for semantic processes covers both regions in adults, but presumably not yet in 9- to 10-year-old children. Again, follow-up studies will help clarifying this issue.

Future investigations might show that the functional segregation and shift of initially interacting brain areas as shown here for developmental trajectories of language comprehension can be viewed as a general principle of cognitive development.

### 5.2. From ventral to dorsal syntax fiber tracts

The capacity to process syntactic complexity as well as semantic plausibility information does not only depend on the selectivity of fronto-temporal cortical regions but is also crucially associated with the functional organization of the connecting white matter fiber tracts. Accordingly, we combined functional magnetic resonance imaging (fMRI) with diffusion tensor imaging (DTI) and behavioral measures in order to systematically track the interplay of cortical connectivity and the acquisition of complex syntax as well the processing of semantic plausibility information from 3 years of age into adulthood. Based on our behavioral and fMRI findings that both syntactic and semantic processing is still limited to the temporal cortex in 3- to 4-year-old children, we provided first evidence that it does not yet depend on long-distance fiber connections with the frontal cortex. The dorsal pathway we identified – a mid and posterior sub-portion of the SLF/AF – did not extend the precentral gyrus and did not enter the IFG. This finding can be aligned with infant data suggesting that the

SLF/AF does not extend parietal and temporal regions (Leroy et al., 2011) or at least terminates in the premotor cortex within the first months of life (Perani et al., 2011). Additionally, there is evidence that the dorsal pathway still undergoes maturational changes at 7 years of age (Brauer et al., 2011). We argue, that the SLF/AF still undergoes pronounced maturational processes between the 4th and the 5th year of life and does not play a functional role for the processing of both complex syntax and semantics. This view is not only supported by our own fMRI data but also by the ERP data introduced in the previous chapter 5.1. suggesting that adult like ELAN-P600 effects – which require intercortical information transfer – do not emerge before the age of 7 (Hahne et al., 2004) for syntactically complex sentences.

Remarkably, also in the ventral pathway – a mid and posterior sub-portion of the ILF – we could not detect a specific involvement in processing syntactic and semantic representations although maturation turned out to be more advanced in this tract. On the basis of these observations, we assume that the maturational processes related to complex syntax and semantics at this age are intralobar, possibly microstructural changes within the left STG and MTG. It remains to be seen if currently available methods, e.g. voxel-based morphometry and cortical thickness measurements on large samples, are sensitive enough to detect these changes. Our findings add an interesting aspect to what we know from the infant literature about the early establishment of interhemispheric connectivities versus the late establishment of intrahemispheric connectivities (Perani et al., 2011). It seems that intralobal maturation steps within the temporal cortex must reach a certain level before intrahemispheric connectivities to the frontal cortex become functionally relevant for processing syntax and semantics. Note, however, that it is plausible that more simple syntactic processes at the phrase level or at the morphosyntactic level

(Schipke et al., 2011) depend on a ventral pathway either via the left ILF or via the left IFOF. Follow up studies will help to clarify this issue.

An adult-like syntax-specialization of a fronto-temporal dorsal tract including the superior longitudinal fasciculus (SLF) and the arcuate fasciculus (AF) is only established at 9 to 10 years of age. However, although a particular specialization on complex syntax is only present in the dorsal tract, the child brain still additionally recruits a ventral pathway covering the inferior fronto-occipital fasciculus (IFOF). This pattern has already been reported for 7-year-old children in the literature (Brauer et al., 2011). Based on our data of 9- to 10-year-old children, we support the view that it is the SLF/AF playing the crucial role for the processing of complex syntactic information while the IFOF rather plays a supplementary role, involved in subprocesses of the actual syntactic analysis such as local phrase structure building (Friederici et al., 2006). Note that we report this functional differentiation only for 9- to 10-year-old children. Brauer et al.'s DTI data, however, taken together with our fMRI data, suggest that a particular specialization on complex syntax in the dorsal tract as seen in a significant correlation between FA values and behavioral performance measures at the age of 9 and 10 years is not yet established at the age of 7 years.

Our probabilistic tracking results indicate that semantic information is propagated from the anterior temporal to the orbitofrontal cortex via a ventral pathway, namely the uncinate fasciculus, in 9- to 10-year-old children. The involvement of this tract in semantic processing has already been discussed in a recent study in adults (Duffau et al., 2009). However, this observation only indirectly supports the view that the pars orbitalis of the left IFG is already involved in semantic processing at 9 to 10 years of age because we found no additional evidence analyzing its hemodynamic activity. Again, further experiments are

needed in order to determine the functional roles of the orbitofrontal cortex and the uncinate fasciculus in semantic processing at this age.

Our data support the hypothesis that, in adults, it is a dorsal tract, linking together the left IFGoper and the left pSTG/MTG via the SLF/AF, which is primarily involved in the processing of complex syntax (Friederici, 2011; Wilson et al., 2011) rather than both a dorsal and a ventral tract (Rolheiser et al., 2011; Papoutsi et al., 2011; Griffiths et al. 2012). We argue that all three studies suggesting an involvement of both a ventral and a dorsal pathway in complex syntax show methodical or conceptual problems. Rolheiser et al. present whole-brain voxelwise correlation clusters which only overlap with the most anterior and the most posterior sub-portions of the ventral tract they identified. A much larger syntax overlap can be seen in the posterior part of the dorsal pathway. Given that the reported clusters are very large, we assume that the described overlaps with the ventral path would not have survived a more restrictive thresholding increasing the distinctivity of the analysis. In Papoutsi et al.'s experiment, complex syntax is not a well-controlled factor. We argue that their phrase disambiguation preference task requires both syntactic and semantic processing and hence does not exclusively isolate syntax. Accordingly, we relate the described effects in the ECFS to semantic processes rather than to complex syntactic processes. A similar problem is present in the study of Griffiths et al. The authors do not provide any analysis enabling themselves to rule out that their Anomalous Prose minus Random Word Order contrast still carries word-level semantic information. Again, this would explain the functional involvement of the ECFS.

We summarize our insights and the existing data in a simple schematic overview (**Figure 5.2.**) focusing on the functional development of white matter fiber tracts connecting cortical areas which are involved in detecting information about syntactic complexity. Given that an isolated semantics effect was only

present in one of our samples and given there are no imaging studies available so far which specifically address this topic, we do not consider the semantics domain.

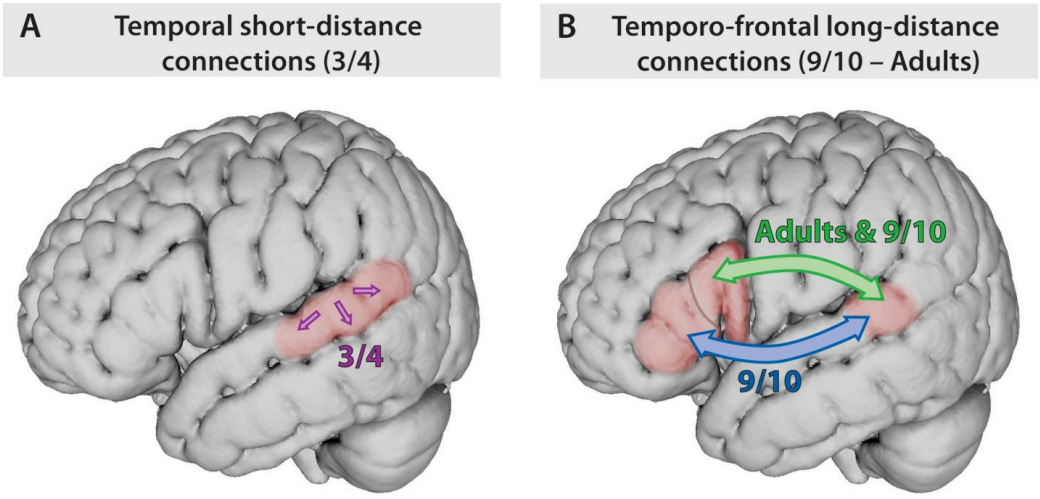


**Figure 5.2.** Development of white matter fiber tracts connecting syntax-selective cortical areas. (**A**) At 3 to 4 years of age, only short-distance connections within mid and posterior portions of the left superior temporal cortex play a role for the processing of complex syntax (purple). (**B**) In 9- to 10-year-old children, the propagation of complex syntactic information depends on a left dorsal tract via the superior longitudinal fasciculus including the arcuate fasciculus (green) while a left ventral tract comprising the inferior fronto-occipital fasciculus supports subprocesses of the actual syntactic analysis (blue). In adults, it is exclusively the dorsal tract playing a functional role for complex syntax (green).

The scheme we introduce, consists of two major parts representing two developmental phases. The first part illustrates the white matter connectivity in 3- to 4-year-old children (A). The second part depicts the trajectory between 9- to 10-year-old children and adults (B).

At 3 to 4 years of age, the processing of complex syntax is limited to mid and posterior portions of the left superior and middle temporal gyri and sulci. As there are no other syntax-selective areas, the information transfer depends solely on short-distance projections rather than on long-distance connections.

In 9- to 10-year-old children, a completely different picture emerges. The increased efficiency in processing syntactically complex sentences at this age goes along with an extended fronto-temporal connectivity. A dorsal pathway via the SLF/AF propagates syntactic information from the dorsal part of the left IFG into posterior parts of the STG and the MTG. A ventral pathway connecting ventral portions of the left IFG with posterior parts of the STG and the MTG via the IFOF plays a supportive role for the transfer of syntactic information. This dual pathway pattern disappears in adults who show a very focused selectivity for complex syntax in the dorsal IFG, i.e. the left pars opercularis, and the posterior portion of the left superior temporal gyrus. Accordingly, the processing of complex syntax depends exclusively on the SLF/AF rather than on a ventral tract in adults.

# REFERENCES

Abe, K., and Watanabe, D. (2011). Songbirds possess the spontaneous ability to discriminate syntactic rules. *Nat. Neurosci.*, *14(8)*, 1067-1074.

Amaro Jr., E., and Barker, G. J. (2006). Study design in fMRI: basic principles. *Brain Cogn.*, *60(3)*, 220-232.

Amunts, K., Schleicher, A., Ditterich, A., and Zilles, K. (2003). Broca's region: cytoarchitectonic asymmetry and developmental changes. *J. Comp. Neurol.*, *465(1)*, 72-89.

Andersson, J. L. R., Hutton, C., Ashburner, J., Turner, R., and Friston, K. (2001). Modeling geometric deformations in EPI time series. *Neuroimage*, *13(5)*, 903-919.

Anwander, A., Tittgemeyer, M., von Cramon, D. Y., Friederici, A. D., and Knösche, T. R. (2007). Connectivity-Based Parcellation of Broca's Area. *Cereb. Cortex*, *17(4)*, 816-825.

Arthurs, O. J., and Boniface, S. (2002). How well do we understand the neural origins of the fMRI BOLD signal? *Trends Neurosci.*, *25(1)*, 27-31.

Bandettini, P. A., Kwong, K. K., Davis, T. L., Tootell, R. B., Wong, E. C., Fox, P. T., Belliveau, J. W., Weisskoff, R. M., and Rosen, B. R. (1997). Characterization of cerebral blood oxygenation and flow changes during prolonged brain activation. *Hum. Brain Mapp.*, *5(2)*, 93-109.

Bandettini, P. A., Wong, E. C., Hinks, R. S., Tikofsky, R. S., and Hyde, J. S. (1992). Time course EPI of human brain function during task activation. *Magn. Reson. Med.*, *25(2)*, 390-397.

Basser, P. J., Mattiello, J., and Le Bihan, D. (1994a). Estimation of the effective self-diffusion tensor from the NMR spin echo. *J. Magn. Reson. B*, *103(3)*, 247-254.

Basser, P. J., Mattiello, J., and Le Bihan, D. (1994b). MR Diffusion Tensor Spectroscopy and Imaging. *Biophysical Journal*, *66(1)*, 259-267.

Ben-Shachar, M., Hendler, T., Kahn, I., Ben-Bashat, D., and Grodzinsky, Y. (2003). The neural reality of syntactic transformations: evidence from functional magnetic resonance imaging. *Psychol. Sci.*, *14(5)*, 433-440.

Ben-Shachar, M., Palti, D., and Grodzinsky, Y. (2004). Neural correlates of syntactic movement: converging evidence from two fMRI experiments. *Neuroimage*, *21(4)*, 1320-1336.

Berry, E., and Bulpitt, A. (2009). Fundamentals of MRI. (New York: Taylor&Francis).

Birn, R. M., Bandettini, P. A., Cox, R. W., Jesmanowicz, A., and Shaker, R. (1998). Magnetic field changes in the human brain due to swallowing or speaking. *Magn. Reson. Med.*, *40(1)*, 55-60.

Birn, R. M., Bandettini, P. A., Cox, R. W., and Shaker, R. (1999). Event-related fMRI of tasks involving brief motion. *Hum. Brain Mapp.*, *7(2)*, 106-114.

Bloch, F., Hansen, W. W., and Packard, M. (1946). Nuclear Induction. *Phys. Rev.*, *69(3-4)*, 127.

Bogels, S., Schriefers, H., Vonk, W., Chwilla, D. J., and Kerkhofs, R. (2010). The interplay between prosody and syntax in sentence processing: the case of subject- and object-control verbs. *J. Cogn. Neurosci.*, *22(5)*, 1036-1053.

Bookheimer, S. (2002). Functional MRI of language: new approaches to understanding the cortical organization of semantic processing. *Annu. Rev. Neurosci.*, *25*, 151-188.

Bornkessel, I., and Schlesewsky, M. (2006). Generalised semantic roles and syntactic templates: A new framework for language comprehension. In: Semantic role universals and argument linking. Theoretical, typological and psycholinguistic perspectives (Ed.: Bornkessel, I., Schlesewsky, M., Comrie, B. & Friederici, A.D.), 327-353, (Berlin: Mouton de Gruyter).

Bornkessel, I., and Schlesewsky, M. (2006). The extended argument dependency model: a neurocognitive approach to sentence comprehension across languages. *Psychol. Rev.*, *113(4)*, 787-821.

Brandt, S., Diessel, H., and Tomasello, M. (2008). The acquisition of German relative clauses: a case study. *J. Child Lang.*, *35(2)*, 325-348.

Brauer, J., Anwander, A., and Friederici, A. D. (2011). Neuroanatomical prerequisites for language functions in the maturing brain. *Cereb. Cortex*, *21(2)*, 459-466.

Brauer, J., and Friederici, A. D. (2007). Functional neural networks of semantic and syntactic processes in the developing brain. *J. Cogn. Neurosci.*, *19(10)*, 1609-1623.

Brauer, J., Neumann, J., and Friederici, A. D. (2008). Temporal dynamics of perisylvian activation during language processing in children and adults. *Neuroimage*, *41(4)*, 1484-1492.

Broca, P. (1863). Localisations des fonctions cérébrales. Siège de la faculté du langage articulé. *Bulletin de la Société d' Anthropologie de Paris*, *4*, 200-204.

Brown, M. A., and Semelka, R. C. (2010). MRI. Basic Principles and Applications. (Hoboken, NJ: Wiley-Blackwell).

Buckner, R. L., Goodman, J., Burock, M., Rotte, M., Koutstaal, W., Schacter, D., Rosen, B., and Dale, A. M. (1998). Functional-anatomic correlates of object priming in humans revealed by rapid presentation event-related fMRI. *Neuron, 20(2)*, 285-296.

Buxton, R. B. (2009). Introduction to Functional Magnetic Resonance Imaging. Principles and Techniques. (Cambridge: Cambridge University Press).

Buxton, R. B., and Frank, L. R. (1997). A model for the coupling between cerebral blood flow and oxygen metabolism during neural stimulation. *J. Cereb. Blood Flow Metab.*, *17(1)*, 64-72.

Buxton, R. B., Uludag, K., Dubowitz, D. J., and Liu, T. T. (2004). Modeling the hemodynamic response to brain activation. *Neuroimage*, *23(1)*, 220-233.

Buxton, R. B., Wong, E. C., and Frank, L. R. (1998). Dynamics of blood flow and oxygenation changes during brain activation: the balloon model. *Magn. Reson. Med.*, *39(6)*, 855-864.

Byars, A. W., Holland, S. K., Strawsburg, R. H., Bommer, W., Dunn, R. S., Schmithorst, V. J., and Plante, E. (2002). Practical aspects of conducting large-scale functional magnetic resonance imaging studies in children. *J. Child Neurol.*, *17(12)*, 885-890.

Caplan, D., Chen, E., and Waters, G. (2008). Task-dependent and task-independent neurovascular responses to syntactic processing. *Cortex*, *44(3)*, 257-275.

Catani, M., Jones, D. K., and ffytche, D. H. (2005). Perisylvian language networks of the human brain. *Ann. Neurol.*, *57(1)*, 8-16.

Constable, R. T., Pugh, K. R., Berroya, E., Mencl, W. E., Westerveld, M., Ni, W., and Shankweiler, D. (2004). Sentence complexity and input modality effects in sentence comprehension: an fMRI study. *Neuroimage*, *22(1)*, 11-21.

Cooke, A., Zurif, E. B., DeVita, C., Alsop, D., Koenig, P., Detre, J., Gee, J., Pinango, M., Balogh, J., and Grossman, M. (2002). Neural basis for sentence comprehension: grammatical and short-term memory components. *Hum. Brain Mapp.*, *15(2)*, 80-94.

Correa, L. M. S. (1995). An Alternative Assessment of Childrens Comprehension of Relative Clauses. *J. Psycholinguist. Res.*, *24(3)*, 183-203.

Cox, R. W. (1996). AFNI: Software for analysis and visualization of functional magnetic resonance neuroimages. *Comput. Biomed. Res.*, *29(3)*, 162-173.

D'Esposito, M., Deouell, L. Y., and Gazzaley, A. (2003). Alterations in the BOLD fMRI signal with ageing and disease: a challenge for neuroimaging. *Nat. Rev. Neurosci.*, *4(11)*, 863-872.

Dale, A. M., and Buckner, R. L. (1997). Selective averaging of rapidly presented individual trials using fMRI. *Hum. Brain Mapp.*, *5(5)*, 329-340.

Damadian, R. (1971). Tumor detection by nuclear magnetic resonance. *Science*, *171(3976)*, 1151-1153.

Darwin, C. R. (1871). The descent of man, and selection in relation to sex. (London: John Murray).

Dehaene-Lambertz, G., Hertz-Pannier, L., and Dubois, J. (2006). Nature and nurture in language acquisition: anatomical and functional brain-imaging studies in infants. *Trends Neurosci.*, *29(7)*, 367-373.

Dikker, S., Rabagliati, H., and Pylkkänen, L. (2009). Sensitivity to syntax in visual cortex. *Cognition*, *110(3)*, 293-321.

Donaldson, D. I., Petersen, S. E., Ollinger, J. M., and Buckner, R. L. (2001). Dissociating state and item components of recognition memory using fMRI. *Neuroimage*, *13(1)*, 129-142.

Dubois, J., Hertz-Pannier, L., Cachia, A., Mangin, J. F., Le Bihan, D., and Dehaene-Lambertz, G. (2009). Structural asymmetries in the infant language and sensori-motor networks. *Cereb. Cortex*, *19(2)*, 414-423.

Duffau, H., Gatignol, P., Moritz-Gasser, S., and Mandonnet, E. (2009). Is the left uncinate fasciculus essential for language? *J. Neurol.*, *256(3)*, 382-389.

Eckstein, K., and Friederici, A. D. (2006). It's early: event-related potential evidence for initial interaction of syntax and prosody in speech comprehension. *J. Cogn. Neurosci.*, *18(10)*, 1696-1711.

Fedorenko, E., Piantadosi, S., and Gibson, E. (2012). Processing relative clauses in supportive contexts. *Cogn. Sci., 36(3)*, 471-497.

Fiebach, C. J., Schlesewsky, M., Lohmann, G., von Cramon, D. Y., and Friederici, A. D. (2005). Revisiting the role of Broca's area in sentence processing: syntactic integration versus syntactic working memory. *Hum. Brain Mapp.*, *24(2)*, 79-91.

Fitch, W. T., and Hauser, M. D. (2004). Computational constraints on syntactic processing in a nonhuman primate. *Science*, *303(5656)*, 377-380.

Flöel, A., de Vries, M. H., Scholz, J., Breitenstein, C., and Johansen-Berg, H. (2009). White matter integrity in the vicinity of Broca's area predicts grammar learning success. *Neuroimage*, *47(4)*, 1974-1981.

Fonov, V., Evans, A. C., Botteron, K., Almli, C. R., McKinstry, R. C., Collins, D. L., and Brain Development Cooperative Group (2011). Unbiased average age-appropriate atlases for pediatric studies. *Neuroimage*, *54(1)*, 313-327.

Fox, A. V. (2011). *TROG-D.* Test zur Überprüfung des Grammatikverständnisses. (Idstein: Schulz-Kirchner).

Friederici, A. D. (1983). Children's sensitivity to function words during sentence comprehension. *Linguistics*, *21*, 717-739.

Friederici, A. D. (2002). Towards a neural basis of auditory sentence processing. *Trends Cogn. Sci.*, *6(2)*, 78-84.

Friederici, A. D. (2005). Neurophysiological markers of early language acquisition: from syllables to sentences. *Trends Cogn. Sci.*, *9(10)*, 481-488.

Friederici, A. D. (2011). The brain basis of language processing: from structure to function. *Physiol. Rev.*, *91(4)*, 1357-1392.

Friederici, A. D. (2012). Language development and the ontogeny of the dorsal pathway. *Front. Evol. Neurosci.*, *4*, 3, 1-7.

Friederici, A. D., Bahlmann, J., Heim, S., Schubotz, R. I., and Anwander, A. (2006). The brain differentiates human and non-human grammars: functional localization and structural connectivity. *Proc. Natl. Acad. Sci. U S A*, *103(7)*, 2458-2463.

Friederici, A. D., Makuuchi, M., and Bahlmann, J. (2009). The role of the posterior superior temporal cortex in sentence comprehension. *Neuroreport*, *20(6)*, 563-568.

Friederici, A. D., Rüschemeyer, S. A., Hahne, A., and Fiebach, C. J. (2003). The role of left inferior frontal and superior temporal cortex in sentence comprehension: localizing syntactic and semantic processes. *Cereb. Cortex*, *13(2)*, 170-177.

Friederici, A. D., von Cramon, D. Y., and Kotz, S. A. (2007). Role of the corpus callosum in speech comprehension: interfacing syntax and prosody. *Neuron*, *53(1)*, 135-145.

Friederici, A. D., Wang, Y., Herrmann, C. S., Maess, B., and Oertel, U. (2000). Localization of early syntactic processes in frontal and temporal cortical areas: a magnetoencephalographic study. *Hum. Brain Mapp.*, *11(1)*, 1-11.

Friederici, A. D., and Weissenborn, J. (2007). Mapping sentence form onto meaning: The syntax-semantic interface. *Brain Res.*, *1146*, 50-58.

Friedrich, M., and Friederici, A. D. (2005). Lexical priming and semantic integration reflected in the event-related potential of 14-month-olds. *Neuroreport*, *16(6)*, 653-656.

Friedrich, M., Weber, C., and Friederici, A. D. (2004). Electrophysiological evidence for delayed mismatch response in infants at-risk for specific language impairment. *Psychophysiology*, *41(5)*, 772-782.

Friston, K. J. (2007). Statistical parametric mapping: the analysis of functional brain images. (London: Elsevier/Academic Press).

Friston, K. J., Fletcher, P., Josephs, O., Holmes, A., Rugg, M. D., and Turner, R. (1998). Event-related fMRI: characterizing differential responses. *Neuroimage*, *7(1)*, 30-40.

Friston, K. J., Jezzard, P., and Turner, R. (1994). Analysis of Functional MRI Time-Series. *Hum. Brain Mapp.*, *1*, 153-171.

Friston, K. J., Josephs, O., Zarahn, E., Holmes, A. P., Rouquette, S., and Poline, J. (2000). To smooth or not to smooth? Bias and efficiency in fMRI time-series analysis. *Neuroimage*, *12(2)*, 196-208.

Friston, K. J., Rotshtein, P., Geng, J. J., Sterzer, P., and Henson, R. N. (2006). A critique of functional localisers. *Neuroimage*, *30(4)*, 1077-1087.

Friston, K. J., Zarahn, E., Josephs, O., Henson, R. N., and Dale, A. M. (1999). Stochastic designs in event-related fMRI. *Neuroimage*, *10(5)*, 607-619.

Gaillard, W. D., Berl, M. M., Moore, E. N., Ritzl, E. K., Rosenberger, L. R., Weinstein, S. L., Conry, J. A., Pearl, P. L., Ritter, F. F., Sato, S., Vezina, L. G., Vaidya, C. J., Wiggs, E., Fratalli, C., Risse, G., Ratner, N. B., Gioia, G., and Theodore, W. H. (2007). Atypical language in lesional and nonlesional complex partial epilepsy. *Neurology*, *69(18)*, 1761-1771.

Galantucci, S., Tartaglia, M. C., Wilson, S. M., Henry, M. L., Filippi, M., Agosta, F., Dronkers, N. F., Henry, R. G., Ogar, J. M., Miller, B. L., and Gorno-Tempini, M. L. (2011). White matter damage in primary progressive aphasias: a diffusion tensor tractography study. *Brain*, *134(10)*, 3011-3029.

Gentner, T. Q., Fenn, K. M., Margoliash, D., and Nusbaum, H. C. (2006). Recursive syntactic pattern learning by songbirds. *Nature*, *440(7088)*, 1204-1207.

Glasser, M. F., and Rilling, J. K. (2008). DTI tractography of the human brain's language pathways. *Cereb. Cortex*, *18(11)*, 2471-2482.

Grainger, J., Dufau, S., Montant, M., Ziegler, J. C., and Fagot, J. (2012). Orthographic processing in baboons (Papio papio). *Science*, *336(6078)*, 245-248.

Griffiths, J. D., Marslen-Wilson, W. D., Stamatakis, E. A., and Tyler, L. K. (2012). Functional Organization of the Neural Language System: Dorsal and Ventral Pathways Are Critical for Syntax. *Cereb. Cortex*, advance access, doi: 10.1093/cercor/bhr386.

Griswold, M. A., Jakob, P. M., Heidemann, R. M., Nittka, M., Jellus, V., Wang, J., Kiefer, B., and Haase, A. (2002). Generalized autocalibrating partially parallel acquisitions (GRAPPA). *Magn. Reson. Med.*, *47(6)*, 1202-1210.

Grodzinsky, Y. (2000). The neurology of syntax: language use without Broca's area. *Behav. Brain Sci.*, *23(1)*, 1-21.

Grodzinsky, Y., and Friederici, A. D. (2006). Neuroimaging of syntax and syntactic processing. *Curr. Opin. Neurobiol.*, *16(2)*, 240-246.

Hagoort, P. (2005). On Broca, brain, and binding: a new framework. *Trends Cogn. Sci.*, *9(9)*, 416-423.

Hahne, A., Eckstein, K., and Friederici, A. D. (2004). Brain signatures of syntactic and semantic processes during children's language development. *J. Cogn. Neurosci.*, *16(7)*, 1302-1318.

Hahne, A., and Friederici, A. D. (1999). Electrophysiological evidence for two steps in syntactic analysis. Early automatic and late controlled processes. *J. Cogn. Neurosci.*, *11(2)*, 194-205.

Hajnal, J. V., Myers, R., Oatridge, A., Schwieso, J. E., Young, I. R., and Bydder, G. M. (1994). Artifacts due to stimulus correlated motion in functional imaging of the brain. *Magn. Res. Med.*, *31(3)*, 283-291.

Hashemi, R. H., Bradley, W. G., and Lisanti, C. L. (2010). MRI. The Basics. (Philadelphia: Lippincott Williams & Wilkins).

Hickok, G., and Poeppel, D. (2007). The cortical organization of speech processing. *Nat. Rev. Neurosci.*, *8(5)*, 393-402.

Humphries, C., Binder, J. R., Medler, D. A., and Liebenthal, E. (2007). Time course of semantic processes during sentence comprehension: an fMRI study. *Neuroimage*, *36(3)*, 924-932.

Humphries, C., Love, T., Swinney, D., and Hickok, G. (2005). Response of anterior temporal cortex to syntactic and prosodic manipulations during sentence processing. *Hum. Brain Mapp.*, *26(2)*, 128-138.

James, W. (1890). The principles of psychology. (London: Macmillan).

Jenkinson, M., Bannister, P., Brady, M., and Smith, S. (2002). Improved optimization for the robust and accurate linear registration and motion correction of brain images. *Neuroimage*, *17(2)*, 825-841.

Josephs, O., Turner, R., and Friston, K. (1997). Event-related fMRI. *Hum. Brain Mapp.*, *5(4)*, 243-248.

Kety, S. S., and Schmidt, C. F. (1945). The Determination of Cerebral Blood Flow in Man by the Use of Nitrous Oxide in Low Concentrations. *American Journal of Physiology*, *143(1)*, 53-66.

Kety, S. S., and Schmidt, C. F. (1948). The Nitrous Oxide Method for the Quantitative Determination of Cerebral Blood Flow in Man: Theory, Procedure and Normal Values. *The Journal of clinical investigation, 27(4)*, 476-483.

Kidd, E. (2011). The acquisition of relative clauses: typology, processing & function. (Amsterdam: John Benjamins).

Kidd, E., Brandt, S., Lieven, E., and Tomasello, M. (2007). Object relatives made easy: A cross-linguistic comparison of the constraints influencing young children's processing of relative clauses. *Lang. Cogn. Process.*, *22(6)*, 860-897.

Kinno, R., Kawamura, M., Shioda, S., and Sakai, K. L. (2008). Neural correlates of noncanonical syntactic processing revealed by a picture-sentence matching task. *Hum. Brain Mapp.*, *29(9)*, 1015-1027.

Knösche, T. R., Maess, B., and Friederici, A. D. (1999). Processing of syntactic information monitored by brain surface current density mapping based on MEG. *Brain Topogr.*, *12(2)*, 75-87.

Kuhl, P. K. (2010). Brain mechanisms in early language acquisition. *Neuron*, *67(5)*, 713-727.

Kumar, A., Welti, D., and Ernst, R. R. (1975). NMR Fourier Zeugmatography. *J. Magn. Res.*, *18(1)*, 69-83.

Kwong, K. K., Belliveau, J. W., Chesler, D. A., Goldberg, I. E., Weisskoff, R. M., Poncelet, B. P., Kennedy, D. N., Hoppel, B. E., Cohen, M. S., Turner, R., Cheng, H., Brady, T. J., and Rosen, B. R. (1992). Dynamic magnetic resonance imaging of human brain activity during primary sensory stimulation. *Proc. Natl. Acad. Sci. U S A*, *89(12)*, 5675-5679.

Lauterbur, P. C. (1973). Image Formation by Induced Local Interactions - Examples Employing Nuclear Magnetic-Resonance. *Nature*, *242(5394)*, 190-191.

Le Bihan, D., Breton, E., Lallemand, D., Grenier, P., Cabanis, E., and Laval-Jeantet, M. (1986). MR imaging of intravoxel incoherent motions: application to diffusion and perfusion in neurologic disorders. *Radiology*, *161(2)*, 401-407.

Lebel, C., and Beaulieu, C. (2009). Lateralization of the arcuate fasciculus from childhood to adulthood and its relation to cognitive abilities in children. *Hum. Brain Mapp.*, *30(11)*, 3563-3573.

Leroy, F., Glasel, H., Dubois, J., Hertz-Pannier, L., Thirion, B., Mangin, J. F., and Dehaene-Lambertz, G. (2011). Early maturation of the linguistic dorsal pathway in human infants. *J. Neurosci.*, *31(4)*, 1500-1506.

Levitt, M. H. (2008). Spin dynamics: basics of nuclear magnetic resonance. (Hoboken, NJ: John Wiley & Sons).

Li, X., Shu, H., Liu, Y., and Li, P. (2006). Mental representation of verb meaning: behavioral and electrophysiological evidence. *J. Cogn. Neurosci.*, *18(10)*, 1774-1787.

Lichtheim, L. (1885). Über Aphasie. *Deutsches Archiv für klinische Medicin*, *36*, 204-268.

Logothetis, N. K., Pauls, J., Augath, M., Trinath, T., and Oeltermann, A. (2001). Neurophysiological investigation of the basis of the fMRI signal. *Nature*, *412(6843)*, 150-157.

Lohmann, G., Muller, K., Bosch, V., Mentzel, H., Hessler, S., Chen, L., Zysset, S., and von Cramon, D. Y. (2001). LIPSIA - a new software system for the evaluation of functional magnetic resonance images of the human brain. *Comput. Med. Imag. Graph.*, *25(6)*, 449-557.

Makuuchi, M., Bahlmann, J., Anwander, A., and Friederici, A. D. (2009). Segregating the core computational faculty of human language from working memory. *Proc. Natl. Acad. Sci. U S A*, *106(20)*, 8362-8367.

Malonek, D., and Grinvald, A. (1996). Interactions between electrical activity and cortical microcirculation revealed by imaging spectroscopy: implications for functional brain mapping. *Science*, *272(5261)*, 551-554.

Männel, C., and Friederici, A. D. (2009). Pauses and intonational phrasing: ERP studies in 5-month-old German infants and adults. *J. Cogn. Neurosci.*, *21(10)*, 1988-2006.

Männel, C., and Friederici, A. D. (2011). Intonational phrase structure processing at different stages of syntax acquisition: ERP studies in 2-, 3-, and 6-year-old children. *Dev. Sci.*, *14(4)*, 786-798.

Mansfield, P. (1977). Multi-Planar Image-Formation Using NMR Spin Echoes. *J. Phys. C Sol. State Phys.*, *10(3)*, 55-58.

Mansfield, P., and Grannell, P. K. (1973). NMR Diffraction in Solids. *J. Phys. C Sol. State Phys.*, *6(22)*, 422-426.

McDaniel, D., McKee, C., and Cairns, H. S. (1996). Methods for assessing children's syntax, language, speech, and communication. (Cambridge, Mass.: MIT Press).

Melchers, P., and Preuss, U. (2009). Kaufman Assessment Battery for Children, Deutsche Version. (Frankfurt am Main: Pearson Assessment).

Moore-Parks, E. N., Burns, E. L., Bazzill, R., Levy, S., Posada, V., and Muller, R. A. (2010). An fMRI study of sentence-embedded lexical-semantic decision in children and adults. *Brain Lang.*, *114(2)*, 90-100.

Mori, S. (2007). Introduction to Diffusion Tensor Imaging. (Amsterdam: Elsevier / Academic Press).

Mori, S., Wakana, S., and Van Zijl, P. C. M. (2005). MRI atlas of human white matter. (Amsterdam: Elsevier).

Moritani, T., Westesson, P.-L., and Ekholm, S. (2009). Diffusion-Weighted MR Imaging of the Brain. (Heidelberg: Springer).

Musso, M., Moro, A., Glauche, V., Rijntjes, M., Reichenbach, J., Buchel, C., and Weiller, C. (2003). Broca's area and the language instinct. *Nat. Neurosci.*, *6(7)*, 774-781.

Muzik, O., Chugani, D. C., Juhasz, C., Shen, C., and Chugani, H. T. (2000). Statistical parametric mapping: assessment of application in children. *Neuroimage*, *12(5)*, 538-549.

Näätänen, R., Lehtokoski, A., Lennes, M., Cheour, M., Huotilainen, M., Iivonen, A., Vainio, M., Alku, P., Ilmoniemi, R. J., Luuk, A., Allik, J., Sinkkonen, J., and Alho, K. (1997). Language-specific phoneme representations revealed by electric and magnetic brain responses. *Nature*, *385(6615)*, 432-434.

Newman, S. D. (2012). The homophone effect during visual word recognition in children: an fMRI study. *Psychol. Res.*, *76(3)*, 280-291.

Newman, S. D., Ikuta, T., and Burns Jr., T. (2010). The effect of semantic relatedness on syntactic analysis: An fMRI study. *Brain Lang.*, *113(2)*, 51-58.

Nunez, S. C., Dapretto, M., Katzir, T., Starr, A., Bramen, J., Kan, E., Bookheimer, S., and Sowell, E. R. (2011). FMRI of syntactic processing in typically developing children: structural correlates in the inferior frontal gyrus. *Dev. Cogn. Neurosci.*, *1(3)*, 313-323.

O'Shaughnessy, E. S., Berl, M. M., Moore, E. N., and Gaillard, W. D. (2008). Pediatric functional magnetic resonance imaging (fMRI): issues and applications. *J. Child Neurol.*, *23(7)*, 791-801.

Oberecker, R., and Friederici, A. D. (2006). Syntactic event-related potential components in 24-month-olds' sentence comprehension. *Neuroreport*, *17(10)*, 1017-1021.

Oberecker, R., Friedrich, M., and Friederici, A. D. (2005). Neural correlates of syntactic processing in two-year-olds. *J. Cogn. Neurosci.*, *17(10)*, 1667-1678.

Obleser, J., and Kotz, S. A. (2010). Expectancy constraints in degraded speech modulate the language comprehension network. *Cereb. Cortex*, *20(3)*, 633-640.

Obleser, J., Scott, S. K., and Eulitz, C. (2006). Now you hear it, now you don't: transient traces of consonants and their nonspeech analogues in the human brain. *Cereb. Cortex*, *16(8)*, 1069-1076.

Ogawa, S., Lee, T. M., Nayak, A. S., and Glynn, P. (1990). Oxygenation-sensitive contrast in magnetic resonance image of rodent brain at high magnetic fields. *Magn. Reson. Med.*, *14(1)*, 68-78.

Ogawa, S., Tank, D. W., Menon, R., Ellermann, J. M., Kim, S. G., Merkle, H., and Ugurbil, K. (1992). Intrinsic signal changes accompanying sensory stimulation: functional brain mapping with magnetic resonance imaging. *Proc. Natl. Acad. Sci. U S A*, *89(13)*, 5951-5955.

Oldfield, R. C. (1971). The assessment and analysis of handedness: the Edinburgh inventory. *Neuropsychologia*, *9(1)*, 97-113.

Paling, M. R., and Brookeman, J. R. (1986). Respiration artifacts in MR imaging: reduction by breath holding. *J. Comput. Assist. Tomogr.*, *10(6)*, 1080-1082.

Pallier, C., Devauchelle, A. D., and Dehaene, S. (2011). Cortical representation of the constituent structure of sentences. *Proc. Natl. Acad. Sci. U S A*, *108(6)*, 2522-2527.

Papoutsi, M., Stamatakis, E. A., Griffiths, J., Marslen-Wilson, W. D., and Tyler, L. K. (2011). Is left fronto-temporal connectivity essential for syntax? Effective connectivity, tractography and performance in left-hemisphere damaged patients. *Neuroimage*, *58(2)*, 656-664.

Pauling, L., and Coryell, C. D. (1936). The magnetic properties and structure of hemoglobin, oxyhemoglobin and carbonmonoxyhemoglobin. *Proc. Natl. Acad. Sci. U S A*, *22*, 210-216.

Perani, D., Saccuman, M. C., Scifo, P., Anwander, A., Spada, D., Baldoli, C., Poloniato, A., Lohmann, G., and Friederici, A. D. (2011). Neural language networks at birth. *Proc. Natl. Acad. Sci. U S A*, *108(38)*, 16056-16061.

Purcell, E. M., Torrey, H. C., and Pound, R. V. (1946). Resonance Absorption by Nuclear Magnetic Moments in a Solid. *Phys. Rev.*, *69(1-2)*, 37-38.

Qayyum, A. (2009). Diffusion-weighted Imaging in the Abdomen and Pelvis: Concepts and Applications. *Radiographics*, *29*, 1797-1810.

Raichle, M. E., and Mintun, M. A. (2006). Brain work and brain imaging. *Annu. Rev. Neurosci.*, *29*, 449-476.

Rauschecker, J. P., and Scott, S. K. (2009). Maps and streams in the auditory cortex: nonhuman primates illuminate human speech processing. *Nat. Neurosci.*, *12(6)*, 718-724.

Reilly, J., and Peelle, J. E. (2008). Effects of semantic impairment on language processing in semantic dementia. *Semin. Speech Lang.*, *29(1)*, 32-43.

Rilling, J. K., Glasser, M. F., Preuss, T. M., Ma, X., Zhao, T., Hu, X., and Behrens, T. E. (2008). The evolution of the arcuate fasciculus revealed with comparative DTI. *Nat. Neurosci.*, *11(4)*, 426-428.

Rogalsky, C., and Hickok, G. (2009). Selective attention to semantic and syntactic features modulates sentence processing networks in anterior temporal cortex. *Cereb. Cortex*, *19(4)*, 786-796.

Rolheiser, T., Stamatakis, E. A., and Tyler, L. K. (2011). Dynamic processing in the human language system: synergy between the arcuate fascicle and extreme capsule. *J. Neurosci.*, *31(47)*, 16949-16957.

Rombouts, S. A., Damoiseaux, J. S., Goekoop, R., Barkhof, F., Scheltens, P., Smith, S. M., and Beckmann, C. F. (2009). Model-free group analysis shows altered BOLD fMRI networks in dementia. *Hum. Brain Mapp.*, *30(1)*, 256-266.

Rosch, E. (1975). Cognitive Representations of Semantic Categories. *J. Exp. Psychol. Gen.*, *104(3)*, 192-233.

Rosen, B. R., Buckner, R. L., and Dale, A. M. (1998). Event-related functional MRI: past, present, and future. *Proc. Natl. Acad. Sci. U S A*, *95(3)*, 773-780.

Roy, C. S., and Sherrington, C. S. (1890). On the Regulation of the Blood-supply of the Brain. *J. Physiol.*, *11(1-2)*, 85-158.

Sakai, K. L. (2005). Language acquisition and brain development. *Science*, *310(5749)*, 815-819.

Sammler, D., Kotz, S. A., Eckstein, K., Ott, D. V., and Friederici, A. D. (2010). Prosody meets syntax: the role of the corpus callosum. *Brain*, *133(9)*, 2643-2655.

Santi, A., and Grodzinsky, Y. (2007). Working memory and syntax interact in Broca's area. *Neuroimage*, *37(1)*, 8-17.

Santi, A., and Grodzinsky, Y. (2010). FMRI adaptation dissociates syntactic complexity dimensions. *Neuroimage*, *51(4)*, 1285-1293.

Saur, D., Kreher, B. W., Schnell, S., Kummerer, D., Kellmeyer, P., Vry, M. S., Umarova, R., Musso, M., Glauche, V., Abel, S., Huber, W., Rijntjes, M., Hennig, J., and Weiller, C. (2008). Ventral and dorsal pathways for language. *Proc. Natl. Acad. Sci. U S A*, *105(46)*, 18035-18040.

Schipke, C. S., Friederici, A. D., and Oberecker, R. (2011). Brain responses to case-marking violations in German preschool children. *Neuroreport*, *22(16)*, 850-854.

Scott, S. K., and Johnsrude, I. S. (2003). The neuroanatomical and functional organization of speech perception. *Trends Neurosci.*, *26(2)*, 100-107.

Silva Pereyra, J. F., Klarman, L., Lin, L. J., and Kuhl, P. K. (2005). Sentence processing in 30-month-old children: an event-related potential study. *Neuroreport*, *16(6)*, 645-648.

Smith, S. M. (2002). Fast robust automated brain extraction. *Hum. Brain Mapp.*, *17(3)*, 143-155.

Smith, S. M., Jenkinson, M., Johansen-Berg, H., Rueckert, D., Nichols, T. E., Mackay, C. E., Watkins, K. E., Ciccarelli, O., Cader, M. Z., Matthews, P. M., and Behrens, T. E. (2006). Tract-based spatial statistics: voxelwise analysis of multi-subject diffusion data. *Neuroimage*, *31(4)*, 1487-1505.

Smith, S. M., Jenkinson, M., Woolrich, M. W., Beckmann, C. F., Behrens, T. E., Johansen-Berg, H., Bannister, P. R., De Luca, M., Drobnjak, I., Flitney, D. E., Niazy, R. K., Saunders, J., Vickers, J., Zhang, Y., De Stefano, N., Brady, J. M., and Matthews, P. M. (2004). Advances in functional and structural MR image analysis and implementation as FSL. *Neuroimage*, *23 (S1)*, S208-219.

Snijders, T. M., Vosse, T., Kempen, G., Van Berkum, J. J., Petersson, K. M., and Hagoort, P. (2009). Retrieval and unification of syntactic structure in sentence comprehension: an FMRI study using word-category ambiguity. *Cereb. Cortex*, *19(7)*, 1493-1503.

Stehling, M. K., Turner, R., and Mansfield, P. (1991). Echo-planar imaging: magnetic resonance imaging in a fraction of a second. *Science*, *254(5028)*, 43-50.

Steinhauer, K., Alter, K., and Friederici, A. D. (1999). Brain potentials indicate immediate use of prosodic cues in natural speech processing. *Nat. Neurosci.*, *2(2)*, 191-196.

Stejskal, E. O., and Tanner, J. E. (1965). Spin Diffusion Measurements: Spin Echoes in the Presence of a Time-Dependent Field Gradient. *J. Chem. Phys.*, *42(1)*, 288-292.

Talairach, J., and Tournoux, P. (1988). Co-planar stereotactic atlas of the human brain. (New York: Thieme).

Thacker, N. A., Burton, E., Lacey, A. J., and Jackson, A. (1999). The effects of motion on parametric fMRI analysis techniques, *Physiological Measurement*, *20(3)*, 251-263.

Thulborn, K. R., Waterton, J. C., Matthews, P. M., and Radda, G. K. (1982). Oxygenation Dependence of the Transverse Relaxation-Time of Water Protons in Whole-Blood at High-Field. *Biochim. Biophys. Acta*, *714(2)*, 265-270.

Tyler, L. K., Marslen-Wilson, W. D., Randall, B., Wright, P., Devereux, B. J., Zhuang, J., Papoutsi, M., and Stamatakis, E. A. (2011). Left inferior frontal cortex and syntax: function, structure and behaviour in patients with left hemisphere damage. *Brain*, *134(2)*, 415-431.

Vandenberghe, R., Nobre, A. C., and Price, C. J. (2002). The response of left temporal cortex to sentences. *J. Cogn. Neurosci.*, *14(4)*, 550-560.

Vannest, J. J., Karunanayaka, P. R., Altaye, M., Schmithorst, V. J., Plante, E. M., Eaton, K. J., Rasmussen, J. M., and Holland, S. K. (2009). Comparison of fMRI data from passive listening and active-response story processing tasks in children. *J. Magn. Reson. Imaging*, *29(4)*, 971-976.

Wansapura, J. P., Holland, S. K., Dunn, R. S., and Ball, W. S., Jr. (1999) NMR relaxation times in the human brain at 3.0 tesla. *J. Magn. Reson. Imaging*, *9(4)*, 531-538.

Weber, C., Hahne, A., Friedrich, M., and Friederici, A. D. (2004). Discrimination of word stress in early infant perception: electrophysiological evidence. *Cogn. Brain Res.*, *18(2)*, 149-161.

Weisskoff, R. M., Baker, J., Belliveau, J. W., Davis, T. L., Kwong, K. K., and Cohen, M. S. (1993). Power spectrum analysis of functional-weighted MR data: what's in the noise? *Proc. Soc. Magn. Reson. Med.*, *(1)*, 7.

Wernicke, C. (1874). Der aphasische Symptomenkomplex. Eine psychologische Studie auf anatomischer Basis. (Breslau: Cohn & Weigert).

Wilke, M., Lidzba, K., Staudt, M., Buchenau, K., Grodd, W., and Krägeloh-Mann, I. (2005). Comprehensive language mapping in children, using functional magnetic resonance imaging: what's missing counts. *Neuroreport*, *16(9)*, 915-919.

Wilke, M., and Schmithorst, V. J. (2006). A combined bootstrap/histogram analysis approach for computing a lateralization index from neuroimaging data. *Neuroimage*, *33(2)*, 522-530.

Wilson, S. M., Dronkers, N. F., Ogar, J. M., Jang, J., Growdon, M. E., Agosta, F., Henry, M. L., Miller, B. L., and Gorno-Tempini, M. L. (2010). Neural correlates of syntactic processing in the nonfluent variant of primary progressive aphasia. *J. Neurosci.*, *30(50)*, 16845-16854.

Wilson, S. M., Galantucci, S., Tartaglia, M. C., Rising, K., Patterson, D. K., Henry, M. L., Ogar, J. M., DeLeon, J., Miller, B. L., and Gorno-Tempini, M. L. (2011). Syntactic processing depends on dorsal language tracts. *Neuron*, *72(2)*, 397-403.

Yetkin, F. Z., Haughton, V. M., Cox, R. W., Hyde, J., Birn, R. M., Wong, E. C., and Prost, R. (1996). Effect of motion outside the field of view on functional MR. *Am. J. Neuroradiol.*, *17(6)*, 1005-1009.

# LIST OF FIGURES

**Chapter 2**



**Chapter 3**

**Chapter 4**

**Chapter 5**

# LIST OF TABLES

### Chapter 4

## Bibliographic Details

---

Michael A. Skeide

"Syntax and semantics networks in the developing brain"

Universität Leipzig

*Dissertation*

154 Seiten, 185 Literaturangaben, 30 Abbildungen, 2 Tabellen

---

Language comprehension crucially depends on the interplay of syntax and semantics. On the one hand, we have to detect the regularities underlying the architecture of a phrase. On the other hand, we have to relate the meanings of this construct to our world knowledge. So far, we do not know much about how the brain regions and their connections, forming the neurobiological basis of syntax and semantics, change their functional organization in the developing brain. In the present thesis, we reported 2 experiments shedding light on this problem. Using event-related functional magnetic resonance imaging (fMRI) in a cross-sectional design, we demonstrated that 3- and 4-year-old children, in contrast to adults, do not process complex syntax and semantics in independent brain regions. A functional specialization comparable to the mature adult brain is still not present at 6 and 7 years of age. It is only at the end of the 10th year of life that neural selectivity for syntax, similar to that of adults, starts to emerge in the left inferior frontal and the left superior temporal cortex. In a second study, we combined the fMRI measures with diffusion tensor imaging

(DTI) and behavioral measures in order to track the interplay of cortical connectivity and the acquisition of syntax and semantics from 3 years of age into adulthood. We showed that in 3- to 4-year-old children the processing of both types of linguistic information is still limited to the temporal cortex and yet does not depend on long-distance fiber connections with the frontal cortex. An adult-like syntax-specialization of a fronto-temporal dorsal tract, including the superior longitudinal fasciculus (SLF) and the arcuate fasciculus (AF), is only established at 9 to 10 years of age. We discussed our findings as a cascade of functional neural interaction, segregation and shift processes marking the developmental trajectories of the relationship between language acquisition and brain maturation.

# Summary


## Introduction

The unique faculty of human beings to produce and to understand a language requires the mastery of very large and complex combinations of linguistic sub-functions. Syntactic rules, determining how words can be grouped together to form a phrase, and lexical-semantic information, enabling the interpretation of the meaning of an utterance on the basis of our world knowledge, are central higher-order language representations. Although only a tight interplay of both functions guarantees language comprehension, recent functional magnetic resonance imaging (fMRI) studies demonstrated that they are processed in clearly segregated neural networks in the adult brain (Bookheimer, 2002; Newman et al., 2010; Friederici, 2011). Complex syntactic processing, on the one hand, is supported by the pars opercularis of the left inferior frontal gyrus (left IFGoper) (Friederici et al., 2006; Makuuchi et al., 2009; Newman et al., 2010; Wilson et al., 2010) and its dorsal connection to the posterior portion of the left superior temporal gyrus (left pSTG) (Newman et al., 2010; Friederici, 2011) via the superior longitudinal fasciculus (SLF) and the arcuate fasciculus (AF) (Wilson et al., 2011). Semantic processing rather depends on a ventral connection identified as the extreme capsule fiber system (ECFS) (Duffau et al., 2009), linking together the pars triangularis and the pars orbitalis of the left inferior frontal gyrus (left IFGtri and left IFGorb) (Newman et al., 2010) with the left middle and superior temporal gyrus (left MTG/STG) (Friederici, 2011). However, how this functional neural architecture establishes in the course of language acquisition and brain maturation, is not yet understood. The existing studies report an interaction of syntactic and semantic processes at the behavioral level until the age of 9 to 10 years (Friederici, 1983) which is in line with

fMRI studies describing pronounced activation overlaps for both types of linguistic information (Brauer and Friederici, 2007; Nunez et al., 2011). Additionally, anatomical MRI studies suggest a late specialization of the syntax supporting IFG (Amunts et al., 2003) as well as dorsal fronto-temporal white matter fiber tracts (Perani et al., 2011; Leroy et al., 2011; Brauer et al., 2011). Thus, the aim of the present dissertation was to elucidate the developmental changes in the functional organization of fronto-temporal cortical regions and their interconnecting white matter fiber tracts as a function of the acquisition of complex syntactic and semantic representations.

**Experiments**

The present thesis comprises 2 studies building upon each other, an fMRI study including 4 different age groups and a diffusion tensor imaging (DTI) study including 3 different age groups.

In the first experiment, we used event-related fMRI in a cross-sectional design to investigate how hemodynamic activation patterns reflecting syntactic and semantic processes differ in children of 3 to 4 years of age, 6 to 7 years of age and 9 to 10 years of age as well as in adults. At the behavioral level, we employed a 2x2 design manipulating syntactic complexity, on the one hand, by contrasting canonical subject relative clauses ("Where is the [subject], who [verb] the [object]?") with more difficult non-canonical object relative clauses ("Where is the [object], who the [subject] [verb]?") and manipulating semantic plausibility, on the other hand, by contrasting semantically plausible sentences (e.g. "the big wolf, who chases the small rabbit") with semantically implausible sentences (e.g. "the small rabbit, who chases the big wolf") based on world knowledge about natural sizes of animals, constraining the plausibility of cer-

tain actions they perform. This paradigm was implemented in a child-friendly picture selection task.

In the second experiment, we used global and local maxima of hemodynamic activation from the preceding fMRI experiment, related either to syntactic or semantic processing, as starting points for probabilistic fiber tracking in 3- to 4-year-old and 9- to 10-year-old children as well as in adults. In order to further corroborate these findings by disentangling the specific and selective contributions of each of the identified white matter fiber tracts to the propagation of either syntactic or semantic information, we assessed linear dependencies between behavioral measures and anatomical DTI measures.

**Results & Discussion**

Our investigations revealed that syntactic and semantic processes interact in the left mSTG/STS at 3 and 4 years of age suggesting that both functions are not represented in independent brain regions yet. Additionally, no domain-specific selectivity could be detected in this age group when assessing candidate regions of interest along the perisylvian cortex. Taking our DTI results into account as well, we argue that at 3 and 4 years of age, the processing of complex syntax and semantics occurs only within the left temporal cortex and does not yet depend on long-distance fiber tracts connecting the left temporal cortex with the left frontal cortex. Our probabilistic fiber tracking results show that a functionally relevant connection from the left mSTG/STS into the left IFG is not established yet. Further evidence for this observation comes from the infant literature (Perani et al., 2011; Leroy et al., 2011) and from a study on 7-year-old children (Brauer et al., 2011). At the behavioral level, we observed that language comprehension is strongly bound to semantic cues at 3 to 4 years of age. This was indicated by the reaction time data – a significant main effect of

semantic implausibility driving a group x semantic implausibility interaction between groups – and was corroborated in a post-hoc interview where the children reported a semantic task solving strategy.

An interaction effect in the left mSTG/STS was still present at 6 and 7 years of age. However, the activation overlap decreased in the older children, making it possible to isolate a main effect of syntactic complexity in the left pSTG as well as a main effect of semantics in the left mSTG/STS which was accompanied by a significantly increased percent signal change for semantics versus syntax in this region of interest. Although the processing efficiency and speed increased in 6- to 7-year-old children compared to 3- to 4-year-old children, the selectivity for complex syntactic and semantic processes was still not pronounced and also limited to the left temporal cortex. However, this might be different with respect to more simple features from both domains which seem to induce frontal cortical activity, too (Schipke et al., 2011; Brauer et al., 2011).

At 9 to 10 years of age, semantics-independent neural selectivity for complex syntax in the left inferior frontal and the left superior temporal cortex, similar to that of adults (Newman et al, 2010; Friederici, 2011) is established. The 9- to 10-year-old children demonstrated a significant main effect of syntactic complexity in the left IFGtri and also a main effect for semantic implausibility in the left anterior superior temporal gyrus and sulcus (aSTG/STS) (Vandenberghe et al., 2002; Rogalsky and Hickok, 2009) but no interaction effect. This finding is in line with event-related potentials (ERP) data demonstrating the emergence of a fronto-temporally distributed ELAN-P600-like component reflecting syntactic processing from age 7 on (Hahne et al., 2004). We further specified this finding observing significantly higher percent signal change rates for complex syntax versus implausible semantics in the left IFGtri, the left IFGoper and the left pSTG at 9 and 10 years of age. The left IFGtri revealed the highest region-

al selectivity and the only significant blood oxygen level dependency (BOLD) effect at the whole-brain level in 9- to 10-year-old children. Similar observations were also made in adults in different languages (Musso et al., 2003; Santi and Grodzinsky, 2007; Caplan et al., 2008; Kinno et al., 2008; Pallier et al., 2011). However, our adult sample rather showed the highest regional selectivity for complex syntax and the only significant BOLD effect at the whole-brain level in the left IFGoper (Friederici et al., 2006; Makuuchi et al., 2009; Newman et al., 2010; Wilson et al., 2010). A recent fMRI study with 10- to 15-year-old children, reporting syntax-related hemodynamic cortical activity in the left IFGoper (Nunez et al., 2011) and a neuroanatomical study demonstrating that the leftward asymmetry of the IFGoper is only present at the age of 11 (Amunts et al., 2003) suggest that an adult-like selectivity for complex syntax in the left IFGoper but not in the left IFGtri seems to establish during early puberty. Given that adults performed most accurate (ceiling level) and fastest in the task given in our experiment, this dorsal selectivity shift within the left IFG seems to go hand in hand with a higher language processing efficiency.

Both in the adults and the 9- to 10-year-old children we identified a dorsal long-distance fiber tract running to the posterior part of the left STG and the left MTG via the left SLF and the left AF when seeding in the left IFGoper. Remarkably, the fractional anisotropy values in this tract positively correlated with the mean response correctness rates related to syntactically complex sentences both in adults and 9- to 10-year-old children, although this seed was only derived from a local activation maximum in the child sample. Crucially, a ventral tract via the left inferior fronto-occipital fasciculus (IFOF), which we isolated in 9- to 10-year-old children using a seed derived from the actual global maximum, did not reveal any correlations. This observation supports a previous DTI patient study showing that syntactic processing depends on dorsal rather than ventral language tracts (Wilson et al., 2011). Additionally, this finding provides

further evidence for the proposed dorsal selectivity shift within the left IFG given that the left SLF/AF connects the left IFGoper with the left superior and middle temporal cortex.

Even at age 9 and 10, children still seem to be more bound to semantic cues in the speech input than adults are. They might still automatically co-process semantic features of an utterance although their syntax processing system is already highly developed. This view is in line with findings from the behavioral literature (Friederici, 1983), but has to be further concretized in future studies. Evidence for the involvement of the anterior portion of the left superior temporal gyrus (left aSTG) in semantic processing, as seen in a BOLD main effect in 9- to 10-year-old children but not in adults, has been previously reported in the adult literature (Vandenberghe et al., 2002; Rogalsky and Hickok, 2009) and was supported by patient data (Reilly and Peelle, 2008). Probabilistic fiber tracking revealed a connection between this region and the orbitofrontal cortex via a ventral pathway including the uncinate fasciculus. The involvement of this tract in semantic processing has already been discussed in a recent study in adults (Duffau et al., 2009) but needs to be further investigated in future studies.

Taken together, we see clear developmental differences both in the functional representations of syntax and semantics and in their structural underpinnings indicating a tight interplay between language acquisition and brain maturation.

# Zusammenfassung

## Einleitung

Die einzigartige Sprachfähigkeit des Menschen setzt die Beherrschung umfangreicher und komplexer linguistischer Subfunktionen voraus. Syntaktische Regeln, die festlegen wie Wörter zu Phrasen kombiniert werden können, und lexikalisch-semantische Informationen, die es uns vor dem Hintergrund unseres Weltwissens ermöglichen, die Bedeutung einer Aussage zu interpretieren, sind grundlegende höhere sprachliche Repräsentationen. Obwohl nur das enge Zusammenspiel beider Funktionen Sprachverständnis sicherstellt, werden sie im erwachsenen Gehirn in klar voneinander abgegrenzten neuronalen Netzwerken verarbeitet, was unter Einsatz funktionaler Magnetresonanztomografie (fMRT) gezeigt werden konnte (Bookheimer, 2002; Newman et al., 2010; Friederici, 2011). Komplexe Syntax wird im pars opercularis des linken inferioren frontalen gyrus (linker IFGoper) (Friederici et al., 2006; Makuuchi et al., 2009; Newman et al., 2010; Wilson et al., 2010) und dem posterioren Anteil des linken superioren temporalen gyrus (linker pSTG) (Newman et al., 2010; Friederici, 2011) verarbeitet, die über den superioren longitudinalen fasciculus (SLF) und den fasciculus arcuatus (AF) dorsal miteinander verbunden sind (Wilson et al., 2011). Semantische Verarbeitung findet hingegen im pars triangularis und im pars orbitalis des linken inferioren frontalen gyrus (linker IFGtri und linker IFGorb) (Newman et al., 2010) statt, die ventral über die capsula extrema (ECFS) (Duffau et al., 2009) mit dem linken mittleren und superioren temporalen gyrus (linker MTG/STG) verbunden sind (Friederici, 2011). Wenig ist bisher darüber bekannt, wie sich diese funktionale neuronale Architektur im Verlauf von Spracherwerb und Gehirnentwicklung ausbildet. In behavioralen Studien wird beschrieben, dass syntaktische und semantische Prozesse bis zu

einem Alter von 9 bis 10 Jahren miteinander interagieren (Friederici, 1983). Dieser Befund ist im Einklang mit fMRT Studien, in denen weitgehend überlappende Aktivierungen für beide Arten linguistischer Informationen berichtet werden (Brauer and Friederici, 2007; Nunez et al., 2011) und auch mit strukturellen MRT Studien, in denen gezeigt wurde, dass sich sowohl der IFG (Amunts et al., 2003) als auch dorsale frontotemporale Nervenfaserbündel spät auf die Syntaxverarbeitung spezialisieren (Perani et al., 2011; Leroy et al., 2011, Brauer et al., 2011). Das Ziel der vorliegenden Arbeit war es also, einen Einblick darin zu gewinnen, wie sich die funktionale Organisation frontotemporaler Cortices und deren Faserverbindungen während des Erwerbs komplexer syntaktischer und semantischer Repräsentationen verändert.

**Experimente**

Die vorliegende Dissertationsschrift umfasst 2 aufeinander aufbauende Studien, eine fMRT Untersuchung mit 4 verschiedenen Altersgruppen und eine Diffusionstensorbildgebungsstudie (DTI) mit 3 verschiedenen Altersgruppen.

Im ersten Experiment haben wir ereigniskorrelierte fMRT eingesetzt, um querschnittlich zu untersuchen, wie sich hämodynamische Aktivierungsmuster für syntaktische und semantische Prozesse im Alter von 3 bis 4, 6 bis 7 und 9 bis 10 Jahren sowie im Erwachsenenalter voneinander unterscheiden. Dafür haben wir ein 2x2 Experimentaldesign verwendet, bei dem wir zum einen die syntaktische Komplexität von Sätzen manipuliert haben, indem kanonische Subjektrelativsätze („Wo ist der [Subjekt], der den [Objekt] [Verb]?“) schwierigeren nicht kanonischen Objektrelativsätzen („Wo ist der [Objekt], den der [Subjekt] [Verb]?“) gegenüber gestellt wurden und bei dem wir zum anderen die semantische Plausibilität von Sätzen auf der Grundlage von Weltwissen darüber, wie die natürliche Größe von Tieren die Plausibilität bestimmter

Handlungen bestimmt, manipuliert haben, indem plausible Sätze („der große Wolf, der den kleinen Hasen jagt“) implausiblen Sätzen („der kleine Hase, der den großen Wolf jagt“) gegenübergestellt wurden. Dieses Paradigma haben wir in eine kindgerechte „Satz-Bild-Zuordnungs-aufgabe“ eingebettet.

Im zweiten Experiment haben wir globale und lokale Maxima syntax- bzw. semantik-relevanter hämodynamischer Aktivität aus dem fMRT Experiment als Startpunkte für probabilistische Traktografie bei 3- bis 4-jährigen und 9- bis 10-jährigen Kindern sowie bei Erwachsenen benutzt. Um diese Befunde dahingehend zu untermauern, dass der spezifische und selektive Beitrag der jeweiligen Nervenfaserbündel zur Übertragung syntaktischer bzw. semantischer Information ermittelt wird, haben wir außerdem Korrelationen zwischen den behavioralen und den anatomischen Maßen untersucht.

**Ergebnisse & Diskussion**

Unsere Untersuchungen haben ergeben, dass bei 3- bis 4-jährigen Kindern syntaktische und semantische Verarbeitungsvorgänge im linken MTG/STG miteinander inter-agieren, was darauf schließen lässt, dass beide Funktionen noch nicht in voneinander unabhängigen Hirnregionen repräsentiert sind. Zudem wiesen sprachrelevante peri-sylvische „regions of interest“ keine domänenspezifische Selektivität auf. Unsere DTI Ergebnisse legen nahe, dass syntaktische und semantische Verarbeitung im Alter von 3 bis 4 Jahren auf den linken temporalen Cortex begrenzt und noch unabhängig von langen Faserverbindungen mit dem linken frontalen Cortex sind. Die Traktografie Daten zeigen, dass eine funktional relevante Verbindung zwischen dem linken MTG/STG und dem linken IFG noch nicht besteht. Weitere Indizien dafür finden sich in der Säuglingsliteratur (Perani et al., 2011; Leroy et al., 2011) und in einer Studie zu 7-jährigen Kindern (Brauer et al., 2011). Auf der

behavioralen Ebene ließ sich das anhand von Reaktionszeitdaten zeigen, da ein signifikanter Haupteffekt für semantische Implau-sibilität ermittelt wurde, der zu einer Interaktion zwischen Gruppe und semantischer Implausibilität führte. Zusätzlich gestützt wurde dieser Befund im Rahmen einer post hoc Befragung, aus der hervorging, dass bei 3- bis 4-jährigen Kinder eine semantische Strategie der Lösung der Aufgabe zugrunde lag.

Ein Interaktionseffekt im linken mSTG/STS war im Alter von 6 bis 7 Jahren immernoch nachweisbar. Die Aktivierungen überlappten jedoch nicht mehr so stark in dieser Alters-gruppe, sodass es möglich war, sowohl einen Haupteffekt für syntaktische Komplexität im linken pSTG als auch einen Haupteffekt für Semantik im linken mSTG/STS zu iso-lieren. Im linken mSTG/STS haben wir darüber hinaus signifikant höhere Signalstärken bei semantischer gegenüber syntaktischer Verarbeitung beobachtet. Obwohl Verarbeit-ungseffektivität und -geschwindigkeit im Alter von 6 und 7 Jahren höher waren als im Alter von 3 und 4 Jahren, war die Selektivität für komplexe syntaktische und semantische Prozesse nur schwach ausgeprägt und begrenzt auf den linken tempo-ralen Cortex. Das muss allerdings nicht für weniger komplexe Eigenschaften aus beiden Domänen gelten, denen offenbar auch neuronale Aktivität im frontalen Cortex zu-grundeliegen (Schipke et al., 2011; Brauer et al., 2011).

Erst im Alter von 9 bis 10 Jahren zeigt sich eine erwachsenenähnliche semantik-unabhängige neuronale Selektivität für komplexe Syntax im linken inferioren frontalen und im linken superioren temporalen Cortex (Newman et al, 2010; Friederici, 2011). Bei den 9- und 10-jährigen Kindern haben wir sowohl einen signifikanten Haupteffekt für syntaktische Komplexität im linken IFGtri als auch einen Haupteffekt für semantische Implausibilität im anterioren Anteil des linken superioren temporalen gyrus und sulcus (Vandenberghe et al., 2002; Rogalsky and Hickok, 2009), aber keinen Interaktionseffekt ermittelt. Dieser

Befund ist vereinbar mit Daten von ereigniskorrelierten Potentialen (ERP), die zeigen, dass ab 7 Jahren frontotemporal verteilte ELAN-P600-ähnliche Komponenten bei der Syntaxverarbeitung nachweisbar sind. Wir konnten diese Beobachtung weiter stützen, da wir bei den 9- und 10-jährigen Kindern signifikant höhere fMRT Signalstärken für syntaktische gegenüber semantischer Verarbeitung im linken IFGtri, IFGoper und pSTG bestimmt haben. Der linke IFGtri wies dabei die höchste regionale Selektivität und den einzigen globalen blood oxygen level dependency (BOLD) Effekt auf. Ähnliche Beobachtungen sind auch bei Erwachsenen gemacht worden (Musso et al., 2003; Santi and Grodzinsky, 2007; Caplan et al., 2008; Kinno et al., 2008; Pallier et al., 2011). In unserer Stichprobe mit Erwachsenen wies jedoch der linke IFGoper sowohl die höchste regionale Selektivität als auch den einzigen globalen BOLD Effekt auf (Friederici et al., 2006; Makuuchi et al., 2009; Newman et al., 2010; Wilson et al., 2010). Eine fMRT Studie mit 10- bis 15-jährigen Kindern, in der syntaxbezogene hämodynamische kortikale Aktivität im linken IFGoper berichtet wurde (Nunez et al., 2011) sowie eine neuroanatomische Studie, in der nachgewiesen wurde, dass die linksgerichtete Asymmetrie des IFGoper erst im Alter von 11 Jahren ausgeprägt ist, legen nahe, dass sich eine erwachsenenähnliche Selektivität für komplexe Syntax im linken IFGoper und nicht im linken IFGtri während der frühen Pubertät etabliert. Die Beobachtung, dass Erwachsene die in unserem Experiment zu lösende Aufgabe am besten und am schnellsten bearbeitet haben, ist ein Anhaltspunkt dafür, dass die dorsal gerichtete Selektivitätsverschiebung innerhalb des linken IFG Hand in Hand mit einer höheren Sprachverarbeitungseffizienz geht.

Sowohl bei den Erwachsenen als auch bei den 9- bis 10-jährigen Kindern haben wir ein langes dorsales Nervenfaserbündel, den linken SLF und AF, identifiziert, das vom linken IFGoper in den posterioren Anteil des linken STG und MTG führt. Bemerkenswerterweise waren die fraktionalen Anisotropiewerte in

diesem Trakt in beiden Altersgruppen mit dem prozentualen Anteil richtiger Antworten für syntaktisch komplexe Sätze korreliert, obwohl der „seed“ für die Kinder lediglich aus einem lokalen Aktivierungsmaximum gewonnen wurde. Ein ventraler Trakt hingegen, der linke inferiore fronto-occipitale fasciculus (IFOF), ausgehend von einem globalen Maximum im linken IFGtri, war nicht mit behavioralen Maßen korreliert. Diese Beobachtung stützt eine DTI Patientenstudie, in der gezeigt wurde, dass syntaktische Verarbeitung in dorsalen und nicht in ventralen Nervenbahnen erfolgt (Wilson et al., 2011). Darüber hinaus liefert der Befund ein weiteres Indiz für die bereits beschriebene dorsal gerichtete Selektivitätsverschiebung innerhalb des linken IFG, da der linke SLF/AF den linken IFGoper mit dem linken superioren und mittleren temporalen Cortex verbindet.

Sogar im Alter von 9 bis 10 Jahren scheinen Kinder immernoch stärker als Erwachsene an semantische Hinweisreize im sprachlichen Input gebunden zu sein und semantische Merkmale automatisch mitzuverarbeiten, obwohl ihr syntaktisches Verarbeitungssystem bereits hoch entwickelt ist, was auch die behaviorale Literatur nahelegt (Friederici, 1983). Diese Beobachtung muss in Folgestudien konkretisiert werden. Hinweise dafür, dass der anteriore Anteil des linken superioren temporalen gyrus (linker aSTG) an der semantischen Verarbeitung beteiligt ist, was wir anhand eines BOLD Haupteffekts bei den 9- bis 10-jährigen Kindern aber nicht bei den Erwachsenen gesehen haben, finden sich in der Literatur zu erwachsenen Probanden (Vandenberghe et al., 2002; Rogalsky and Hickok, 2009) einschließlich Patienten (Reilly and Peelle, 2008). Unter Einsatz probabilistischer Traktografie haben wir eine ventrale Verbindung zwischen dem linken aSTG und dem frontalen orbitalen Cortex über den fasciculus uncinatus identifiziert. Die Beobachtung, dass dieser Trakt eine Rolle für die Verarbeitung semantischer Information spielt, ist bereits in

einer Erwachsenenstudie diskutiert worden (Duffau et al., 2009), bedarf jedoch weiterer Reproduktionen in Folgestudien.

Insgesamt haben wir klare Entwicklungsunterschiede sowohl hinsichtlich der hirnfunktionalen Repräsentationen von Syntax und Semantik als auch hinsichtlich deren hirnstrukturellen Grundlagen festgestellt, die für einen engen Zusammenhang zwischen Spracherwerb und Gehirnentwicklung sprechen.

# Curriculum Vitae

## Personal details

| | |
|---|---|
| ***Name*** | Michael Artur Skeide |
| ***Date of birth*** | 07 June 1984 |
| ***Place of birth*** | Wernigerode, Germany |

## Education

| | |
|---|---|
| ***since 09/2009*** | PhD student in the Neuropsychology department of the Max Planck Institute for Human Cognitive and Brain Sciences, Leipzig, Germany |
| ***06/2009 – 08/2009*** | Summer School at Harvard University, Cambridge, MA, U.S.A., Courses in Neurobiology and Brain Imaging Methods |
| ***06/2009*** | M. A. (Magister Artium) from Ruprecht-Karls-University, Heidelberg, Germany |
| ***09/2005 – 06/2009*** | Undergraduate studies in Linguistics and Philosophy at the Ruprecht-Karls-University, Heidelberg, Germany |
| ***06/2004*** | A-Levels (Abitur), Gymnasium Stadtfeld, Wernigerode, Germany |

## Professional Experience

***04/2008 – 08/2009*** Student Assistant of Prof. Dr. Arnulf Deppermann, Pragmatics Department, Institute for the German Language, Mannheim, Germany

***09/2008 – 08/2009*** Intern, Department of Cognitive Neuroscience (Prof. Dr. Christian Fiebach), Department of Psychology, Ruprecht-Karls-University, Heidelberg, Germany

# Publikationen, Vorträge, Präsentationen

## Artikel

Skeide, M. A., Brauer, J., and Friederici, A. D. (under review). *Cognitive development means functional neural segregation*.

## Hochschulschriften

Skeide, M. A. (2009). *Protoconversational Conflict Behavior in the Infant's Playground*. Master Thesis, University of Heidelberg, Germany.

## Poster

Skeide, M. A., Brauer, J., and Friederici, A. D. (2012). *Maturational differences in language-relevant frontotemporal white matter fiber tracts*. Poster presented at the 19th Cognitive Neuroscience Society Annual Meeting, Chicago, IL, USA.

Hubert, A., Meyer, L., Skeide, M. A., and Friederici, A. D. (2011). *Childrens' language comprehension abilities correlate with grey matter density in the left inferior parietal lobe*. Poster presented at the 17th Annual HBM Meeting, Quebec City, QC, Canada.

Skeide, M. A., Friederici, A. D., and Brauer, J. (2011). *Brain representations for syntactic and semantic processing in 9- to 10-year old children*. Poster presented at the 41st Annual Meeting of the Society for Neuroscience, Washington, DC, USA.

## Selbstständigkeitserklärung

Hiermit erkläre ich, dass die vorliegende Arbeit ohne unzulässige Hilfe und ohne Verwendung anderer als der angegebenen Hilfsmittel angefertigt wurde und dass die aus fremden Quellen direkt oder indirekt übernommenen Gedanken in der Arbeit als solche kenntlich gemacht worden sind.

Michael A. Skeide Leipzig, den 22. August 2012

## MPI Series in Human Cognitive and Brain Sciences:

1 Anja Hahne
*Charakteristika syntaktischer und semantischer Prozesse bei der auditiven Sprachverarbeitung: Evidenz aus ereigniskorrelierten Potentialstudien*

2 Ricarda Schubotz
*Erinnern kurzer Zeitdauern: Behaviorale und neurophysiologische Korrelate einer Arbeitsgedächtnisfunktion*

3 Volker Bosch
*Das Halten von Information im Arbeitsgedächtnis: Dissoziationen langsamer corticaler Potentiale*

4 Jorge Jovicich
*An investigation of the use of Gradient- and Spin-Echo (GRASE) imaging for functional MRI of the human brain*

5 Rosemary C. Dymond
*Spatial Specificity and Temporal Accuracy in Functional Magnetic Resonance Investigations*

6 Stefan Zysset
*Eine experimentalpsychologische Studie zu Gedächtnisabrufprozessen unter Verwendung der funktionellen Magnetresonanztomographie*

7 Ulrich Hartmann
*Ein mechanisches Finite-Elemente-Modell des menschlichen Kopfes*

8 Bertram Opitz
*Funktionelle Neuroanatomie der Verarbeitung einfacher und komplexer akustischer Reize: Integration haemodynamischer und elektrophysiologischer Maße*

9 Gisela Müller-Plath
*Formale Modellierung visueller Suchstrategien mit Anwendungen bei der Lokalisation von Hirnfunktionen und in der Diagnostik von Aufmerksamkeitsstörungen*

10 Thomas Jacobsen
*Characteristics of processing morphological structural and inherent case in language comprehension*

11 Stefan Kölsch
*Brain and Music*
*A contribution to the investigation of central auditory processing with a new electrophysiological approach*

12 Stefan Frisch
*Verb-Argument-Struktur, Kasus und thematische Interpretation beim Sprachverstehen*

13 Markus Ullsperger
*The role of retrieval inhibition in directed forgetting – an event-related brain potential analysis*

14 Martin Koch
*Measurement of the Self-Diffusion Tensor of Water in the Human Brain*

15 Axel Hutt
*Methoden zur Untersuchung der Dynamik raumzeitlicher Signale*

16 Frithjof Kruggel
*Detektion und Quantifizierung von Hirnaktivität mit der funktionellen Magnetresonanztomographie*

17 Anja Dove
*Lokalisierung an internen Kontrollprozessen beteiligter Hirngebiete mithilfe des Aufgabenwechselparadigmas und der ereigniskorrelierten funktionellen Magnetresonanztomographie*

18 Karsten Steinhauer
*Hirnphysiologische Korrelate prosodischer Satzverarbeitung bei gesprochener und geschriebener Sprache*

19 Silke Urban
*Verbinformationen im Satzverstehen*

20 Katja Werheid
*Implizites Sequenzlernen bei Morbus Parkinson*

21 Doreen Nessler
*Is it Memory or Illusion? Electrophysiological Characteristics of True and False Recognition*

22 Christoph Herrmann
*Die Bedeutung von 40-Hz-Oszillationen für kognitive Prozesse*

23 Christian Fiebach
*Working Memory and Syntax during Sentence Processing.*
*A neurocognitive investigation with event-related brain potentials and functional magnetic resonance imaging*

24 Grit Hein
*Lokalisation von Doppelaufgabendefiziten bei gesunden älteren Personen und neurologischen Patienten*

25 Monica de Filippis
*Die visuelle Verarbeitung unbeachteter Wörter. Ein elektrophysiologischer Ansatz*

26 Ulrich Müller
*Die katecholaminerge Modulation präfrontaler kognitiver Funktionen beim Menschen*

27 Kristina Uhl
*Kontrollfunktion des Arbeitsgedächtnisses über interferierende Information*

28 Ina Bornkessel
*The Argument Dependency Model: A Neurocognitive Approach to Incremental Interpretation*

29 Sonja Lattner
*Neurophysiologische Untersuchungen zur auditorischen Verarbeitung von Stimminformationen*

30 Christin Grünewald
*Die Rolle motorischer Schemata bei der Objektrepräsentation: Untersuchungen mit funktioneller Magnetresonanztomographie*

31 Annett Schirmer
*Emotional Speech Perception: Electrophysiological Insights into the Processing of Emotional Prosody and Word Valence in Men and Women*

32 André J. Szameitat
*Die Funktionalität des lateral-präfrontalen Cortex für die Verarbeitung von Doppelaufgaben*

33 Susanne Wagner
*Verbales Arbeitsgedächtnis und die Verarbeitung ambiger Wörter in Wort- und Satzkontexten*

34 Sophie Manthey
*Hirn und Handlung: Untersuchung der Handlungsrepräsentation im ventralen prämotorischen Cortex mit Hilfe der funktionellen Magnet-Resonanz-Tomographie*

35 Stefan Heim
*Towards a Common Neural Network Model of Language Production and Comprehension: fMRI Evidence for the Processing of Phonological and Syntactic Information in Single Words*

36 Claudia Friedrich
*Prosody and spoken word recognition: Behavioral and ERP correlates*

37 Ulrike Lex
*Sprachlateralisierung bei Rechts- und Linkshändern mit funktioneller Magnetresonanztomographie*

38 Thomas Arnold
*Computergestützte Befundung klinischer Elektroenzephalogramme*

39 Carsten H. Wolters
*Influence of Tissue Conductivity Inhomogeneity and Anisotropy on EEG/MEG based Source Localization in the Human Brain*

40 Ansgar Hantsch
*Fisch oder Karpfen? Lexikale Aktivierung von Benennungsalternative bei der Objektbenennung*

41 Peggy Bungert
*Zentralnervöse Verarbeitung akustischer Informationen Signalidentifikation, Signallateralisation und zeitgebundene Informationsverarbeitung bei Patienten mit erworbenen Hirnschädigungen*

42 Daniel Senkowski
*Neuronal correlates of selective attention: An investigation of electrophysiological brain responses in the EEG and MEG*

43 Gert Wollny
*Analysis of Changes in Temporal Series of Medical Images*

44 Angelika Wolf
*Sprachverstehen mit Cochlea-Implantat: EKP-Studien mit postlingual ertaubten erwachsenen CI-Trägern*

45 Kirsten G. Volz
*Brain correlates of uncertain decisions: Types and degrees of uncertainty*

46 Hagen Huttner
*Magnetresonanztomographische Untersuchungen über die anatomische Variabilität des Frontallappens des menschlichen Großhirns*

47 Dirk Köster
*Morphology and Spoken Word Comprehension: Electrophysiological Investigations of Internal Compound Structure*

48 Claudia A. Hruska
*Einflüsse kontextueller und prosodischer Informationen in der auditorischen Satzverarbeitung: Untersuchungen mit ereigniskorrelierten Hirnpotentialen*

49 Hannes Ruge
*Eine Analyse des raum-zeitlichen Musters neuronaler Aktivierung im Aufgabenwechselparadigma zur Untersuchung handlungssteuernder Prozesse*

50 Ricarda I. Schubotz
*Human premotor cortex: Beyond motor performance*

51 Clemens von Zerssen
*Bewusstes Erinnern und falsches Wiedererkennen: Eine funktionelle MRT Studie neuroanatomischer Gedächtniskorrelate*

52 Christiane Weber
*Rhythm is gonna get you.*
*Electrophysiological markers of rhythmic processing in infants with and without risk for Specific Language Impairment (SLI)*

53 Marc Schönwiesner
*Functional Mapping of Basic Acoustic Parameters in the Human Central Auditory System*

54 Katja Fiehler
*Temporospatial characteristics of error correction*

55 Britta Stolterfoht
*Processing Word Order Variations and Ellipses: The Interplay of Syntax and Information Structure during Sentence Comprehension*

56 Claudia Danielmeier
*Neuronale Grundlagen der Interferenz zwischen Handlung und visueller Wahrnehmung*

57 Margret Hund-Georgiadis
*Die Organisation von Sprache und ihre Reorganisation bei ausgewählten, neurologischen Erkrankungen gemessen mit funktioneller Magnetresonanztomographie – Einflüsse von Händigkeit, Läsion, Performanz und Perfusion*

58 Jutta L. Mueller
*Mechanisms of auditory sentence comprehension in first and second language: An electrophysiological miniature grammar study*

59 Franziska Biedermann
*Auditorische Diskriminationsleistungen nach unilateralen Läsionen im Di- und Telenzephalon*

60 Shirley-Ann Rüschemeyer
*The Processing of Lexical Semantic and Syntactic Information in Spoken Sentences: Neuroimaging and Behavioral Studies of Native and Non-Native Speakers*

61 Kerstin Leuckefeld
*The Development of Argument Processing Mechanisms in German. An Electrophysiological Investigation with School-Aged Children and Adults*

62 Axel Christian Kühn
*Bestimmung der Lateralisierung von Sprachprozessen unter besondere Berücksichtigung des temporalen Cortex, gemessen mit fMRT*

63 Ann Pannekamp
*Prosodische Informationsverarbeitung bei normalsprachlichem und deviantem Satzmaterial: Untersuchungen mit ereigniskorrelierten Hirnpotentialen*

64 Jan Derrfuß
*Functional specialization in the lateral frontal cortex: The role of the inferior frontal junction in cognitive control*

65 Andrea Mona Philipp
*The cognitive representation of tasks – Exploring the role of response modalities using the task-switching paradigm*

66 Ulrike Toepel
*Contrastive Topic and Focus Information in Discourse – Prosodic Realisation and Electrophysiological Brain Correlates*

67 Karsten Müller
*Die Anwendung von Spektral- und Waveletanalyse zur Untersuchung der Dynamik von BOLD-Zeitreihen verschiedener Hirnareale*

68 Sonja A.Kotz
*The role of the basal ganglia in auditory language processing: Evidence from ERP lesion studies and functional neuroimaging*

69 Sonja Rossi
*The role of proficiency in syntactic second language processing: Evidence from event-related brain potentials in German and Italian*

70 Birte U. Forstmann
*Behavioral and neural correlates of endogenous control processes in task switching*

71 Silke Paulmann
*Electrophysiological Evidence on the Processing of Emotional Prosody: Insights from Healthy and Patient Populations*

72 Matthias L. Schroeter
*Enlightening the Brain – Optical Imaging in Cognitive Neuroscience*

73 Julia Reinholz
*Interhemispheric interaction in object- and word-related visual areas*

74 Evelyn C. Ferstl
*The Functional Neuroanatomy of Text Comprehension*

75 Miriam Gade
*Aufgabeninhibition als Mechanismus der Konfliktreduktion zwischen Aufgabenrepräsentationen*

76 Juliane Hofmann
*Phonological, Morphological, and Semantic Aspects of Grammatical Gender Processing in German*

77 Petra Augurzky
*Attaching Relative Clauses in German – The Role of Implicit and Explicit Prosody in Sentence Processing*

78 Uta Wolfensteller
*Habituelle und arbiträre sensomotorische Verknüpfungen im lateralen prämotorischen Kortex des Menschen*

79 Päivi Sivonen
*Event-related brain activation in speech perception: From sensory to cognitive processes*

80 Yun Nan
*Music phrase structure perception: the neural basis, the effects of acculturation and musical training*

81 Katrin Schulze
*Neural Correlates of Working Memory for Verbal and Tonal Stimuli in Nonmusicians and Musicians With and Without Absolute Pitch*

82 Korinna Eckstein
*Interaktion von Syntax und Prosodie beim Sprachverstehen: Untersuchungen anhand ereigniskorrelierter Hirnpotentiale*

83 Florian Th. Siebörger
*Funktionelle Neuroanatomie des Textverstehens: Kohärenzbildung bei Witzen und anderen ungewöhnlichen Texten*

84 Diana Böttger
*Aktivität im Gamma-Frequenzbereich des EEG: Einfluss demographischer Faktoren und kognitiver Korrelate*

85 Jörg Bahlmann
*Neural correlates of the processing of linear and hierarchical artificial grammar rules: Electrophysiological and neuroimaging studies*

86 Jan Zwickel
*Specific Interference Effects Between Temporally Overlapping Action and Perception*

87 Markus Ullsperger
*Functional Neuroanatomy of Performance Monitoring: fMRI, ERP, and Patient Studies*

88 Susanne Dietrich
*Vom Brüllen zum Wort – MRT-Studien zur kognitiven Verarbeitung emotionaler Vokalisationen*

89 Maren Schmidt-Kassow
*What's Beat got to do with ist? The Influence of Meter on Syntactic Processing: ERP Evidence from Healthy and Patient populations*

90 Monika Lück
*Die Verarbeitung morphologisch komplexer Wörter bei Kindern im Schulalter: Neurophysiologische Korrelate der Entwicklung*

91 Diana P. Szameitat
*Perzeption und akustische Eigenschaften von Emotionen in menschlichem Lachen*

92 Beate Sabisch
*Mechanisms of auditory sentence comprehension in children with specific language impairment and children with developmental dyslexia: A neurophysiological investigation*

93 Regine Oberecker
*Grammatikverarbeitung im Kindesalter: EKP-Studien zum auditorischen Satzverstehen*

94 Şükrü Barış Demiral
*Incremental Argument Interpretation in Turkish Sentence Comprehension*

95 Henning Holle
*The Comprehension of Co-Speech Iconic Gestures: Behavioral, Electrophysiological and Neuroimaging Studies*

96 Marcel Braß
*Das inferior frontale Kreuzungsareal und seine Rolle bei der kognitiven Kontrolle unseres Verhaltens*

97 Anna S. Hasting
*Syntax in a blink: Early and automatic processing of syntactic rules as revealed by event-related brain potentials*

98 Sebastian Jentschke
*Neural Correlates of Processing Syntax in Music and Language – Influences of Development, Musical Training and Language Impairment*

99 Amelie Mahlstedt
*The Acquisition of Case marking Information as a Cue to Argument Interpretation in German*
*An Electrophysiological Investigation with Pre-school Children*

100 Nikolaus Steinbeis
*Investigating the meaning of music using EEG and fMRI*

101 Tilmann A. Klein
*Learning from errors: Genetic evidence for a central role of dopamine in human performance monitoring*

102 Franziska Maria Korb
*Die funktionelle Spezialisierung des lateralen präfrontalen Cortex: Untersuchungen mittels funktioneller Magnetresonanztomographie*

103 Sonja Fleischhauer
*Neuronale Verarbeitung emotionaler Prosodie und Syntax: die Rolle des verbalen Arbeitsgedächtnisses*

104 Friederike Sophie Haupt
*The component mapping problem: An investigation of grammatical function reanalysis in differing experimental contexts using eventrelated brain potentials*

105 Jens Brauer
*Functional development and structural maturation in the brain's neural network underlying language comprehension*

106 Philipp Kanske
*Exploring executive attention in emotion: ERP and fMRI evidence*

107 Julia Grieser Painter
*Music, meaning, and a semantic space for musical sounds*

108 Daniela Sammler
*The Neuroanatomical Overlap of Syntax Processing in Music and Language - Evidence from Lesion and Intracranial ERP Studies*

109 Norbert Zmyj
*Selective Imitation in One-Year-Olds: How a Model's Characteristics Influence Imitation*

110 Thomas Fritz
*Emotion investigated with music of variable valence – neurophysiology and cultural influence*

111 Stefanie Regel
*The comprehension of figurative language: Electrophysiological evidence on the processing of irony*

112 Miriam Beisert
*Transformation Rules in Tool Use*

113 Veronika Krieghoff
*Neural correlates of Intentional Actions*

114 Andreja Bubić
*Violation of expectations in sequence processing*

115 Claudia Männel
*Prosodic processing during language acquisition: Electrophysiological studies on intonational phrase processing*

116 Konstanze Albrecht
*Brain correlates of cognitive processes underlying intertemporal choice for self and other*

117 Katrin Sakreida
*Nicht-motorische Funktionen des prämotorischen Kortex: Patientenstudien und funktionelle Bildgebung*

118 Susann Wolff
*The interplay of free word order and pro-drop in incremental sentence processing: Neurophysiological evidence from Japanese*

119 Tim Raettig
*The Cortical Infrastructure of Language Processing: Evidence from Functional and Anatomical Neuroimaging*

120 Maria Golde
*Premotor cortex contributions to abstract and action-related relational processing*

121 Daniel S. Margulies
*Resting-State Functional Connectivity fMRI: A new approach for assessing functional neuroanatomy in humans with applications to neuroanatomical, developmental and clinical questions*

122 Franziska Süß
*The interplay between attention and syntactic processes in the adult and developing brain: ERP evidences*

123 Stefan Bode
*From stimuli to motor responses: Decoding rules and decision mechanisms in the human brain*

124 Christiane Diefenbach
*Interactions between sentence comprehension and concurrent action: The role of movement effects and timing*

125 Moritz M. Daum
*Mechanismen der frühkindlichen Entwicklung des Handlungsverständnisses*

126 Jürgen Dukart
*Contribution of FDG-PET and MRI to improve Understanding, Detection and Differentiation of Dementia*

127 Kamal Kumar Choudhary
*Incremental Argument Interpretation in a Split Ergative Language: Neurophysiological Evidence from Hindi*

128 Peggy Sparenberg
*Filling the Gap: Temporal and Motor Aspects of the Mental Simulation of Occluded Actions*

129 Luming Wang
*The Influence of Animacy and Context on Word Order Processing: Neurophysiological Evidence from Mandarin Chinese*

130 Barbara Ettrich
*Beeinträchtigung frontomedianer Funktionen bei Schädel-Hirn-Trauma*

131 Sandra Dietrich
*Coordination of Unimanual Continuous Movements with External Events*

132 R. Muralikrishnan
*An Electrophysiological Investigation Of Tamil Dative-Subject Constructions*

133 Christian Obermeier
*Exploring the significance of task, timing and background noise on gesture-speech integration*

134 Björn Herrmann
*Grammar and perception: Dissociation of early auditory processes in the brain*

135 Eugenia Solano-Castiella
*In vivo anatomical segmentation of the human amygdala and parcellation of emotional processing*

136 Marco Taubert
*Plastizität im sensomotorischen System – Lerninduzierte Veränderungen in der Struktur und Funktion des menschlichen Gehirns*

137 Patricia Garrido Vásquez
*Emotion Processing in Parkinson's Disease: The Role of Motor Symptom Asymmetry*

138 Michael Schwartze
*Adaptation to temporal structure*

139 Christine S. Schipke
*Processing Mechanisms of Argument Structure and Case-marking in Child Development: Neural Correlates and Behavioral Evidence*

140 Sarah Jessen
*Emotion Perception in the Multisensory Brain*

141 Jane Neumann
*Beyond activation detection: Advancing computational techniques for the analysis of functional MRI data*

142 Franziska Knolle
*Knowing what's next: The role of the cerebellum in generating*